Journal of Systematic Palaeontology, 2015
http://dx.doi.org/10.1080/14772019.2015.1119211

Taylor & Francis
Taylor & Francis Group

The ammonoids from the Late Permian *Paratirolites* Limestone of Julfa (East Azerbaijan, Iran)

Dieter Korn[a]*, Abbas Ghaderi[b], Lucyna Leda[a], Martin Schobben[a] and Ali Reza Ashouri[b]

[a]*Museum für Naturkunde, Leibniz-Institut for Research on Evolution and Biodiversity, Invalidenstraße 43, 10115 Berlin, Germany;* [b]*Department of Geology, Faculty of Sciences, Ferdowsi University of Mashhad, Azadi Square, 9177948974, Mashhad, Iran*

(Received 10 January 2015; accepted 22 September 2015)

The Changhsingian (Late Permian), 4 to 5 m thick *Paratirolites* Limestone has yielded diverse ammonoid assemblages composed of the genera *Neoaganides*, *Pseudogastrioceras*, *Dzhulfites*, *Paratirolites*, *Julfotirolites*, *Alibashites*, *Abichites*, *Stoyanowites* and *Arasella*. The succession of ammonoid species allows for a subdivision of the rock unit into eight biozones, in ascending order: *Dzhulfites zalensis* Zone, *Paratirolites trapezoidalis* Zone, *Paratirolites kittli* Zone, *Stoyanowites dieneri* Zone, *Alibashites mojsisovicsi* Zone, *Abichites abichi* Zone, *Abichites stoyanowi* Zone and *Arasella minuta* Zone. The following 20 new species are described by two of us (DK and AG): *Neoaganides ultimus* sp. nov., *Pseudogastrioceras relicuum* sp. nov., *Dzhulfites zalensis* sp. nov., *Dzhulfites hebes* sp. nov., *Paratirolites coronatus* sp. nov., *Paratirolites birunii* sp. nov., *Paratirolites quadratus* sp. nov., *Paratirolites multiconus* sp. nov., *Paratirolites serus* sp. nov., *Julfotirolites kozuri* sp. nov., *Alibashites ferdowsii* sp. nov., *Alibashites uncinatus* sp. nov., *Alibashites stepanovi* sp. nov., *Abichites subtrapezoidalis* sp. nov., *Abichites alibashiensis* sp. nov., *Abichites ariaeii* sp. nov., *Abichites paucinodus* sp. nov., *Abichites shahriari* sp. nov., *Abichites terminalis* sp. nov. and *Stoyanowites aspinosus* sp. nov. After the time-equivalent Chinese occurrences, the material described here is the most diverse assemblage known from the critical interval before the end-Permian mass extinction.

http://zoobank.org/urn:lsid:zoobank.org:pub:75D71EE8-27A2-48B1-805B-52E98578A7B8

Keywords: Late Permian; Changhsingian; *Paratirolites* Limestone; Ammonoidea; Iran; biostratigraphy

Introduction

Ammonoids are among the most celebrated victims of the end-Permian mass extinction event. They very nearly became extinct, with the survival of only a few lineages of which only one gave rise to the majority of the Mesozoic ammonoids (e.g. Glenister & Furnish 1981; House 1988; Leonova 2002, 2011; Villier & Korn 2004; Brayard *et al*. 2009).

Studies on the evolutionary history of Permian ammonoids have shown that the group experienced a severe end-Guadalupian extinction event, at which mainly the goniatitic and prolecanitic ammonoids were significantly reduced, while the ceratitic ammonoids remained unaffected (e.g. Spinosa *et al*. 1975). In the aftermath of this crisis, only the ceratites experienced a rapid diversification during the early Wuchiapingian and were then the cardinal ammonoid clade for the duration of the Late Permian, outnumbering the reduced goniatitic and prolecanitic ammonoids in terms of species richness (e.g. Ruzhencev 1959, 1962, 1963, 1965; Zhao *et al*. 1978; Bando 1979; Taraz *et al*. 1981; Leonova 2002, 2011; Brayard *et al*. 2009).

The ceratitic ammonoid clades show differential evolutionary tempos and dominances during the Late Permian. In the Wuchiapingian, ammonoid assemblages are dominated by the diverse araxoceratids (superfamily Otoceratoidea); this group is unimportant in the Changhsingian but survived the end-Permian extinction event and has, along with *Otoceras*, an earliest Triassic representative (e.g. Ruzhencev 1962; Tozer 1979). By contrast, the second Late Permian group of ceratitic ammonoids, the xenodiscids (superfamily Xenodiscoidea), are much less important in the Wuchiapingian but very diverse with a number of independent lineages in the Changhsingian. However, this ammonoid group experienced a mass extinction at the end-Permian crisis, with few survivors.

The Changhsingian Stage can be subdivided in terms of ammonoid evolution, but there are only two regions known with species-rich occurrences. These are the Transcaucasian−Iranian region (e.g. Shevyrev 1965, 1968; Stepanov *et al*. 1969; Teichert *et al*. 1973; Bando

*Corresponding author. Email: dieter.korn@mfn-berlin.de

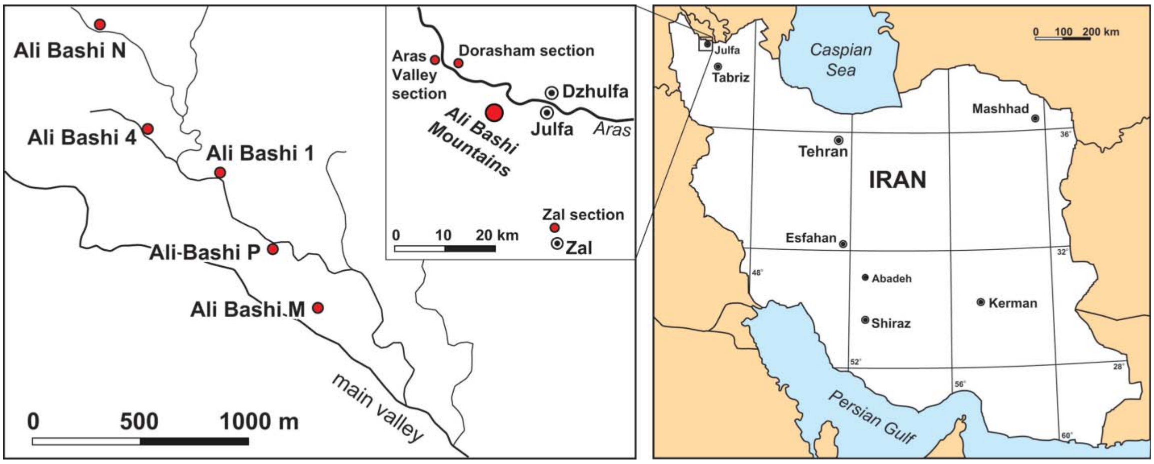

Figure 1. Geographical position of Permian–Triassic boundary sections in the Transcaucasus–NW Iran region (after Arakelyan *et al*. 1965); sections investigated in this study are highlighted.

1979; Taraz *et al*. 1981; Zakharov 1983, 1992; Zakharov & Rybalka 1987; Ghaderi *et al*. 2014b) and South China (e.g. Zhao *et al*. 1978; Zheng 1981; Liang 1983; Yang 1987; Yang & Yang 1992). The two regions display different ammonoid successions and are, in terms of detailed ammonoid stratigraphy, very difficult to correlate. In the Transcaucasian–Iranian sections, the paratirolitid ammonoids (= family Dzhulfitidae) became dominant at the end of the Changhsingian Stage, while in South China the families Tapashanitidae, Pseudotirolitidae and Pleuronodoceratidae are the most common.

In the Transcaucasian–Iranian region, ammonoids occur rather frequently in the 4 to 5 m thick *Paratirolites* Limestone, which is the youngest Late Permian carbonate formation that occurs regularly in the entire region (Fig. 1). The formation was first described by Stoyanow (1910), a pioneer in the study of the latest Permian ammonoids from the Transcaucasus. He described the genus *Paratirolites* and also four species, which can be attributed to *Paratirolites* or related genera.

Here we present the first description of the ammonoids from the *Paratirolites* Limestone based on material collected bed by bed. Earlier publications (e.g. Shevyrev 1965, 1968) treated the *Paratirolites* Limestone as a uniform rock unit. Hence, they were not able to provide evidence for a stratigraphical succession of the various species, their evolutionary patterns or their possible phylogenetic relationships. We demonstrate that the *Paratirolites* Limestone contains a remarkable ammonoid record in terms of morphological evolution and diversity.

Palaeogeographical distribution of Changhsingian ammonoids

Occurrences of Changhsingian ammonoids

Late Changhsingian ammonoids are known from only a few places worldwide, and there are only two regions from which rather diverse ammonoid assemblages have been described:

1. Transcaucasian–Central Iranian region. This region had a Late Permian position in the Central Tethys (Fig. 2) close to the equator (Muttoni *et al*. 2009a, b). Based on previous investigations (Stoyanow 1910; Shevyrev 1965, 1968; Stepanov *et al*. 1969; Teichert *et al*. 1973; Zakharov 1983, 1992; Zakharov & Rybalka 1987) and our own investigations, the following ammonoid families and genera characterize the *Paratirolites* Limestone:

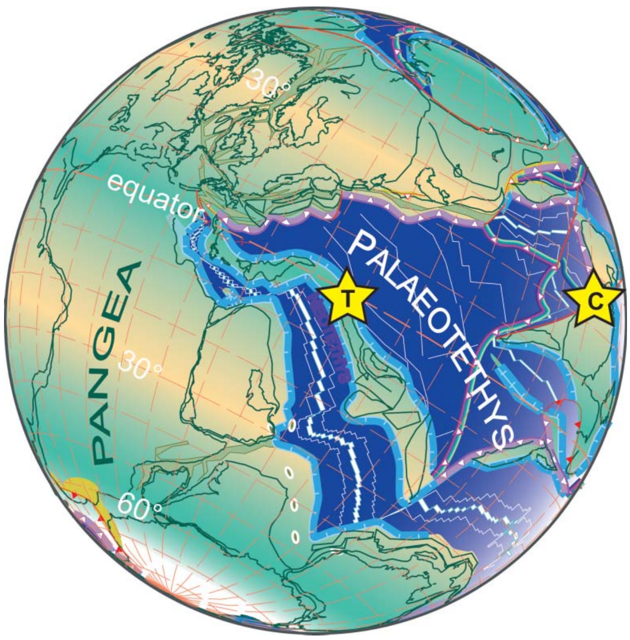

Figure 2. Palaeogeographical position of the Julfa area (after Stampfli & Borel 2002). T = Transcaucasus–NW Iran region; C = South China.

Pseudohaloritidae (*Neoaganides*);
Paragastrioceratidae (*Pseudogastrioceras*);
Dzhulfitidae (*Dzhulfites*, *Paratirolites*, *Julfotirolites*, *Alibashites*, *Abichites*, *Stoyanowites*);
Xenodoiscidae (*Arasella*).

Other genera previously reported from the *Paratirolites* Limestone need to be discussed. Bando (1973) described the otoceratid genus and species *Julfotoceras tarazi* (a species with close morphological similarities to the Wuchiapingian genus *Vedioceras*) from Ali Bashi, and stated that the single specimen was from the 'lowermost Triassic' (= *Paratirolites* Limestone). During our field investigations, we did not find any evidence for otoceratids in the *Paratirolites* Limestone; therefore, we suspect that the specimen may have come from the upper part of the Julfa Formation, which is also a red nodular limestone formation and contains specimens of *Vedioceras* and related genera.

Teichert & Kummel (in Teichert *et al.* 1973) listed poorly preserved specimens from Ali Bashi under the names *Strigogoniatites*, *Pleuronodoceras*, *Pseudotirolites* and *Tapashanites*, but these ammonoids were not collected in situ; it is therefore possible that they derive from lower horizons. Because of their poor preservation, they are probably not attributable to distinct genera.

Rostovcev (in Zakharov 1983) described the new species '*Pseudotirolites azariani*' from Dorasham but did not illustrate a suture line. According to the conch shape and sculpture, this species probably belongs to *Paratirolites kittli*.

The Changhsingian interval below the *Paratirolites* Limestone has yielded a number of ammonoid species, which belong to the following taxa (Shevyrev 1965, 1968; own collections):

Paragastrioceratidae (*Pseudogastrioceras*);
Xenodiscidae (*Xenodiscus*, *Xenaspis*, *Phisonites*, *Iranites*, *Shevyrevites*);
Dzhulfitidae (*Dzhulfites*).

2. South China. This region had a Late Permian latitude of about 20° N (Liu *et al.* 1999) (Fig. 2). A number of monographs (e.g. Zhao *et al.* 1978; Zheng 1981; Liang 1983; Yang 1987; Yang & Yang 1992) have contributed to the knowledge of the ammonoid assemblages, which are composed of the following families and genera (note that many of the listed genera were regarded as synonyms by Leonova 2002):

Pseudohaloritidae (Neoaganides, Qinglongites);
Paragastrioceratidae (Pseudogastrioceras, Strigogoniatites);
Neostacheoceratidae (Stacheoceras);
Cyclolobidae (Changhsingoceras, Cyclolobus);
Paraceltitidae (Meitianoceras);
Xenodiscidae (Xenodiscus, Penglaites);
Huananoceratidae (Huananoceras);
Tapashanitidae (Tapashanites, Mingyuexiaceras, Pseudostephanites, Sinoceltites);
Liuchengoceratidae (Liuchengoceras, Rongjiangoceras, Wangrenoceras);
Pseudotirolitidae (Chaotianoceras, Dushanoceras, Pachydiscoceras, Pernodoceras, Pseudotirolites, Schizoloboceras, Shangsites, Trigonogastrites);
Pleuronodoceratidae (Longmenshanoceras, Pentagonoceras, Pleuronodoceras, Qianjiangoceras, Rotodiscoceras).

The list above shows remarkable differences in the Changhsingian ammonoid assemblages between the two regions. Common taxa in the two sedimentary basins appear to be restricted to those that do not play a major role in terms of frequency within their occurrences. Of the genus *Pseudogastrioceras*, for instance, only two specimens have been recorded by us in the *Paratirolites* Limestone of NW Iran, and *Neoaganides* is represented by only four specimens. In contrast, the family Dzhulfitidae represents more than 97% of the ammonoid specimens from the *Paratirolites* Limestone of the NW Iranian sections. Representatives of the family are completely lacking in South China.

The latter observation requires special attention. In South China, many of the Late Changhsingian ceratitic ammonoids share a number of morphological characters, such as: (1) conch geometry extremely discoidal and subevolute to evolute; (2) whorl cross section pentagonal with tectiform or keeled venter; (3) suture line possesses a short external lobe with unserrated or weakly serrated prongs; and (4) sculpture has weak radial ribs.

In contrast to the Chinese Changhsingian ceratites, the members of the Central Tethyan family Dzhulfitidae appear to be more variable in their morphology. While the coiling rate of most of the species is rather similar, variation in the shape of the whorl cross section is wide (ranging from strongly depressed trapezoidal to compressed oval). The suture lines are more variable and in many of the species show much stronger serration of the lobes, best seen in the prongs of the external lobe (Fig. 3). The sculpture or ornament ranges from the development of coarse conical nodes, to a nearly smooth shell ornamented with growth lines.

The significant difference in the composition of ammonoid assemblages between the main regions (Central Tethys and South China) is a major obstacle for a global scheme of ammonoid stratigraphy for the Changhsingian. In both regions, the ammonoid faunas consist of two components: (1) goniatitic ammonoids, which play only a subordinate role in species richness as well as specimen abundance; and (2) ceratitic ammonoids, which became

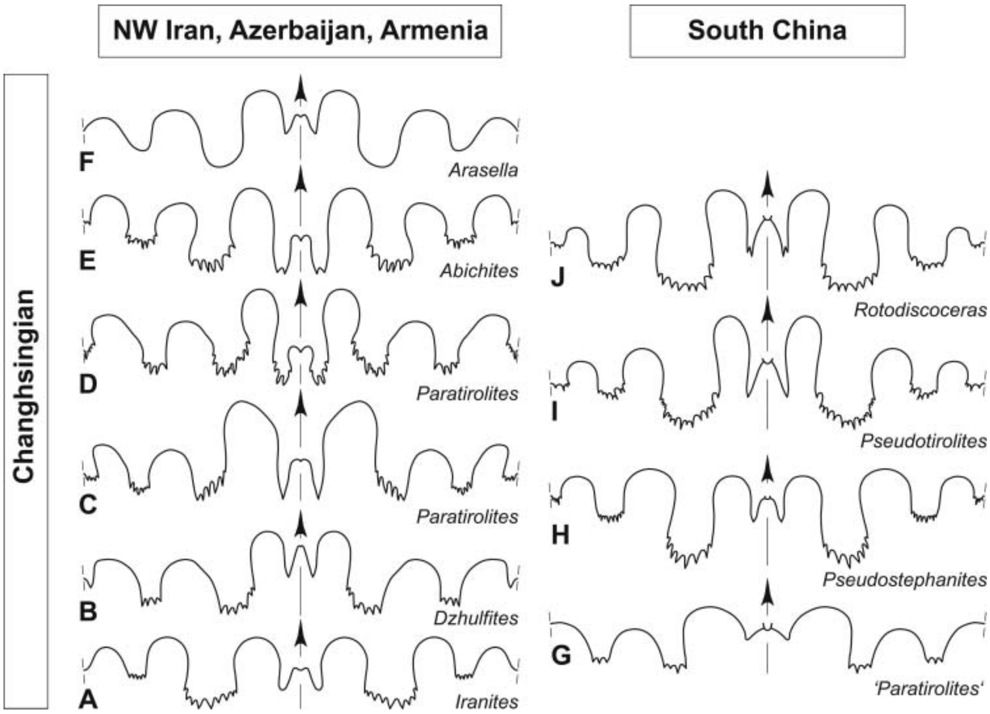

Figure 3. Suture lines of representatives of Changhsingian ammonoids from the Transcaucasus−NW Iran and South China; for comparison the suture lines are figured at the same size (A−B are from Shevyrev 1965; G is from Liang 1983; H−J are from Zhao *et al*. 1978). **A,** *Iranites transcaucasinus* (Shevyrev, 1965); **B,** *Dzhulfites spinosus* Shevyrev, 1965; **C,** *Paratirolites birunii* sp. nov.; **D,** *Paratirolites kittli* Stoyanow, 1910; **E,** *Abichites subtrapezoidalis* sp. nov.; **F,** *Arasella minuta* (Zakharov, 1983); **G,** '*Paratirolites guizhouensis*' Liang, 1983; **H,** *Pseudostephanites nodosus* Zhao, Liang & Zheng, 1978; **I,** *Pseudotirolites orientalis* Chao, 1965; **H,** *Rotodiscoceras asiaticum* Chao & Liang, 1966.

dominant in the Late Permian and dominate the late Changhsingian assemblages. Only some of the goniatitic genera (*Neoaganides*, *Pseudogastrioceras*) occur in both regions, but they are long ranging (e.g. Leonova 2002) and thus not suitable for a distinctive age assignment. On the other hand, the species-rich ceratitic ammonoids display pronounced biogeographical separation without co-occurring genera (or even families).

Paratirolites in South China?

The genus *Paratirolites* has been reported from the area of Anshun in the province of Guizhou (Zhao *et al*. 1978; Zheng 1981; Liang 1983), but these records are highly questionable. Only fragments have been illustrated; indeed, the conch with conical nodes resembles *Paratirolites*, but the suture line of '*Paratirolites guizhouensis*' figured by Liang (1983) clearly shows that at least this species to have a very low and wide external lobe (Fig. 3G) which cannot be assigned to *Paratirolites*. These South Chinese specimens assigned to *Paratirolites* were found in association with specimens assigned to *Shevyrevites shevyrevi*; however, these determinations are also somewhat ambiguous because of the poor preservation of the material. Zhao *et al*. (1978) placed a '*Paratirolites*−*Shevyrevites* Genus Zone' in the early Changhsingian. It was probably this putative (but incorrectly postulated) occurrence of *Paratirolites* that was used by Zhao *et al*. (1978) for the statement that the Transcaucasian *Paratirolites* Limestone does not represent the latest Permian, but rather an interval in the early Changhisingian.

Based on the occurrence of the putative *Paratirolites*, Liang (1983, p. 614) stated: "This indicates that the Dorashemian stage is definitely equivalent to the lower Changhsingian of South China". This statement can be refuted because '*Paratirolites guizhouensis*' is not a *Paratirolites* and most probably does not even belong in the family Dzhulfitidae. If it belongs there at all, it may just be a very early representative of this family. Ammonoids with a suture line similar to that of '*Paratirolites guizhouensis*', i.e. with a very short and wide external lobe, occur in the NW Iranian sections below the *Paratirolites* Limestone. It is therefore much more likely that the *Paratirolites* Limestone in fact represents the late Changhsingian of the South Chinese sections, as already concluded from the investigation of conodonts (Kozur 2005, 2007; Shen & Mei 2010; Ghaderi *et al*. 2014b).

Tozer (1979) suggested that the South Chinese species *Schizoloboceras fusuiense* Zhao, Liang & Zheng, 1978 is congeneric with *Paratirolites vediensis*, but this conclusion does not take account of the major sutural differences between *Schizoloboceras* and *Paratirolites*. *Schizoloboceras* has, like the other representatives of the family Pseudotirolitidae, a very short external lobe, in which the prongs are usually unserrated and in some cases bifid. There is therefore no evidence that the two genera are identical.

Biostratigraphy of Late Permian ammonoids

The Permian–Triassic rock succession near Julfa

The sedimentary succession of the Permian–Triassic boundary beds in the region of Julfa can be subdivided into three major units (Ruzhencev *et al*. 1965; Stepanov *et al*. 1969; Rostovtsev & Azaryan 1973; Teichert *et al*. 1973; Ghaderi *et al*. 2013, 2014b; Leda *et al*. 2014; Schobben *et al*. 2014, 2015), in ascending order:

1. The Middle Permian Gnishik and Khachik formations (both together about 475 m thick), composed of massive shallow-water limestone (Stepanov *et al*. 1969).
2. The Late Permian succession of approximately 57 m thickness with the Julfa Formation (Wuchiapingian in age), the Changhsingian Ali Bashi Formation (which includes the shale-dominated Zal Member and the *Paratirolites* Limestone Member) and the latest Permian 'Boundary Clay' (= Aras Member), which formally represents the lower part of the Elikah Formation (Ghaderi *et al*. 2014b). The sharp but continuous transition from the *Paratirolites* Limestone into the Aras Member marks the end-Permian mass extinction event (Leda *et al*. 2014).
3. The Early Triassic carbonatic portion of the Elikah Formation, with the *Claraia* Beds in the lower portion, reaching about 280 m in thickness (Stepanov *et al*. 1969).

Two questions regarding biostratigraphical aspects have to be addressed: (1) how can the ammonoid faunas from the *Paratirolites* Limestone be incorporated into a global stratigraphical scheme of the Late Permian? (2) how can the succession of ammonoids within the *Paratirolites* Limestone be subdivided in terms of biozones?

The *Paratirolites* Limestone

The *Paratirolites* Limestone, named after the Late Permian ammonoid genus *Paratirolites*, is the youngest Permian carbonate formation in the sections of Transcaucasia and north-western Iran. It is an approximately 4 to 5 m thick succession of intensely red-coloured and sometimes pink to grey nodular limestone; the individual beds reach thicknesses of 25 cm and are separated by shaly intervals ranging in thickness between a few millimetres and 20 cm (Figs 4, 5). The shale content is much higher in the lower part of the unit, while in the upper 3 m, shale interbeds usually do not reach a thickness of more than 2 cm. Most of the limestone beds possess a rich content of skeletal remains, but the fossils are often fragmentarily preserved. Ghaderi *et al*. (2014a) described some brachiopods from the rock unit. Leda *et al*. (2014) identified the carbonate microfacies of the rock unit as nodular burrowed bioclastic wackestone or argillaceous lime mudstone indicating a deeper shelf/outer ramp depositional setting. Study of the oxygen isotopes of conodont phosphate and brachiopod calcite by Schobben *et al*. (2014) indicated that a clear temperature trend cannot be observed within the *Paratirolites* Limestone, where the temperatures range between 27 and 33°C. However, a sudden increase of 8°C occurs at the extinction horizon and confirms the results by Joachimski *et al*. (2012) for South China.

Figure 4. The Permian–Triassic boundary beds at the Ali Bashi N section. From bottom to top: *Paratirolites* Limestone (Late Permian; about 4 m thick), Aras Member ('boundary clay'; about 1.5 m thick, covered by scree) and *Claraia* Beds (Early Triassic).

The term '*Paratirolites* Limestone' was coined by Stepanov *et al*. (1969), who published the first description of the Permian–Triassic boundary beds in the Ali Bashi Mountains 9 km west of Julfa (East Azerbaijan, Iran). Teichert *et al*. (1973) adopted the term and provided an extensive historical overview of the research history of the Permian–Triassic boundary in Transcaucasia. However, similar terms have been used earlier, for example by Ruzhencev *et al*. (1965) and Shevyrev (1965) for the

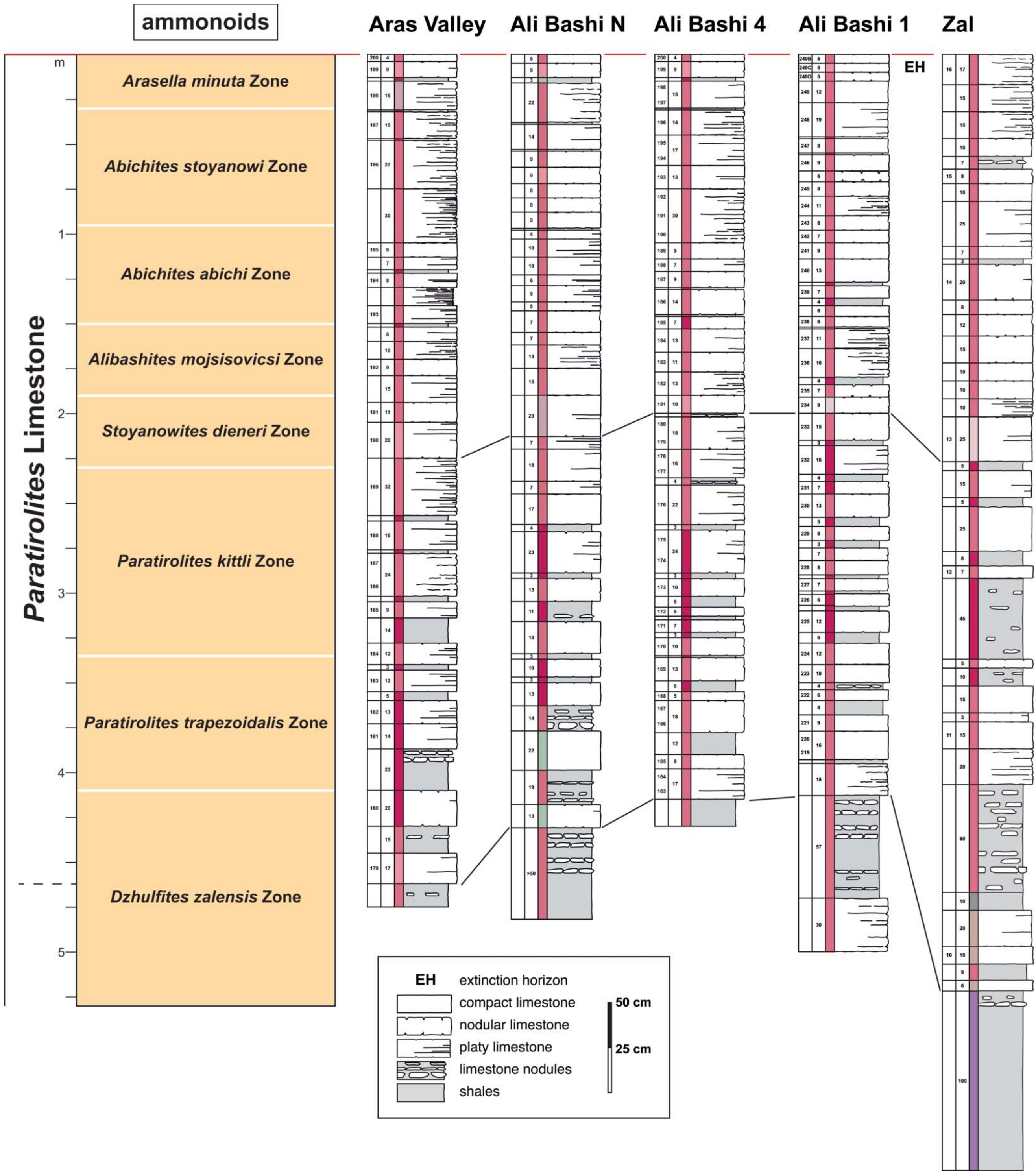

Figure 5. Columnar sections of the *Paratirolites* Limestone in the Aras Valley, Ali Bashi 4, Ali Bashi 1 and Zal sections, with their ammonoid zonation.

Permian−Triassic succession in the classical Dorasham section (Nakhichevan, Azerbaijan).

In all these articles, the *Paratirolites* Limestone has been treated as a uniform rock unit; a lithostratigraphical or biostratigraphical subdivision has not been achieved. One reason for the lack of a subdivision may be the superficial lithofacies similarity throughout the unit, but another reason may be the rather scarce occurrence of macrofaunas. For instance, Ruzhencev & Shevyrev (1965) listed only 116 ammonoid specimens from the *Paratirolites* Limestone of the various Transcaucasian localities. This is a comparatively low number when the intensive fieldwork of the Russian team is considered. Teichert *et al*. (1973), when describing the Ali Bashi sections, had even fewer specimens (only about 75), most of which were float collections without reference to a distinct horizon.

In contrast to the mentioned studies on ammonoids, microfossils have been shown to allow zonation within the *Paratirolites* Limestone. Kozur (2005, 2007) and Shen & Mei (2010), for instance, showed six conodont zones (*Clarkina bachmanni* Zone to *C. hauschkei* Zone) for the *Paratirolites* Limestone. Ghaderi (in Ghaderi *et al*. 2014b) largely confirmed this subdivision and also defined six zones (*Clarkina changxingensis* Zone to *C. hauschkei* Zone). It is thus obvious that the *Paratirolites* Limestone can no longer be treated as a single, uniform rock unit.

In four field campaigns between 2010 and 2013, we intensely investigated the *Paratirolites* Limestone in outcrops in the vicinity of Julfa and collected more than 310 determined ammonoid specimens from this rock unit. We measured five complete sections in the Ali Bashi Mountains, one in the Aras Valley 2 km west of the classical Dorasham locality, and one 2.2 km north−northwest of Zal, 22 km south of Julfa. With this study, we will demonstrate the potential for a more detailed ammonoid zonation within the *Paratirolites* Limestone. Another aim of the study is the documentation of the extinction patterns of Late Permian ammonoid faunas.

All of the ammonoids collected in situ were measured regarding their position in the rock column with respect to the extinction horizon. In the following, the stratigraphical position is thus explained in metres below this horizon (which is equal to the top surface of the *Paratirolites* Limestone).

Investigated outcrops

Outcrops of the Late Permian *Paratirolites* Limestone are known from north and south of the Aras (Araxes) River in the vicinity of Dzhulfa (Nakhichevan; Azerbaijan) and Julfa (East Azerbaijan; Iran) (Figs 1, 5).

1. Aras Valley (39.015° N, 45.434° E). This section was first described by Ghaderi *et al*. (2014b) and Leda *et al*. (2014); it is located about 19 km west-northwest of the towns of Dzhulfa and Julfa immediately west of the Aras (Araxes) River. At this place, the Aras River marks the political boundary between Iran and the province of Nakhichevan (Azerbaijan), and Late Permian rocks are exposed on both sides. The new Aras Valley section has a position approximately 2 km north-west of the famous Dorasham II section described by Ruzhencev *et al*. (1965).

2. Kuh-e-Ali Bashi (= Ali Bashi Mountains; 9 km west of Julfa). The *Paratirolites* Limestone is exposed in a number of parallel sections over an extension of about 1.5 km. We studied five of the numerous sections, which are positioned along a strike from west-northwest to east-southeast:

(a) Ali Bashi N section (38.941° N, 45.516° E). This section has not been studied previously. It begins in the higher portion of the Ali Bashi Formation and ranges into the Elikah Formation. The *Paratirolites* Limestone is well exposed and can be investigated over an outcrop length of 200 m.

(b) Ali Bashi 4 section of Teichert *et al*. (1973) (38.942° N, 45.516° E). This is the section figured by Stepanov *et al*. (1969). It is the most complete of all the sections in the Ali Bashi Mountains and ranges from the *Codonofusiella* Beds (exposed in the stream at the base of the section) into the Elikah Formation. The lower part of the Ali Bashi Formation is poorly exposed because of a scree cover. The *Paratirolites* Limestone, the Boundary Clay and the base of the carbonate member of the Elikah Formation are perfectly exposed over a distance of 100 m.

(c) Ali Bashi 1 section of Teichert *et al*. (1973) (38.940° N, 45.520° E). The section begins in the upper part of the Julfa Beds and exposes the shaly part of the Ali Bashi Formation, the *Paratirolites* Limestone, the Boundary Clay and the base of the carbonate member of the Elikah Formation. The *Paratirolites* Limestone is rather well exposed over a distance of 50 m.

(d) Ali Bashi P section (38.937° N, 45.523° E). This is a small outcrop at the south side of the side valley and exposes the upper portion of the *Paratirolites* Limestone.

(e) Ali Bashi M section (38.936° N, 45.524° E). The section is located on the north side of the main valley and exposes the *Paratirolites* Limestone as well as the base of the Elikah Formation in several small exposures. Kozur (2005) studied this section for its conodont stratigraphy; it was named 'Ali Bashi locality 1' there.

3. Zal (22 km SSW of Julfa and 2.2 km north-northwest of the village of Zal) (38.733° N, 45.580° E). In this section, the entire Late Permian succession is exposed; the section ranges high up into the Early Triassic Elikah Formation.

Ammonoid zonation within the *Paratirolites* Limestone

An ammonoid zonation for the *Paratirolites* Limestone did not exist until the preliminary proposal by Korn (in Ghaderi *et al*. 2014b). In the major previous investigations (e.g. Shevyrev 1965, 1968; Stepanov *et al*. 1969; Teichert *et al*. 1973), the unit has not been subdivided and the ammonoid findings were not assigned to specific horizons.

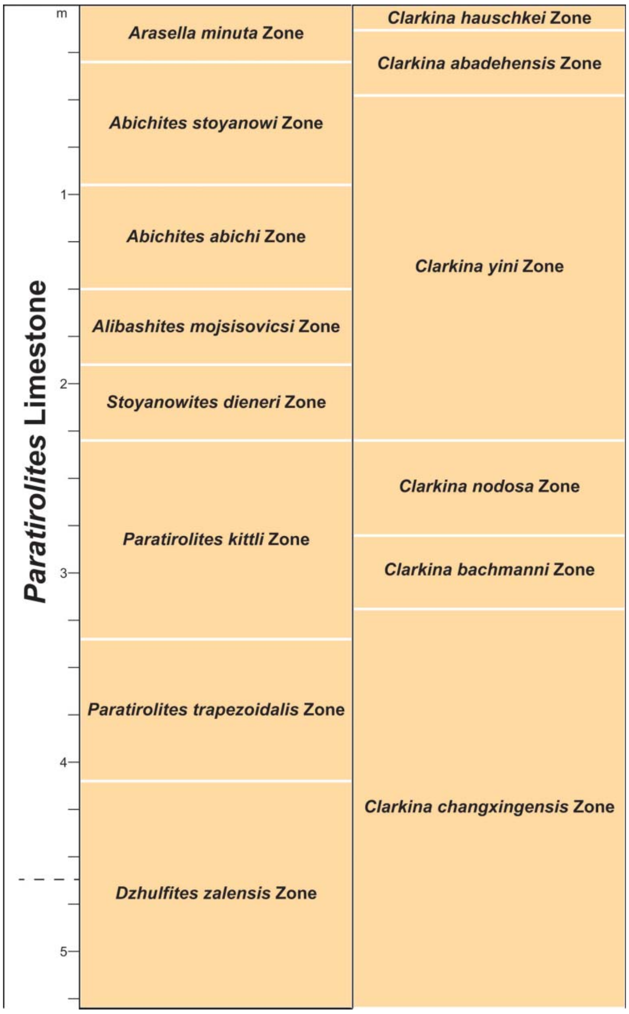

Figure 6. Correlation of the ammonoid stratigraphy with the conodont stratigraphy (from Ghaderi *et al*. 2014b) for the sections in the Transcaucasus−North-west Iran.

During our field investigations, we paid particular attention to the precise position of the ammonoid specimens in the rock column; all in situ collected specimens were recorded with detailed lithostratigraphical information (in terms of position below the extinction horizon, which is equivalent to the top surface of the *Paratirolites* Limestone). We collected more than 230 specimens in this way.

The morphological evolution of the paratirolitid ammonoids allows for a subdivision of the *Paratirolites* Limestone into eight biozones, which only partly correlate with the conodont biozones (Fig. 6). Five separable ammonoid zones (defined by first occurrences of index species) were distinguished within the *Paratirolites* Limestone by Ghaderi *et al*. (2014b); however, this zonation is revised and refined here, in ascending order:

1. ***Dzhulfites zalensis* Zone.** This zone may begin already below the *Paratirolites* Limestone, but scarce fossil content precludes a precise statement. The name-giving species occurs, in the Zal section, in a horizon 5.30 m below the extinction horizon −that is, at the border of the Zal member and the *Paratirolites* Limestone. The zone is characterized by the two species *D. zalensis* sp. nov. and *D. hebes* sp. nov., which probably have a successive occurrence. The zone has a thickness of about 1.20 m.
2. ***Paratirolites trapezoidalis* Zone.** This zone also has a position at the base of the *Paratirolites* Limestone, where the taxonomic diversity of the ammonoid faunas is still rather low. The interval contains paratirolitid ammonoids with unsubdivided or bifid prongs of the external lobe. *Paratirolites trapezoidalis* Shevyrev, 1965 best defines the base of this interval, which is difficult to recognize because of the rarity of fossils at the base of the *Paratirolites* Limestone. The index fossil was recorded, in the Ali Bashi 4 section, from a horizon 4.10 m below the extinction horizon. The thickness of this zone is thus about 0.75 m.
3. ***Paratirolites kittli* Zone.** This interval shows the main occurrence of the genus *Paratirolites*, of which also *Paratirolites vediensis* Shevyrev, 1965 can be used as an index fossil besides the nominate species *Paratirolites kittli* Stoyanow, 1910. Even without distinct species attribution, specimens of this zone are usually clearly assigned to this zone because of the strongly serrated external, adventive and lateral lobes. This interval is, in the Aras Valley and Ali Bashi sections, often very fossiliferous and thus easily recognizable. In the Ali Bashi N section, *P. kittli* occurs first at 3.35 m below the extinction horizon, indicating a thickness of about 1.05 m for this zone.
4. ***Stoyanowites dieneri* Zone.** The entry of paratirolitids with laterally compressed whorl sections, among which *Paratirolites dieneri* Stoyanow, 1910 is the type species of the new genus *Stoyanowites*, characterizes the next biozone within the *Paratirolites* Limestone. In the Aras Valley section, this species occurs first at 2.30 m below the extinction horizon; the *Stoyanowites dieneri* Zone thus has a thickness of 0.40 m in this section.
5. ***Alibashites mojsisovicsi* Zone.** With the entry of the genus *Alibashites*, species richness within the *Paratirolites* Limestone reaches its maximum. Almost simultaneously, several species of this genus as well as the genus *Abichites* appear, making the zone easily recognizable. The *Alibashites mojsisovicsi* Zone has a thickness of 0.40 m in the sections.
6. ***Abichites abichi* Zone.** *Abichites abichi* Shevyrev, 1965 marks the base of this zone, in which the genus *Abichites* is dominant. The zone has a thickness of 0.55 m.
7. ***Abichites stoyanowi* Zone.** A higher portion of the *Paratirolites* Limestone is dominated by paratirolitid ammonoids with quadrate or slightly compressed

whorl cross sections and weakened sculpture. Such forms usually belong to the genus *Abichites*, which possesses a suture line with bifid or unsubdivided prongs of the external lobe. The index fossil *Abichites stoyanowi* (Kiparisova, 1947) occurs, in the Aras Valley section, with first specimens at 0.95 m below the extinction horizon. The thickness of this zone is thus about 0.65 m.

8. ***Arasella minuta* Zone.** At the top of the *Paratirolites* Limestone is a thin interval, about 0.30 m thick, which is dominated by very small ammonoids with simple suture lines. *Arasella minuta* (Zakharov, 1983) is the most common of these and can be used for the definition of this zone, which ends at the top surface of the *Paratirolites* Limestone (= mass extinction horizon).

The occurrence of ammonoid species is irregular in the *Paratirolites* Limestone. While in the lower portion, during the *Dzhulfites zalensis* and *Paratirolites trapezoidalis* zones only one or two species co-occur, species richness increases in the *Paratirolites kittli* Zone with up to five co-occurring species. The highest diversity was recorded in the *Alibashites mojsisovicsi* Zone with nine species; thereafter a discontinuous decrease is observed. Immediately below the extinction horizon, three species were recorded (Fig. 7).

Material and methods

More than 340 ammonoid specimens collected during four field campaigns between 2010 and 2013 were available for study. Three hundred and twelve of these specimens

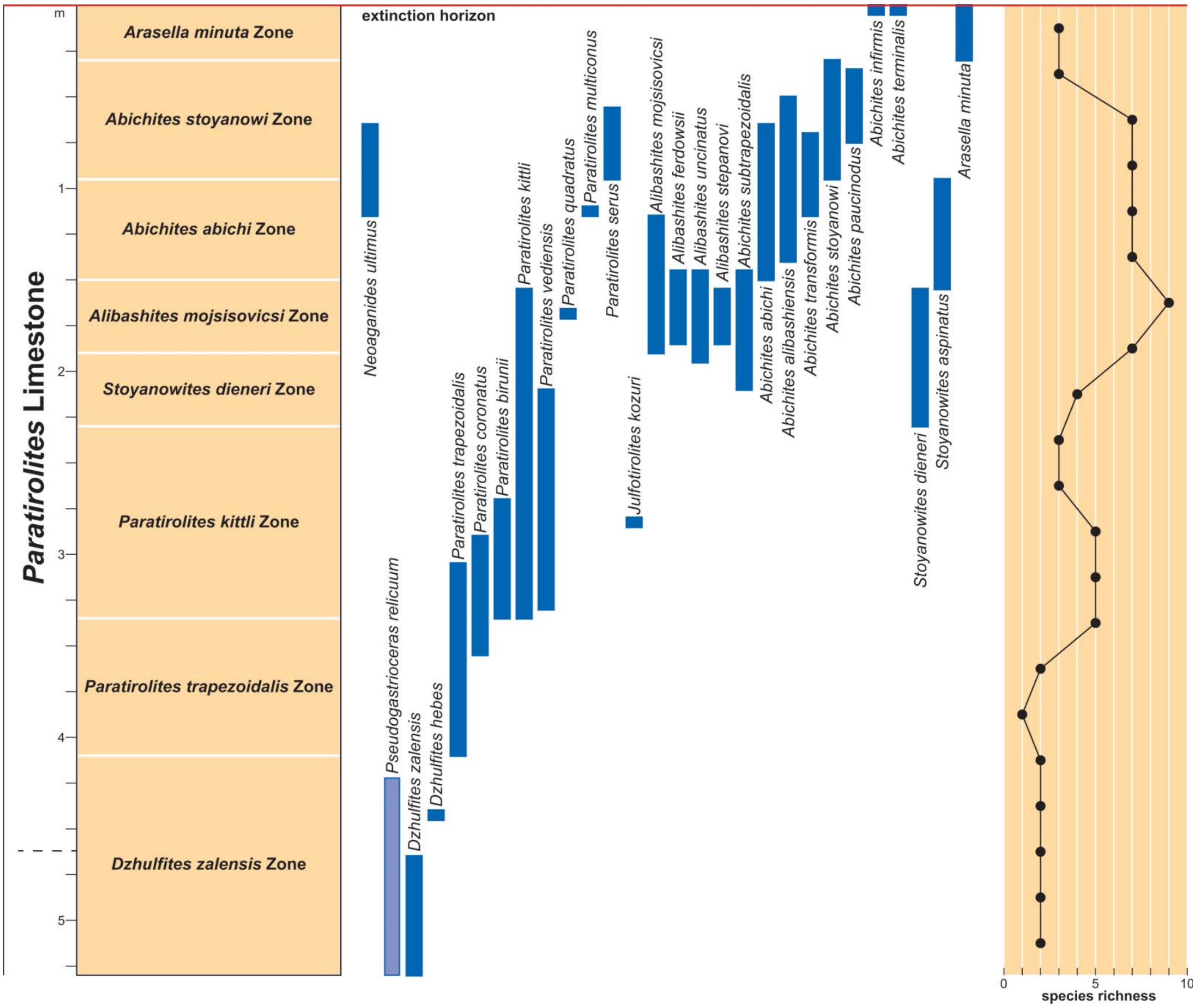

Figure 7. The stratigraphical occurrence of ammonoid species in the *Paratirolites* Limestone of the Julfa region, and species richness in rock intervals of 0.25 m.

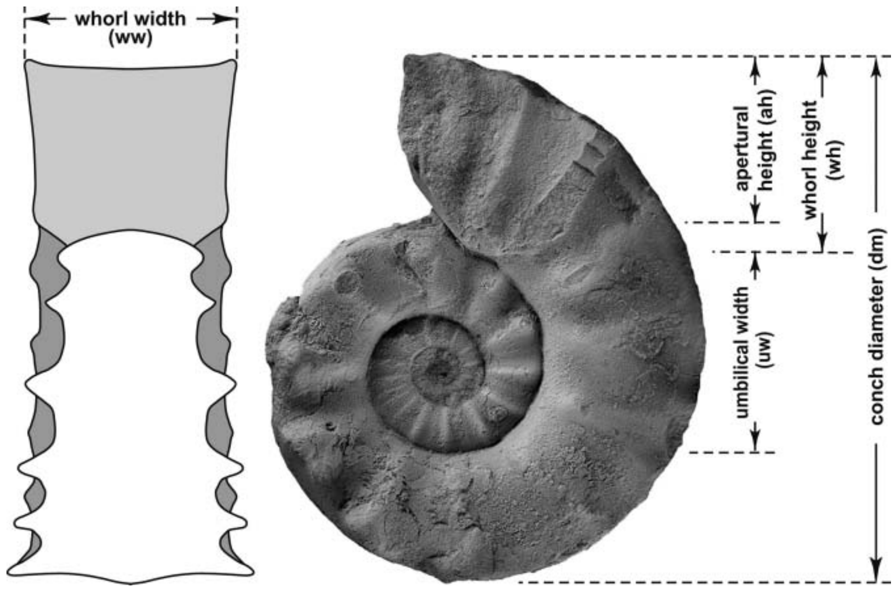

Figure 8. Descriptive terms for the conch geometry of the ammonoids described here.

were determined (Suuplemental material Table 1); they derive from the following localities: Aras Valley (142 specimens); Ali Bashi N (116 specimens); Ali Bashi 4 (19 specimens); Ali Bashi 1 (nine specimens); Ali Bashi P (seven specimens); Ali Bashi M (one specimen); Zal (16 specimens).

All specimens are preserved as internal moulds; shell material is extremely rare as it was dissolved in early diagenesis, and when present it is restricted to the inner whorls. Preservation of the specimens is therefore poor. In many cases, the specimens are preserved only from the lower side facing the sediment, while the upper side was eroded or dissolved during burial of the specimens (Leda *et al*. 2014). Preparation of the specimens often benefits from the presence of a thin clay film separating the ammonoid moulds and the surrounding sediment.

In the following, two of us (DK and AG) describe 28 ammonoid species from the *Paratirolites* Limestone. It appears that the total ammonoid diversity of this unit is not yet complete. There are a number of fragmentary or poorly preserved specimens left undescribed; these could not be attributed to any of the species described herein, therefore these fragments may represent other new species.

Descriptive terminology for conch morphology is after Korn (2010). Abbreviations of conch dimensions (Fig. 8) are: **dm**, conch diameter; **ww**, whorl width; **wh**, whorl height; **uw** (= $dm_1-wh_1-wh_2$), umbilical width; **ah**, aperture height. The whorl expansion rate (**WER**) was calculated as $[dm/(dm - ah)]^2$. The imprint zone rate (**IZR**) characterizes the whorl overlap, and can be calculated as (wh−ah)/wh. A list of measurements of the studied specimens is provided in Supplemental material Table 1.

For the shape of the cross sections, an additional explanation of terminology is given (Fig. 9), distinguishing

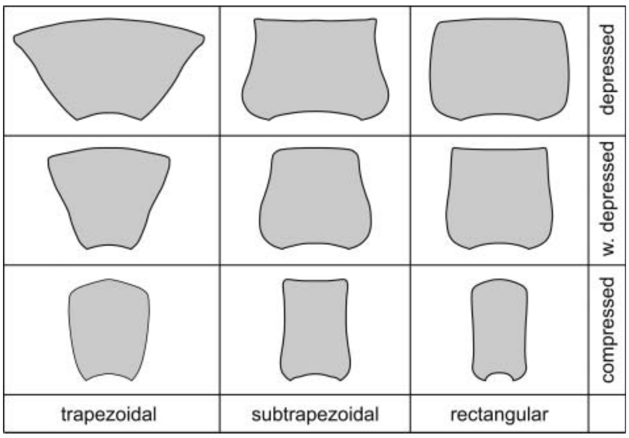

Figure 9. Descriptive terms for the whorl profiles of the ammonoids described here.

between trapezoidal, quadrate, subtrapezoidal, circular and oval. The terminology of the suture line follows Korn *et al.* (2003), meaning that a difference between an A-mode (goniatitic) and a U-mode (prolecanitic and thus also ceratitic) sutural ontogeny, as proposed by Schindewolf (1929), is not accepted. The sutural elements described here are therefore external (**E**), adventive (**A**), lateral (**L**), umbilical (**U**) and internal (**I**) lobes (Fig. 10). The suture lines in the figures are drawn, where possible, from umbilical seam to umbilical seam. Solid lines refer to empirical sutures, dotted lines to reconstructions by mirroring.

The stratigraphical position of individual specimens and the range of species are given in metres below the extinction horizon (top surface of the *Paratirolites* Limestone).

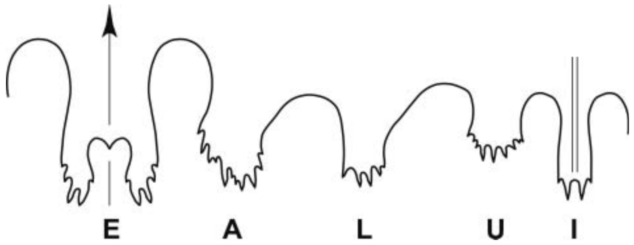

Figure 10. Descriptive terms for the suture lines of the paratirolitid ammonoids, exemplified by *Paratirolites kittli* Stoyanow, 1910, specimen MB.C.25215, Aras Valley, −2.65 m; at 55.8 mm dm, 20.2 mm wh. E, external lobe; A, adventive lobe; L, lateral lobe; U, umbilical lobe; I, internal lobe.

Institutional abbreviations

MB.C.: Cephalopod collection of the Museum für Naturkunde, Berlin; **PIN**: Palaeontological Institute of the Academy of Sciences, Moscow.

Systematic palaeontology (DK and AG)

Order **Goniatitida** Hyatt, 1884
Suborder **Tornoceratina** Wedekind, 1914
Superfamily **Pseudohaloritoida** Ruzhencev, 1957
Family **Pseudohaloritidae** Ruzhencev, 1957
Subfamily **Shouchangoceratinae** Zhao & Zheng, 1977

Included genera. *Aulacaganides* Zhou, 1985; *Elephantoceras* Zhao & Zheng, 1977; *Erinoceras* Zhao & Zheng, 1977; *Lianyuanoceras* Zhou, 1985; *Neoaganides* Plummer & Scott, 1937; *Qinglongites* Zheng, 1981; *Sangzhites* Zhao & Zheng, 1977; *Shangraoceras* Zhao & Zheng, 1977; *Shouchangoceras* Zhao & Zheng, 1977; *Sosioceras* Frest, Glenister & Furnish, 1981.

Genus ***Neoaganides*** Plummer & Scott, 1937

Type species. *Neoaganides grahamensis* Plummer & Scott, 1937, by original designation.

Included species. *Neoaganides costatus* Yang & Yang, 1992, p. 596 (Hubei); *Neoaganides dictyon* Zhou, 1987, p. 310 (Hunan); *Neoaganides gigantus* Liang, 1983, p. 608 (Hunan); *Neoaganides grahamensis* Plummer & Scott, 1937, p. 350 (Texas); *Neoaganides laevigatus* Yang & Yang, 1997, p. 596 (Hubei); *Neoaganides meitianensis* Zheng, 1984, p. 310 (Hunan); *Imitoceras* (*Aganides*) *multiseptatus* Chao, 1940, p. 70 (Hunan); *Neoaganides nesenensis* Frest, Glenister & Furnish, 1981, p. 23 (N. Iran); *Neoaganides paulus* Zhao, Liang & Zheng, 1978, p. 72 (Jiangxi); *Neoaganides rectilobatus* Ruzhencev, 1950, p. 89 (South Urals); *Neoaganides tabantalensis* Ruzhencev, 1952, p. 58 (South Urals); *Neoaganides ultimus* sp. nov. (North-west Iran); *Neoaganides xiaoheensis* Xu, 1977, p. 560 (Hunan).

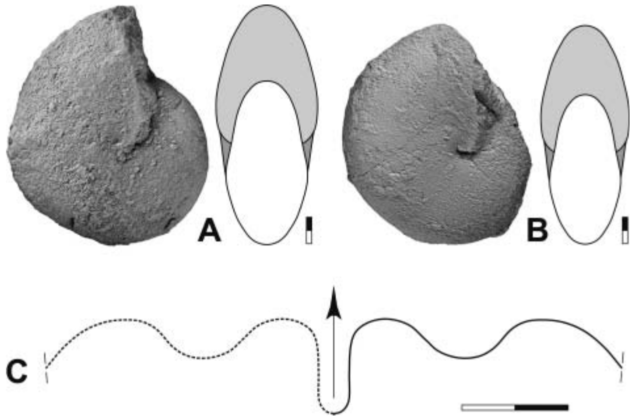

Figure 11. *Neoaganides ultimus* sp. nov. **A,** lateral view, holotype, MB.C.25169, Ali Bashi 1, −0.65 m; **B,** dorsal view, paratype, MB.C.25170, Ali Bashi 4, −1.05 m; **C,** holotype, MB. C.25169, suture line at 6.1 mm ww, 5.8 mm wh. Scale bar = 2 mm.

Neoaganides ultimus sp. nov.
(Fig. 11)

Derivation of name. From Latin *ultimus*, the last, because of its high stratigraphical occurrence in the Late Permian.

Holotype. MB.C.25169 (Fig. 11A).

Type locality and horizon. Ali Bashi 1 section; 0.65 m below the top of the *Paratirolites* Limestone (*Abichites stoyanowi* Zone).

Material. Four specimens (Aras Valley, Ali Bashi N, Ali Bashi 4, Ali Bashi 1).

Diagnosis. *Neoaganides* with lenticular conch (ww/dm = 0.40−0.45). Suture line with very shallow adventive lobe.

Description. All specimens show very similar conch proportions as exemplified by the holotype. The specimen is rather poorly preserved, being coated by a thin clay film (Fig. 11A). It has a conch diameter of 18 mm and is thinly discoidal (ww/dm = 0.42) with a completely closed umbilicus. The conch is widest at the umbilical margin, from which the flanks converge towards the narrowly rounded venter. The coiling rate is moderately high (WER = 2.00). The suture line of the holotype has a deep, parallel-sided external lobe and a very shallow (less than half the depth of the external lobe), broadly rounded adventive lobe (Fig. 11C).

Remarks. Teichert *et al*. (1973, p. 404, pl. 4, figs 5, 6) and Frest *et al*. (1981, p. 25, pl. 3, figs 20−22, text-fig. 15) described and figured two specimens from “the middle of the Ali Bashi Formation” in open nomenclature under

'*Neoaganides* sp. nov.' and '*Neoaganides* sp. 2', respectively. It is not clear if they are conspecific, but they differ from the specimens from the *Paratirolites* Limestone in their larger size (up to 32 mm dm), their more parallel flanks and the presence of shallow ribs on the flanks at 15 mm dm.

Neoaganides nesenensis from the Wuchiapingian Nesen Formation of the Alborz Mountains (Frest *et al.* 1981) is based on a specimen of 23 mm dm. It has a wider conch (ww/dm = 0.47) than *N. ultimus* (ww/dm = 0.42) with less strongly converging flanks. The coiling rate is much higher in *N. nesenensis* (WER = 2.35) than in *N. ultimus* (WER = 2.00).

Neoaganides ultimus differs from all other species of the genus in the very shallow adventive lobe. Usually the adventive lobe is as deep as the external lobe, but in *N. ultimus* it reaches less than half of the depth.

Stratigraphical range. *Paratirolites* Limestone; 1.15 to 0.65 m below the extinction horizon (upper part of the *Abichites abichi* Zone and lower part of the *Abichites stoyanowi* Zone).

Suborder **Goniatitina** Hyatt, 1884
Superfamily **Neoicoceratoidea** Hyatt, 1900
Family **Paragastrioceratidae** Ruzhencev, 1951
Subfamily **Pseudogastrioceratinae** Furnish, 1966

Included genera. *Altudoceras* Ruzhencev, 1940; *Chekiangoceras* Ruzhencev, 1974; *Daubichites* Popov, 1963; *Metagastrioceras* Zhao, Liang & Zheng, 1978; *Pseudogastrioceras* Spath, 1930; *Retiogastrioceras* Zhao, Liang & Zheng, 1978; *Roadoceras* Zhou, 1985; *Sabaliceras* Yang & Yang, 1992; *Stenolobulites* Mikesh, Glenister & Furnish, 1988; *Strigogoniatites* Spath, 1934.

Genus ***Pseudogastrioceras*** Spath, 1930

Type species. *Goniatites Abichianus* von Möller, 1879, by original designation.

Included species. *Goniatites abichianus* von Möller, 1879, p. 230 (Azerbaijan); *Pseudogastrioceras gigantum* Zhao, Liang & Zheng, 1978, p. 74 (Jiangxi); *Pseudogastrioceras guangxiense* Zhao, Liang & Zheng, 1978, p. 73 (Guangxi); *Pseudogastrioceras guizhouense* Zhao, Liang & Zheng, 1978, p. 74 (Guizhou); *Pseudogastrioceras jiangxiense* Zhao, Liang & Zheng, 1978, p. 74 (Jiangxi); *Pseudogastrioceras relicuum* sp. nov. (North-west Iran); *Pseudogastrioceras szechuanense* Chao, 1965, p. 1821 (Sichuan).

Pseudogastrioceras relicuum sp. nov.
(Fig. 12)

Derivation of name. From Latin *relicuum* = the remaining, because the species is the last one of the group.

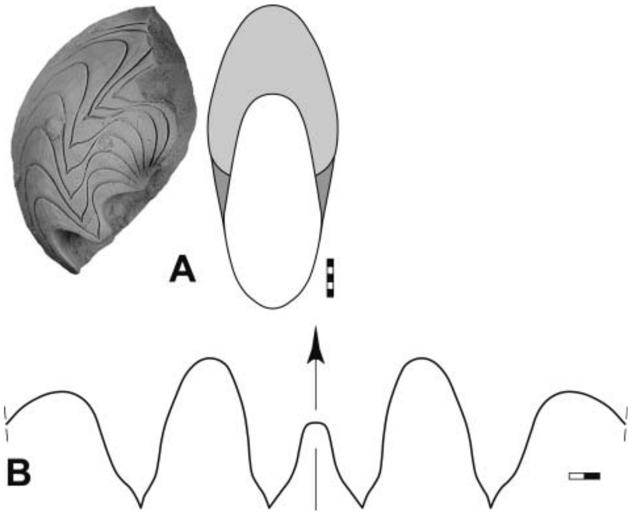

Figure 12. *Pseudogastrioceras relicuum* sp. nov., holotype, MB.C.25173, Ali Bashi N, float. **A,** lateral and dorsal views; **B,** suture line at 20.3 mm ww, 16.9 mm wh. Scale bars: A = 5 mm; B = 2 mm.

Holotype. MB.C.25173 (Fig. 12).

Type locality and horizon. Ali Bashi N section; *Paratirolites* Limestone, float.

Material. Only the holotype; a second specimen is still in situ at the base of the *Paratirolites* Limestone in the Aras Valley section.

Diagnosis. *Pseudogastrioceras* with moderately large conch; diameter attaining 70 mm. Conch shape thinly discoidal (ww/dm = 0.40–0.45), involute (uw/dm = 0.05) with converging flanks and broadly rounded venter. Ornament with about 15 faint spiral lines on the venter.

Description. Only one incomplete specimen (Fig. 12) is available for study, and hence a detailed description of the species is impossible. The overall conch geometry, the ornament and the suture line are typical for *Pseudogastrioceras*. The holotype is a fragment of a phragmocone, which was approximately 40 mm in diameter; it is thinly discoidal with a very narrow umbilicus (ww/dm = 0.42; uw/dm = 0.05–0.10). The last three septa of the specimen show conspicuous crowding, so it can be assumed that it is an adult individual. The ww/wh ratio of the specimen is 0.80. The flanks converge strongly towards the rounded venter. No parts of the shell are preserved; the internal mould is smooth except for about 15 faint spiral lines on the venter. The suture line, drawn at a phragmocone whorl height of 20 mm (Fig. 12B), is typical for *Pseudogastrioceras* with a wide external lobe and an unsubdivided median saddle reaching half of the external lobe depth. The V-shaped adventive lobe is slightly asymmetric with a slightly curved dorsal flank.

Remarks. *Pseudogastrioceras abichianum* is a very common component in the lower part of the Wuchiapingian Julfa Formation of the sections in the vicinity of the Aras Valley (Ruzhencev & Shevyrev 1965). This species can reach a large diameter with phragmocone dimensions of 80 mm in diameter, which is twice the value of the Changhsingian specimen described here. In contrast to *P. relicuum* with about 15 spiral lines restricted to the venter, *P. abichianum* has, at a similar conch diameter, about 30 much stronger spiral lines, which extend across the venter and the outer flanks. The umbilicus is possibly a little wider in *P. abichianum*.

The new species mainly differs from the South Chinese species described by Zhao *et al*. (1978) in the shape of the external lobe, in which the prongs are asymmetrical with a concave dorsal flank.

Stratigraphical range. *Paratirolites* Limestone; most probably only in the lower part (*Dzhulfites zalensis* Zone). The position is assumed, as at the type locality fossils older than the *Paratirolites* Limestone have not been found. A second specimen, which has not been extracted from the outcrop, has a position approximately 4 m below the extinction horizon at the type locality.

Order **Ceratitida** Hyatt, 1884
Suborder **Paraceltitina** Shevyrev, 1968
Superfamily **Xenodiscoidea** Frech, 1902
Family **Dzhulfitidae** Shevyrev, 1965

Included genera. *Dzhulfites* Shevyrev, 1965; *Paratirolites* Stoyanow, 1910; *Julfotirolites* gen. nov.; *Alibashites* gen. nov.; *Abichites* Shevyrev, 1965; *Stoyanowites* Korn, 2014.

Diagnosis. Representatives of the superfamily Xenodiscoidea with small to large conch, in which the ontogeny displays up to four stages, beginning with a unsculptured initial stage followed by a juvenile stage with transverse ribs, a subadult stage with coarse ribs often ending in pronounced ventrolateral nodes or spines and an adult stage with weakening of the sculpture. Suture line usually with serrated external, adventive, lateral and umbilical lobes; some species with simple prongs of the external lobe.

Description. Nearly all of the species in the family have some conch, ornament and suture line characters in common. Two of these characters are the coiling rate (the WER ranges between 2.00 and 2.40) and the umbilical width (the uw/dm ratio ranges between 0.35 and 0.45). Most of the species included in the family Dzhulfitidae share a distinct ontogeny, in which four growth stages can be separated:

1. The initial stage (up to about 5 mm dm) is widely evolute with oval or circular whorl cross section; it does not possess ribs or spines.
2. The juvenile stage (between 5 and 15 mm dm) has an oval or circular whorl cross section; it is weakly ornamented with faint ribs on the midflank.
3. The subadult stage usually ends with a conspicuous change in the conch ornament; the diameter of this change differs between the various species within the family. The subadult stage is the most diagnostic for many of the species; it best displays differences in the general shape of the whorl cross section (circular, oval, quadrate, rectangular, pear-shaped or trapezoidal), the shape of the venter (rounded, flattened, tectiform or concave), the sculpture (in many cases with coarse ribs, which often form distinctive ventrolateral nodes or spines) and the suture line (which varies in the depth of the external lobe, the degree of serration of the external, adventive and lateral lobe and the width and shape of the saddles). In most of the specimens, the position of the end of the subadult stage is indicated by the conspicuous crowding of the last septa produced during ontogeny.
4. The adult stage represents the terminal body chamber. The species of the family Dzhulfitidae often differ in the shape of the conch cross section and sculpture of the body chamber. In most of the species, the beginning of the terminal body chamber coincides with a more or less sudden change in the ornamentation, such as weakening of the ribs or nodes. Rather often, the adult stage is similar in various species despite significant differences in the subadult stage.

The suture line is a somewhat variable character among the representatives of the family Dzhulfitidae and can be used for taxonomic purposes with some limitations. The principal sutural formula is (E1 Em E1) A L U I, of which E1, A, L and U often display ceratitic serration (i.e. with small notches at the base of the lobes). The study of a rich material from Julfa demonstrates:

1. The genera and species within the family can sometimes be separated by means of suture line characters, particularly depth of the external lobe and the number of notches.
2. Intraspecific variation in size, shape and the degree of serration of the individual lobes occurs in some of the species; specimens from one stratigraphical position and with closely resembling conch and ornament features may possess rather different suture lines.
3. A general simplification trend of the suture lines occurs within the *Paratirolites* Limestone; the suture lines of the paratirolitid ammonoids show the strongest serration near the base of the rock unit, where in some of the specimens the notching of the lobes begins to extend to the lower flanks of the saddles. Towards the top of the *Paratirolites* Limestone, a nearly continuous decrease in the number of secondary notches is observable.

4. The prongs of the external lobe are often unserrated in the specimens from the base and top of the *Paratirolites* Limestone, while specimens from the middle part show more or less strong secondary subdivision of the E lobe.
5. Many specimens show asymmetrical suture lines, particularly visible in the different numbers of notches of sutural elements on both sides of the conch. In some specimens, the prongs of the external lobe are bifid on one side and unserrated on the other.
6. In most of the species, the external lobe has the same depth as the adventive lobe; it is only rarely shorter, as in the genus *Stoyanowites*, and only in this respect resembles the majority of the Changhsingian ammonoids described from South China.

Remarks. Shevyrev (1965) introduced the family Dzhulfitidae particularly for species already described by Stoyanow (1910) from the *Paratirolites* Limestone. But, unfortunately, he chose the rather poorly known *Dzhulfites* as the name-giving genus, which itself was based on *Dzhulfites spinosus* Shevyrev, 1965, then known by 10 moderately preserved specimens. Shevyrev's (1965) choice is even more incomprehensible as he could have defined the family Paratirolitidae based on better and more specific material**.**

Dzhulfites is the name-giving genus but occupies a rather marginal position in the morphological spectrum of the family. Two of the most characteristic features for the paratirolitid ammonoids – the deep external lobe and the often-strong secondary serration of lobes – are absent in this genus. Another problem with this genus is that the two species *D. spinosus* and *D. nodosus* have been described from incomplete specimens. *Dzhulfites spinosus* displays a conch morphology with a trapezoidal whorl cross section and ornament with conical ventral ateral nodes that would speak for its incorporation in *Paratirolites*, but the suture line is characterized by a short external lobe, which in contrast to *Paratirolites* does not reach the depth of the adventive lobe. As *D. spinosus* is the type species of the genus *Dzhulfites*, it needs to be clearly separated from the stratigraphically older species of *Paratirolites*.

Shevyrev's family contained the three genera *Dzhulfites* Shevyrev, 1965, *Paratirolites* Stoyanow, 1910 and *Abichites* Shevyrev, 1965. According to Shevyrev (1965), only the latter two occur in the *Paratirolites* Limestone, while *Dzhulfites* should be restricted to an older ammonoid zone, separated by the '*Bernhardites* Zone' (now *Shevyrevites* Zone) from the beds with *Paratirolites*.

In total, Shevyrev (1965) separated 10 species within the three genera of the family, most founded on rather well-preserved material and supported by good illustrations of the suture lines. However, he did not discuss possible intraspecific variability within the material, and he figured only one or two specimens of each species.

The lack of such a discussion led Teichert & Kummel to lump together many of the species earlier described by Stoyanow (1910) and Shevyrev (1965, 1968). Teichert & Kummel (in Teichert *et al*. 1973) argued for the extensive variability of the discussed species and regarded only one genus (*Paratirolites*) with three species (one species of each of Shevyrev's genera) as justified. One has to bear in mind, however, that Teichert & Kummel had only about 60 specimens under study, most of them being fragments collected from float below the outcrops of the *Paratirolites* Limestone. Unlike Shevyrev (1965), these authors did not provide a sufficient reasoning for their approach to the taxonomy and classification of the paratirolitid ammonoids. Instead, they expressed a very vague reasoning for why they used a strikingly restricted concept, which is mainly based on the interpretation of the *Paratirolites* Limestone as a uniform rock unit (Teichert *et al*. 1973, p. 413):

"Because of fragmentary preservation, our collection is not suited for a detailed analysis of this variation. However, because the specimens are all from a single unit (approximately 3 m thick) within a very limited geographical range, we believe it more prudent to assume they are a single species; otherwise the only limit on the number of species recognized would be the number of specimens available."

Although Shevyrev (1965, 1968) probably had better arguments (particularly because he studied the better material) for his species concept for the paratirolitids, other authors tended to follow Teichert *et al*. (1973). Bando (1979) and Taraz *et al*. (1981), for instance, when discussing the Late Permian and Early Triassic ammonoids from the Hambast Mountains, 55 km ESE of Abadeh (Central Iran), almost fully adopted the restrictive scheme proposed by Teichert *et al*. (1973). Moreover, in these two publications, they suggested rather long stratigraphical occurrences for each of the three separated species, which should occur between "one to ten meters below the base of the Lower Triassic *Claraia* beds" (Bando 1979, p. 135). Interestingly, Bando (1979, p. 134), who had 135 specimens of *Paratirolites* (in the wider sense) from the Hambast Mountains, also did not provide a scientific reason for following Teichert *et al*. (1973): "The present writer also believes the *Dzhulfites* and *Abichites* are synonymy of *Paratirolites* [sic]".

In her compilation of the Permian ammonoid genera and species, Leonova (2002) followed the view of Shevyrev and accepted all of his genera and species. Our investigation of the rich material from the north-western Iranian localities (more than 300 specimens, about 250 of which have been collected in situ) largely supports the species concept for the paratirolitids as proposed by Shevyrev (1965, 1968) and suggests that the species richness for paratirolitids is higher. Our material shows that the morphological characters (conch shape, suture line and sculpture) show a stratigraphical succession.

Genus ***Dzhulfites*** Shevyrev, 1965

Type species. *Dzhulfites spinosus* Shevyrev, 1965, by original designation.

Included species. *Dzhulfites hebes* sp. nov. (North-west Iran); *Dzhulfites nodosus* Shevyrev, 1965 (Azerbaijan); *Dzhulfites spinosus* Shevyrev, 1965 (Azerbaijan); *Dzhulfites zalensis* sp. nov. (North-west Iran).

Diagnosis. Representatives of the family Dzhulfitidae with moderately large to large conch; maximum adult diameters are between 80 and 120 mm. Subadult stage with trapezoidal whorl cross section, adult stage variable. Subadult stage with small to large conical ventrolateral nodes, adult stage with weakening sculpture. Suture line with external lobe that does not reach the depth of the adventive lobe; prongs of the external lobe simple or bifid.

Remarks. Shevyrev (1965) distinguished *Dzhulfites* and *Paratirolites* by using the shape of the external lobe, which was thought to be short with unserrated prongs in *Dzhulfites* but deep and serrated in *Paratirolites*. The two genera were reported to be separated stratigraphically by a complete ammonoid zone in which they were lacking; *Dzhulfites* was recorded well below the *Paratirolites* Limestone. Our investigations revealed that *Dzhulfites* may possess weakly subdivided prongs of the external lobe (Fig. 13A), and representatives of *Paratirolites* with an unserrated external lobe also occur in the *Paratirolites* Limestone, particularly at its base. However, the depth of the external lobe is a diagnostic character separating the two genera.

It might be argued that the secondary subdivision of the external lobe is rather plastic and thus not a clear distinguishing criterion for the two genera, a view seemingly corroborated by the occasional finding of paratirolitids with an asymmetrical external lobe (see below, *Abichites subtrapezoidalis* from the upper part of the *Paratirolites* Limestone). However, our material from the base of the *Paratirolites* Limestone demonstrates that conch shapes and ornament are always correlated with distinct suture lines and that all species of *Paratirolites* have a deep external lobe. The depth of the external lobe is thus a stable character, and hence *Dzhulfites* is regarded as separable from *Paratirolites*.

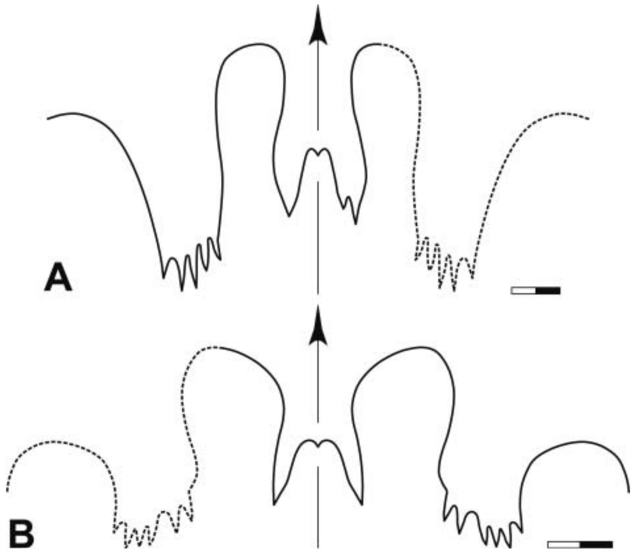

Figure 13. *Dzhulfites spinosus* Shevyrev, 1965, suture lines. **A,** MB.C.25174, Aras Valley, float; at 25.5 mm ww, 15.2 mm wh; **B,** MB.C.25175, Aras Valley, float; at 17.5 mm ww, 10.0 mm wh. Scale bars = 2 mm.

In contrast to the statements given by Ruzhencev & Shevyrev (1965) and Shevyrev (1965, 1968), but according to our collections, it is clear that *Dzhulfites* still occurs in the *Paratirolites* Limestone. However, the genus is restricted to the lowest part of the rock unit and almost reaches the lowest occurrence of the genus *Paratirolites*.

Dzhulfiites zalensis sp. nov.
(Fig. 14)

Derivation of name. Named after the type locality.

Holotype. MB.C.25176, Weyer collection 2002 (Fig. 14A).

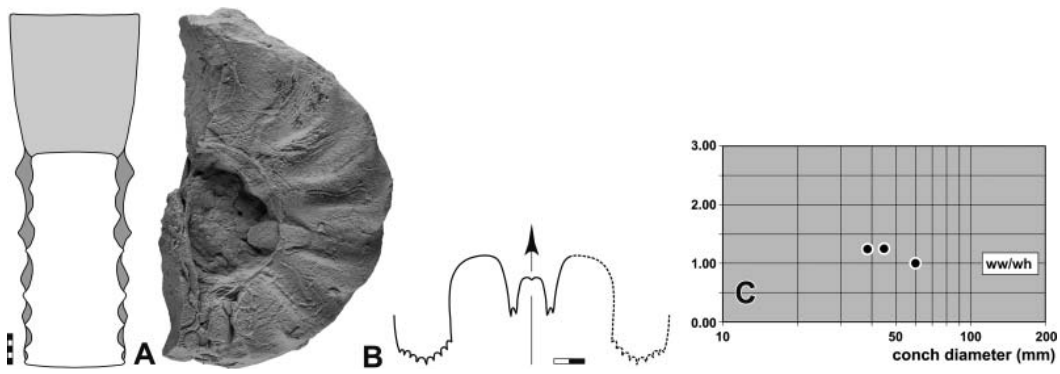

Figure 14. *Dzhulfites zalensis* sp. nov., holotype, MB.C.25176, Zal, −5.30 m. **A,** lateral and dorsal views; **B,** suture line at 18.7 mm ww, 16.3 mm wh; **C,** whorl cross section proportions Scale bars: A = 5 mm; B = 2mm.

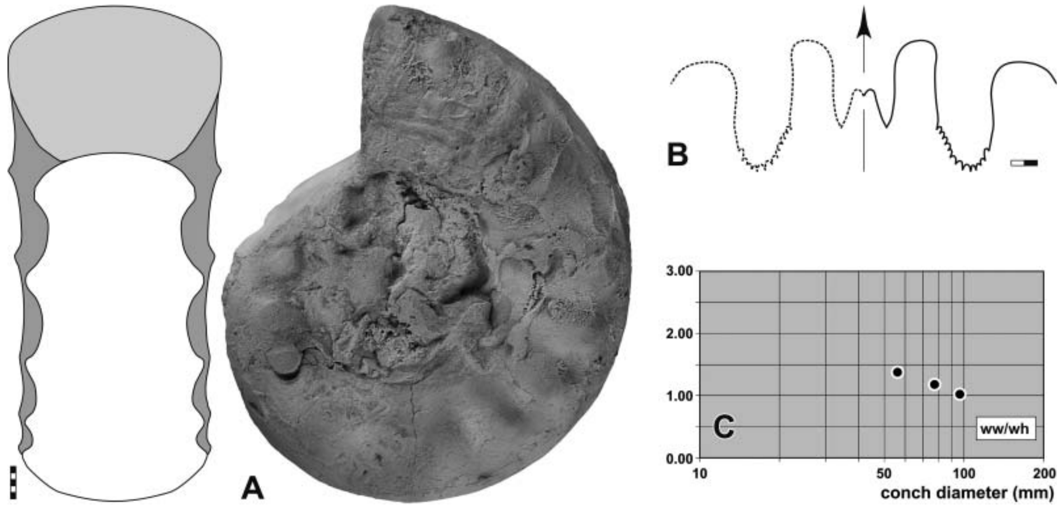

Figure 15. *Dzhulfites hebes* sp. nov. **A,** lateral and dorsal views, holotype, MB.C.25181, Ali Bashi N, −4.40 m; **B,** suture line, paratype, MB.C.25182, Ali Bashi N, −4.40 m; at approximately 23 mm wh. **C,** whorl cross section proportions. Scale bars: A = 5 mm; B = 2 mm.

Type locality and horizon. Zal section; 5.30 m below the top of the *Paratirolites* Limestone (*Dzhulfites zalensis* Zone).

Material. Eighteen specimens (Aras Valley, Zal).

Diagnosis. *Dzhulfites* with a conch reaching 70 mm dm. Subadult stage with trapezoidal, weakly depressed whorl cross section (ww/wh = 1.25) and broadly arched venter; 15 coarse ribs ending in hook-shaped ventrolateral nodes per volution. Adult stage with trapezoidal and weakly depressed whorl cross section (ww/wh = 1.05), flat venter and angular ventrolateral shoulder; without change of sculpture. Prongs of the external lobe bifid; altogether about 18 notches of the E, A and L lobes.

Description. Holotype is a partly corroded, incomplete specimen with 58 mm conch diameter (Fig. 14A). Half of the last volution belongs to the body chamber; of the phragmocone, the last three chambers are visible showing a closer spacing of the last two. The whorl profile is trapezoidal and weakly depressed (ww/wh = 1.05) with a flat venter separated from the flanks by an angular ventrolateral shoulder. The body chamber shows a sculpture with seven coarse ribs per half volution. These ribs extend with a slightly concave course across the flank and turn forward and end in a hook-shaped node at the ventrolateral shoulder. The venter is smooth.

Only small parts of the suture line can be seen in the holotype (Fig. 14B). They show the small external lobe with bifid prongs and the much deeper, U-shaped adventive lobe with numerous small denticles.

Remarks. *Dzhulfites zalensis* differs from the other species of the genus in the narrower umbilicus, the completely flat venter in the adult stage and the angular ventrolateral shoulder. The ribs ending in hook-shape ventrolateral nodes are another criterion and make a separation from species of the genus *Paratirolites* easy.

Stratigraphical range. *Paratirolites* Limestone; 5.30 to 4.65 m below the extinction horizon (*Dzhulfites zalensis* Zone).

Dzhulfiites hebes sp. nov.
(Fig. 15)

Derivation of name. After Latin *hebes* = blunt, referring to the shape of the conical nodes.

Holotype. MB.C.25181 (Fig. 15A).

Type locality and horizon. Ali Bashi N section; 4.40 m below the top of the *Paratirolites* Limestone (*Dzhulfites zalensis* Zone).

Material. Two specimens from Ali Bashi N.

Diagnosis. *Dzhulfites* with a conch reaching 100 mm dm. Subadult stage with oval, weakly depressed whorl cross section (ww/wh = 1.35) and broadly rounded venter; 10 coarse conical lateral nodes per volution. Adult stage with trapezoidal and weakly depressed whorl cross section (ww/wh = 1.05), broadly rounded venter and rounded ventrolateral shoulder; about 15 coarse ventrolateral nodes. Prongs of the external lobe simple; altogether about 24 notches of the E, A and L lobes.

Description. Holotype MB.C.25181 is a specimen with conch diameter of 77 mm (Fig. 15A). The conch is discoidal at the end of the phragmocone (56 mm dm) and possesses an oval weakly depressed whorl cross section (ww/wh = 1.35) with broadly rounded venter. The sculpture consists of coarse, rounded nodes with a position on the midflank. There is no significant change in ornamentation on the body chamber, which also shows coarse nodes but with a position in a more ventrolateral direction. The body chamber shows a transformation of the whorl profile towards a trapezoidal shape with rounded venter.

Paratype MB.C.25182 (Ali Bashi N, −4.40 m) allows the study of the ventral portion of the suture line (Fig. 15B). It shows the short external lobe (about two-thirds of the adventive lobe depth) with simple V-shaped prongs. The adventive lobe is very narrow and almost parallel sided with numerous small denticles.

Remarks. *Dzhulfites hebes* differs from the other species of *Dzhulfites* in the shape of the venter, which is broadly rounded in the new species, but more or less flattened in the others. *Paratirolites kittli* is a species with similar conch morphology, but has the deep external lobe, which is much shorter in *Dzhulfites hebes*.

Stratigraphical range. *Paratirolites* Limestone; 4.40 m below the extinction horizon (upper part of the *Dzhulfites zalensis* Zone).

Genus ***Paratirolites*** Stoyanow, 1910

Type species. *Paratirolites kittli* Stoyanow, 1910, by original designation.

Included species. *Paratirolites birunii* sp. nov. (North-west Iran); *Paratirolites coronatus* sp. nov. (North-west Iran); *Paratirolites kittli* Stoyanow, 1910 (Azerbaijan); *Paratirolites multiconus* sp. nov. (North-west Iran); *Paratirolites quadratus* sp. nov. (North-west Iran; *Paratirolites serus* sp. nov. (North-west Iran); *Paratirolites trapezoidalis* Shevyrev, 1965 (Azerbaijan); *Paratirolites vediensis* Shevyrev, 1965 (Armenia); *Stephanites* (?) *waageni* Stoyanow, 1910 (Azerbaijan) (synonym of *Paratirolites kittli* Stoyanow, 1910); *Paratirolites compressus* Ehiro, 1996 (Japan); *Xenodiscus douvillei* Diener, 1914 (Madagascar).

Diagnosis. Representatives of the family Dzhulfitidae with moderately large to very large conch; maximum adult diameters are between 60 and 250 mm. Adult stage with trapezoidal whorl cross section. Subadult stage with large conical ventrolateral nodes; adult stage with significantly weakening sculpture. Suture line with deep external lobe; the depths of external lobe and adventive lobe are nearly identical.

Remarks. The continuous nature of conch, suture and ornament characters within the family Dzhulfitidae make an unequivocal definition of the genus *Paratirolites* rather difficult. The distribution of characters within the species of the family Dzhulfitidae let us assume that *Paratirolites* is paraphyletic, from which the genera *Alibashites*, *Stoyanowites* and *Abichites* derived. Therefore, the genus *Paratirolites* will here be defined by the use of some key characters but also by the absence of other features.

The main characters of the genus *Paratirolites* are the following:

1. The subadult stage is characterized by the presence of a trapezoidal, weakly to moderately depressed whorl cross section (ww/wh = 1.10−1.80) with pronounced ventrolateral shoulder and more or less flattened venter.
2. The adult stage has a trapezoidal whorl cross section.
3. The subadult stage possesses a sculpture with 10 to 20 pronounced conical ventrolateral nodes per volution.
4. The sculpture becomes strikingly weaker on the adult body chamber; the nodes become much less dominant or even disappear on the mature body chamber.
5. The suture line possesses a deep external lobe; the external lobe is as deep as the adventive lobe or even deeper.

Shevyrev (1965, 1968) separated *Paratirolites* from *Dzhulfites* on the basis of the suture lines. *Dzhulfites* was thought to possess a shallow external lobe with unsubdivided prongs, while *Paratirolites* should have an external lobe with serrated prongs. The strictly in-situ collected new material demonstrates that such a separation is problematic for several reasons:

1. Some specimens within the family Dzhulfitidae show asymmetrical suture lines; it is not uncommon that one prong is simple and the other one bifid.
2. Morphologically very similar specimens may differ rather widely; unsubdivided and serrated prongs of the external lobe may occur in the same horizons.
3. The complexity of the suture lines within the family Dzhulfitidae displays a distinct temporal pattern; stratigraphically older and also younger species tend to possess simple external lobes, while species in the middle portion of the *Paratirolites* Limestone show a stronger serration.

In summary, *Paratirolites* differs from the other genera of the family Dzhulfitidae as follows:

1. *Dzhulfites* possesses a shorter external lobe, which does not reach the depth of the adventive lobe. This is in contrast to *Paratirolites*, which shows an external lobe as deep as the adventive lobe or even deeper. This appears to be the only criterion to separate the two genera.
2. *Stoyanowites* also shows a shallow external lobe (like *Dzhulfites*) and has a much weaker sculpture without conical ventrolateral nodes in the subadult stage.

3. *Alibashites* has an intermediate morphological position between *Paratirolites* and *Abichites*. It possesses the subadult sculpture with conical ventrolateral nodes of *Paratirolites*, but lacks the trapezoidal whorl profile of that genus. The species of *Alibashites* still possess conical nodes in the subadult stage, but species of the genus show a subtrapezoidal or quadrate whorl cross section in the adult stage.
4. *Abichites* occurs in the upper portion of the *Paratirolites* Limestone and can be interpreted as descendent from *Paratirolites*, morphologically and stratigraphically. *Abichites* has a subadult and adult conch morphology with a rectangular or oval whorl profile and does not show the strong ventrolateral nodes developed in *Paratirolites* and *Alibashites*.
5. *Paratirolites compressus* Ehiro, 1966 from the Kitakami Massif of Japan is based on poorly preserved material, which cannot be attributed to *Paratirolites* with certainty.
6. *Xenodiscus Douvillei* Diener, 1914 from Madagascar is also described from insufficiently preserved material. The species was intensely discussed by Tozer (1969), who concluded that it is a Permian species belonging to *Paratirolites*. However, the shape of the conch with the angular coiling of the comparatively rather narrow umbilicus and the sculpture composed of a few conical nodes makes a placement in the Early Triassic genus *Tirolites* more likely.

Paratirolites trapezoidalis Shevyrev, 1965
(Fig. 16)

1965 *Paratirolites trapezoidalis* Shevyrev: 177, pl. 24, fig. 1.
1968 *Paratirolites trapezoidalis* Shevyrev; Shevyrev: 92, pl. 4, fig. 1.
2014b *Paratirolites trapezoidalis* Shevyrev; Korn in Ghaderi *et al.*: text-fig. 7E.

Holotype. PIN 1252/129; illustrated by Shevyrev (1965, pl. 24, fig. 1).

Type locality and horizon. Dorasham 2 (Azerbaijan); *Paratirolites* Limestone.

Material. Twelve specimens (Aras Valley, Ali Bashi N, Ali Bashi 4).

Diagnosis. *Paratirolites* with a conch reaching 120 mm dm. Subadult stage with trapezoidal, depressed whorl cross section (ww/wh = 1.50) and flattened, slightly tectiform venter; 10−12 coarse ribs, which end in coarse conical ventrolateral nodes, per volution. Adult stage with strongly trapezoidal and weakly depressed whorl cross section (ww/wh = 1.40), flattened venter and angular ventrolateral shoulder; weak straight riblets and numerous small ventrolateral nodes. Prongs of the external lobe usually unsubdivided; altogether 12−16 notches of the E, A and L lobes.

Description. Specimen MB.C.25183 (Ali Bashi 4, −3.20 m) is a fragmentary, slightly deformed specimen of 84 mm conch diameter; three-quarters of a volution of the body chamber as well as small parts of the phragmocone are preserved (Fig. 16A). The conch is thinly discoidal and subevolute in the last volution (ww/dm = 0.45; uw/dm = 0.35) and shows a ventrally weakly depressed trapezoidal whorl cross section (ww/wh = 1.40) with an angular ventrolateral shoulder. This separates the flanks from the flattened venter, which possesses a very shallow keel. The phragmocone shows a trapezoidal whorl cross section and prominent conical ventrolateral nodes (about six per half volution). These nodes become rapidly much weaker on the adult body chamber; here they originate from rounded and shallow, straight riblets. These riblets are strongest on the outer flanks; on the venter they are barely visible and extend with a broad semicircular projection. About 10 of these ribs and nodes can be counted on half a volution.

The suture line of specimen MB.C.25183, drawn at a whorl height of 16 mm (corresponding to a phragmocone diameter of about 45 mm), shows a parallel-sided external lobe with narrow V-shaped asymmetric prongs (Fig. 16E). The wide venter accommodates the nearly symmetric, parallel-sided ventrolateral saddle and the slightly asymmetrical, strongly serrated adventive lobe, in which the lobe base has a semicircular outline. In the serrated lateral lobe, which has a position on the midflank, the base is almost horizontal. It possesses four small notches and has diverging flanks.

Specimen MB.C.25184 (Ali Bashi N, −3.45 m) is an immature individual with 54 mm conch diameter, of which the last half volution belongs to the body chamber (Fig. 16B). The conch is thinly discoidal and subevolute in the last volution (ww/dm = 0.45; uw/dm = 0.43) and possesses a weakly depressed trapezoidal whorl cross section (ww/wh = 1.40) with flattened diverging flanks, a subangular ventrolateral shoulder and a broadly rounded venter. The last volution possesses 11 strong ventrolateral nodes, which positions do not correspond on both sides of the conch.

The suture line of specimen MB.C.25184 (drawn at 10.5 mm whorl height; about 33 mm phragmocone diameter) has a parallel-sided external lobe with nearly symmetrical prongs that possess two small notches (Fig. 16F). The ventrolateral saddle is tongue-shaped and nearly symmetrical. The asymmetrical adventive lobe is almost as deep as the external lobe; it is much deeper on the dorsal side and possesses about seven little notches.

Remarks. *Paratirolites trapezoidalis* differs from *P. birunii* in the much wider whorl cross section in the adult stage at 80 mm dm (ww/wh = 1.40 in *P. trapezoidalis* but

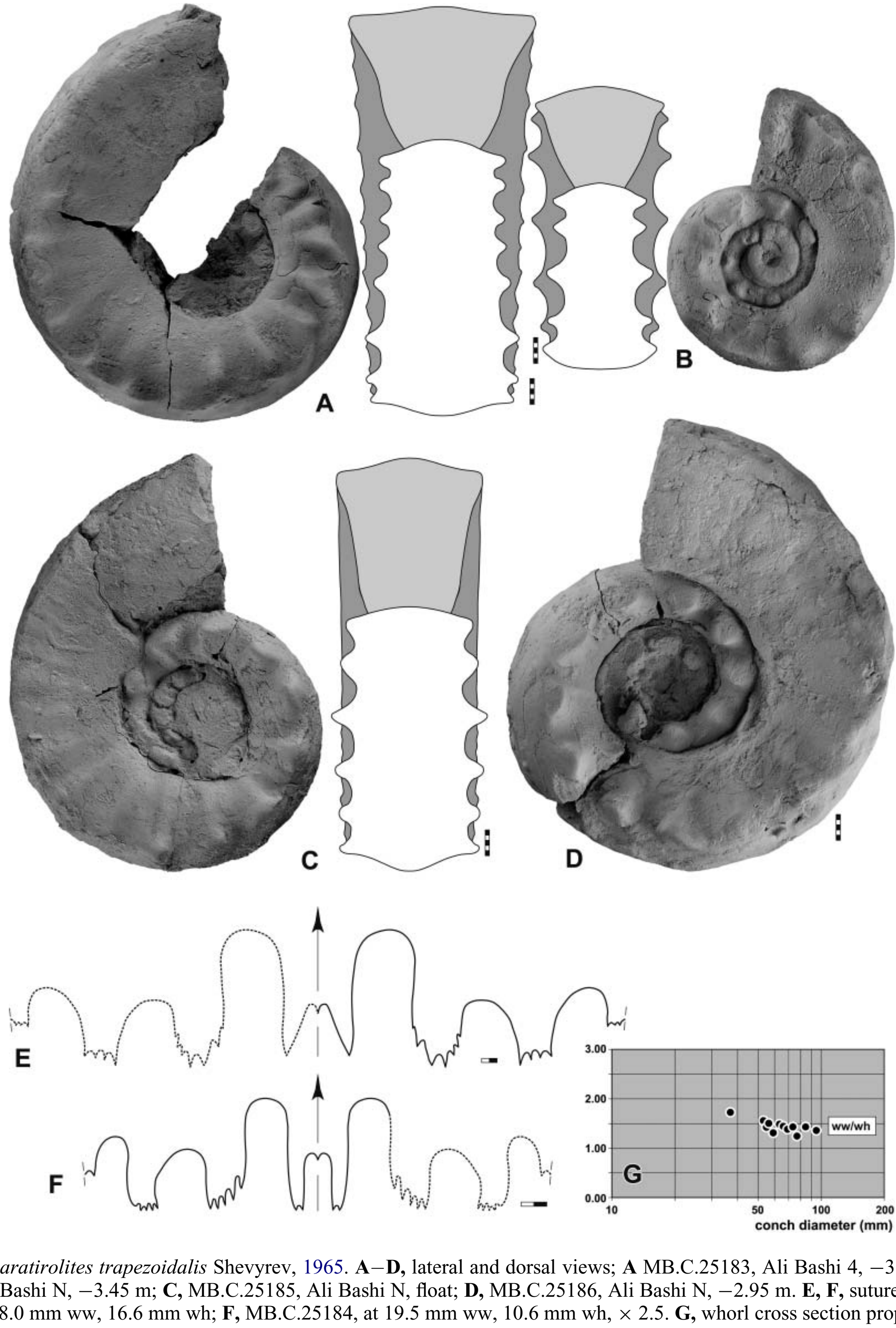

Figure 16. *Paratirolites trapezoidalis* Shevyrev, 1965. **A−D,** lateral and dorsal views; **A** MB.C.25183, Ali Bashi 4, −3.20 m; **B,** MB.C.25184, Ali Bashi N, −3.45 m; **C,** MB.C.25185, Ali Bashi N, float; **D,** MB.C.25186, Ali Bashi N, −2.95 m. **E, F,** suture lines; **E,** MB.C.25183, at 38.0 mm ww, 16.6 mm wh; **F,** MB.C.25184, at 19.5 mm ww, 10.6 mm wh, × 2.5. **G,** whorl cross section proportions. Scale bars: A−D = 5 mm; E, F = 2 mm.

only 0.80 in *P. birunii*). *Paratirolites vediensis* has a similar conch shape, but differs from *P. trapezoidalis* in the stronger ventrolateral nodes in the adult stage. *Paratirolites coronatus* has an even wider whorl cross section (ww/wh = 1.60−1.80 in *P. coronatus* but only 1.40 in *P. trapezoidalis*); the species has also less coarse but more numerous ventrolateral nodes in the subadult stage (15 in *P. coronatus* but only 10 in *P. trapezoidalis*).

A superficially similar species is the stratigraphically older *Dzhulfites spinosus*, which has the same conch shape and sculpture in the subadult growth stage. The two species, however, are easily separable by the depth of the external lobe; in *P. trapezoidalis* it is as deep as the adventive lobe but in *D. spinosus* much shallower.

Stratigraphical range. *Paratirolites* Limestone; 4.10 to 3.05 m below the extinction horizon (*Paratirolites trapezoidalis* Zone and lower part of the *Paratirolites kittli* Zone).

Paratirolites coronatus sp. nov.
(Figs 17, 18)

Derivation of name. From Latin *corona* = crown, because of the shape of the whorl profile.

Holotype. MB.C.25195 (Fig. 17A).

Type locality and horizon. Aras Valley section; 2.90 m below the top of the *Paratirolites* Limestone (*Paratirolites kittli* Zone).

Material. Five specimens (Aras Valley, Ali Bashi N).

Diagnosis. *Paratirolites* with a conch reaching 125 mm dm. Subadult stage with trapezoidal, moderately depressed whorl cross section (ww/wh = 1.60−1.80) and flattened tectiform venter; 15 coarse conical ventrolateral nodes per volution. Adult stage with extremely trapezoidal and moderately depressed whorl cross section (ww/wh = 1.60−1.90), flattened tectiform venter and subangular ventrolateral shoulder; weak ventrolateral nodes. Prongs of the external lobe trifid or multiply serrated; altogether 11−24 notches of the E, A and L lobes.

Description. Holotype MB.C.25195 is a rather well-preserved specimen with 77 mm conch diameter (Fig. 17A). It shows the partly weathered body chamber (last half volution) and about half of a volution of the phragmocone. The conch is pachyconic and subevolute in the last volution (ww/dm = 0.69; uw/dm = 0.41), and possesses a ventrally moderately depressed trapezoidal whorl cross section (ww/wh = 1.72). During the last half volution, a significant widening of the whorl can be recorded; at 56 mm dm the ww/dm ratio is only 0.56 (ww/wh = 1.72). The specimen shows flat, strongly diverging flanks, which are separated from the slightly curved venter by an angular ventrolateral shoulder. The sculpture changes significantly on the last preserved volution; the first 300° show shallow ribs on the flank, which end in conical ventrolateral nodes, but the last 60° display a sudden weakening of the ribs. The ventrolateral nodes are very small in this growth stage.

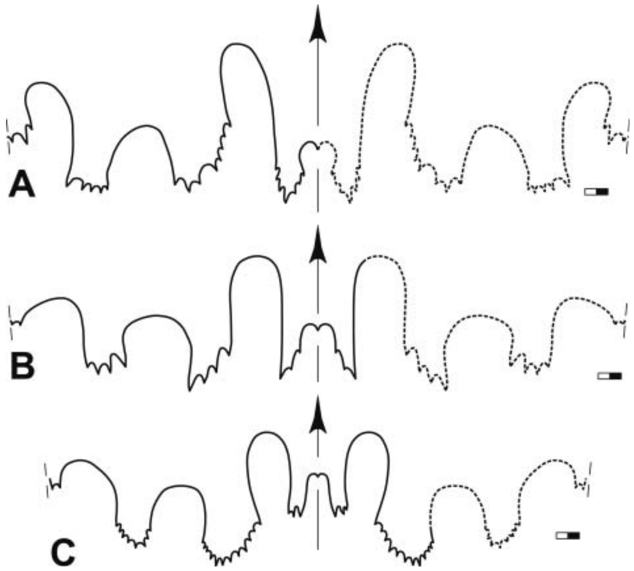

Figure 18. *Paratirolites coronatus* sp. nov., suture lines. **A,** MB.C.25196, Aras Valley, float; at 18.0 mm wh; **B,** holotype, MB.C.25195, Aras Valley, −2.90 m; at 31.5 mm ww, 17.3 mm wh; **C,** MB.C.25197, Aras Valley, −3.55 m; at 15.8 mm wh. Scale bars = 2 mm.

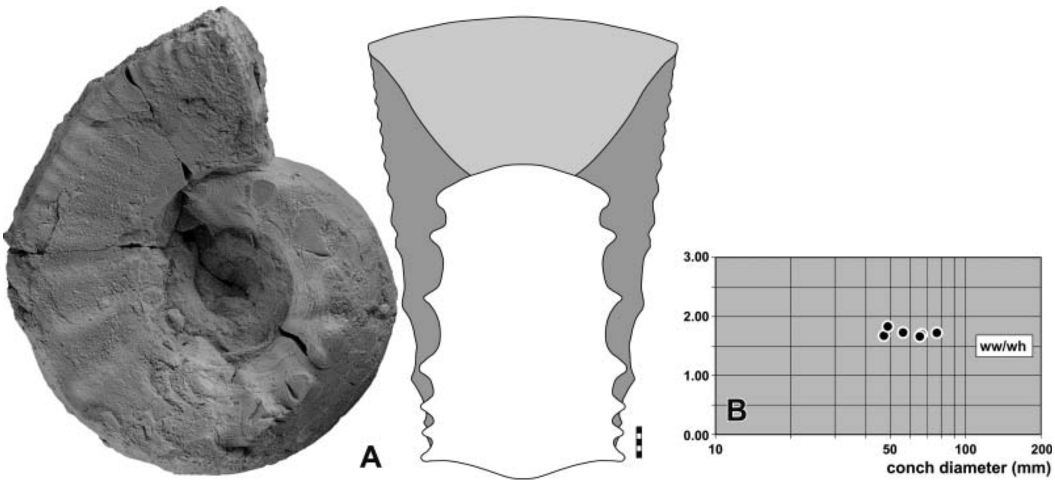

Figure 17. *Paratirolites coronatus* sp. nov. **A,** lateral and dorsal views, holotype, MB.C.25195, Aras Valley, −2.90 m; **B,** whorl cross section proportions. Scale bar = 5 mm.

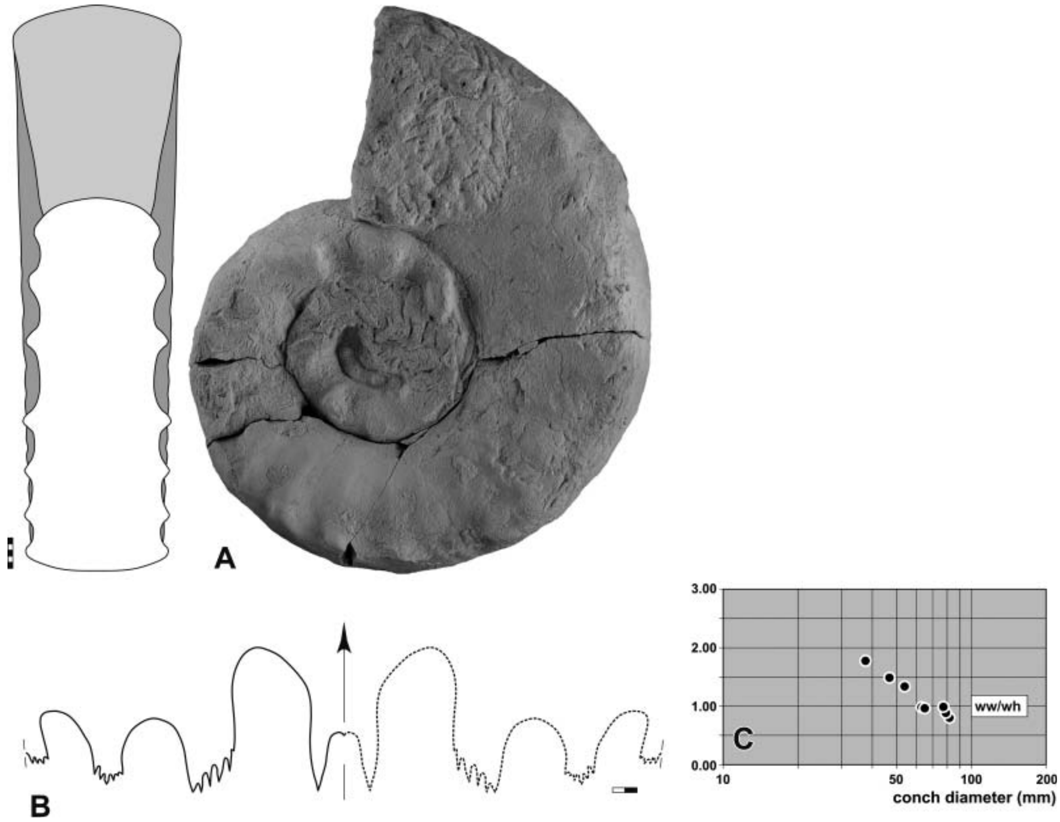

Figure 19. *Paratirolites birunii* sp. nov. **A,** holotype, MB.C.25200, Ali Bashi 4, −3.20 m; **B,** paratype, MB.C.25201, Ali Bashi N, −3.35 m; at 30.0 mm ww, 15.6 mm wh; **C,** whorl cross section proportions. Scale bars: A = 5 mm; B = 2 mm.

The suture line of holotype MB.C.25195 (at 17 mm whorl height; about 55 mm phragmocone diameter) shows a narrow external lobe with parallel flanks and asymmetrical prongs that show two little additional notches on their ventral flank (Fig. 18B). The symmetric ventrolateral saddle is rather narrow and continuously rounded. The adventive lobe is asymmetrical and much deeper on the dorsal side; it possesses four rather large notches.

The suture lines drawn from several specimens demonstrate a wide morphological range in general shape and degree of secondary subdivision of individual elements (Fig. 18). Specimen MB.C.25196 (Aras Valley, float; at approximately 47 mm dm) possesses a deep V-shaped external lobe with strongly serrated prongs, while this lobe is small and short in specimen MB.C.25197 (Aras Valley, −3.55 m; at approximately 44 mm dm). In the latter, the prongs possess only three small notches.

Remarks. *Paratirolites coronatus* is the paratirolitid with the widest conch, resulting from the coronate ventrolateral shoulder. Therefore, it cannot be confused with any other species. *Paratirolites coronatus* differs from *P. vediensis* and the other species in the more strongly trapezoidal whorl cross section of the adult stage.

Stratigraphical range. *Paratirolites* Limestone; 3.55 to 2.90 m below the extinction horizon (uppermost part of the *Paratirolites trapezoidalis* Zone and lower part of the *Paratirolites kittli* Zone).

Paratirolites birunii sp. nov.
(Fig. 19)

Derivation of name. After Abu al-Rayhan Muhammad ibn Ahmad al-Biruni (973−1048), a Persian Muslim scholar and polymath from the Khwarezm region.

Holotype. MB.C.25200 (Fig. 19A).

Type locality and horizon. Ali Bashi 4 section; 3.20 m below the top of the *Paratirolites* Limestone (*Paratirolites kittli* Zone).

Material. Ten specimens (Aras Valley, Ali Bashi N, Ali Bashi 4).

Diagnosis. *Paratirolites* with a conch reaching 115 mm dm. Subadult stage with trapezoidal, weakly depressed whorl cross section (ww/wh = 1.35) and broadly rounded venter; 10 strong ventrolateral nodes per volution. Adult stage with trapezoidal and weakly compressed whorl cross section (ww/wh = 0.80), slightly flattened tectiform venter and subangular ventrolateral shoulder; numerous small ventrolateral nodes. Prongs of the external lobe simple or bifid; altogether 12−14 notches of the E, A and L lobes.

Description. Holotype MB.C.25200 is a more or less complete but somewhat corroded specimen with 82 mm conch diameter; preserved in the specimen are the partly weathered body chamber and the last two and a half whorls of the phragmocone (Fig. 19A). The conch is thinly discoidal and subevolute in the last volution (ww/dm = 0.29; uw/dm = 0.41) and possesses a laterally compressed trapezoidal whorl cross section (ww/wh = 0.79) with a subangular ventrolateral shoulder and a flattened venter. In the penultimate volution, prominent conical ventrolateral nodes (about five per half volution) are the dominant sculpture elements; these become rapidly much weaker and more densely spaced on the adult body chamber (about 20 per half volution).

Paratype MB.C.25201 (Ali Bashi N, −3.35 m) shows a suture line with a narrow, Y-shaped external lobe at a whorl height of 16 mm (corresponding to a phragmocone diameter of about 45 mm). Its flanks are almost parallel in the lower part and diverge strongly in the upper half; the prongs of the external lobe are very narrow and lanceolate. The wide venter accommodates the asymmetrical, dorsally slightly inclined ventrolateral saddle and the asymmetrical, strongly serrated adventive lobe that is deeper on its dorsal side. The lateral and umbilical lobes, both on the inner half of the flank, are much smaller than the adventive lobe and are also strongly serrated (Fig. 19B).

Remarks. *Paratirolites birunii* differs from *P. trapezoidalis* in the much narrower whorl cross section of the adult stage at 80 mm dm (ww/wh = 0.80 in *P. birunii* but 1.40 in *P. trapezoidalis*). The species differs from *P. kittli*, which shows similar conch proportions, in the coarser and fewer conical nodes (10 in *P. birunii* but 20 in *P. kittli*) of the subadult stage.

Stratigraphical range. *Paratirolites* Limestone; 3.35 to 2.70 m below the extinction horizon (*Paratirolites kittli* Zone).

Paratirolites kittli Stoyanow, 1910
(Figs 20−22)

1910 *Paratirolites kittli* Stoyanow: 82, pl. 9, figs 1, 2.
1910 *Stephanites*? *waageni* Stoyanow: 89, pl. 8, fig. 3.
?1910 *Stephanites* sp. indet. Stoyanow: 89, pl. 7, fig. 8.
1934 *Paratirolites kittli* Stoyanow; Spath: 366, text-fig. 125a−d.
1934 *Paratirolites waageni* (Stoyanow); Spath: 367.
1947 *Paratirolites kittli* Stoyanow; Voinova *et al.*: 169, pl. 40, fig. 4, text-fig. 67.

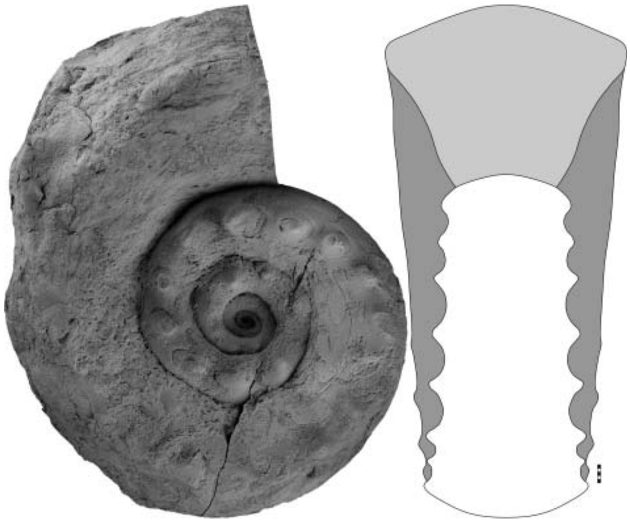

Figure 20. *Paratirolites kittli* Stoyanow, 1910, lateral and dorsal views of MB.C.25210, Ali Bashi N, −2.65 m. Scale bar = 5 mm.

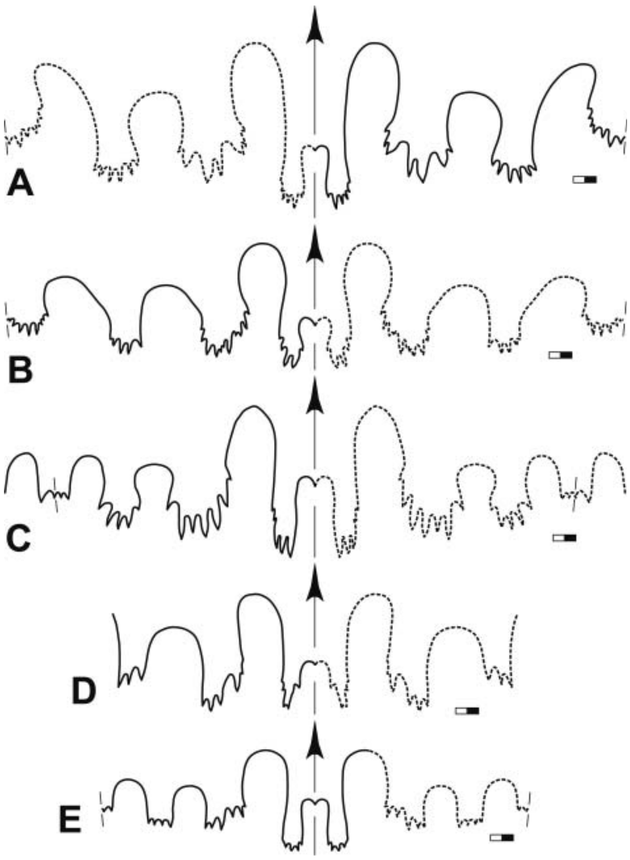

Figure 21. *Paratirolites kittli* Stoyanow, 1910, suture lines. **A,** MB.C.25215, Aras Valley, −2.65 m; at 55.8 mm dm, 20.2 mm wh; **B,** MB.C.25211, Aras Valley, float; at 17.8 mm wh; **C,** MB.C.25212, Aras Valley, −3.30 m; at 21.0 mm ww, 16.7 mm wh; **D,** MB.C.25213, Ali Bashi N, −2.95 m; at 15.5 mm wh; **E,** MB.C.25216, Ali Bashi N, −3.10 m; at 39.7 mm dm, 18.7 mm ww, 13.9 mm wh. Scale bars = 2 mm.

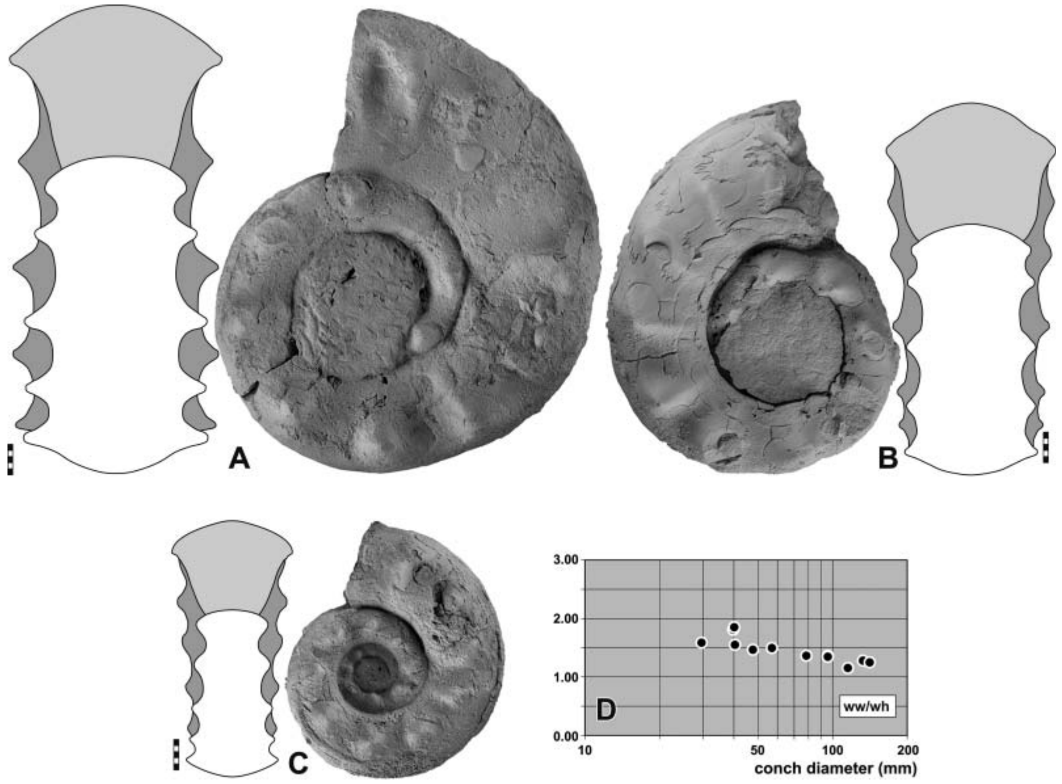

Figure 22. *Paratirolites kittli* Stoyanow, 1910. **A−C,** lateral and dorsal views; **A**, MB.C.25214, Ali Bashi N, −3.30 m; **B,** MB.C.25215, Aras Valley, −2.65 m; **C,** MB.C.25216, Ali Bashi N, −3.10 m. **D,** whorl cross section. Scale bars = 5 mm.

1947 *Stephanites*? *waageni* (Stoyanow); Voinova *et al*.: 167, pl. 40, fig. 3.

1957 *Paratirolites kittli* Stoyanow; Kummel: 179, text-fig. 1a, b.

1958 *Paratirolites kittli* Stoyanow; Voinova *et al*., pl. 8, fig. 5a, b.

1965 *Paratirolites kittli* Stoyanow; Shevyrev: 174, pl. 22, fig. 4.

1965 *Paratirolites waageni* (Stoyanow); Shevyrev: 175, pl. 22, figs 5, 6.

1968 *Paratirolites kittli* Stoyanow; Shevyrev: 90, pl. 3, fig. 1.

1968 *Paratirolites waageni* (Stoyanow); Shevyrev: 90, pl. 2, figs 6, 7.

1983 *Pseudotirolites azariani* Rostovcev in Zakharov: 154, pl. 15, fig. 5.

Lectotype. The specimen figured by Stoyanow (1910, pl. 9, fig. 1).

Type locality and horizon. Dorasham (Azerbaijan); *Paratirolites* Limestone.

Material. Fifty-four specimens (Aras Valley, Ali Bashi N, Ali Bashi 4).

Diagnosis. *Paratirolites* with a conch reaching 190 mm dm. Subadult stage with rounded trapezoidal, weakly to moderately depressed whorl cross section (ww/wh = 1.30−1.60) and rounded venter; 10−12 very coarse ventrolateral nodes per volution. Adult stage with strongly trapezoidal and weakly depressed whorl cross section (ww/wh = 1.00−1.30), flattened tectiform venter and subangular ventrolateral shoulder; weak ventrolateral nodes. Prongs of the external lobe usually multiply serrated; altogether 12−21 notches of the E, A and L lobes.

Description. Specimen MB.C.25210 (Ali Bashi N, −2.65 m) is a more or less complete specimen with 140 mm conch diameter. Its body chamber is strongly weathered but the last two volutions of the phragmocone are rather well preserved (Fig. 20). The conch is thinly discoidal and subevolute in the last volution (ww/dm = 0.40; uw/dm = 0.42) and shows a weakly depressed trapezoidal whorl cross section (ww/wh = 1.12) with flattened diverging flanks, a subangular ventrolateral shoulder and a broadly rounded venter. A similar whorl cross section can also be seen in the subadult stage at about 60 mm conch diameter. Particularly the penultimate volution (up to 60 mm dm) displays prominent conical ventrolateral nodes (10 per volution); these nodes become weaker and more densely spaced on the last preserved volution.

Specimen MB.C.25217 (Ali Bashi N, −3.35 m) is another rather complete specimen with 132 mm conch diameter; it also has a strongly corroded body chamber. The conch is thinly discoidal and subevolute in the last volution (ww/dm = 0.42; uw/dm = 0.43) and possesses a weakly depressed trapezoidal whorl cross section (ww/wh = 1.27). The flanks are flattened and diverge strongly; they are separated from the slightly flattened venter by a subangular ventrolateral shoulder. Strong ventrolateral nodes are developed up to a conch diameter of about 96 mm; they are particularly prominent on the penultimate volution (10 per volution). On the last preserved volution these nodes become significantly weaker.

The suture line of specimen MB.C.25212 (Aras Valley, −3.30 m; drawn at 16.7 mm whorl height, referring to about 50 mm phragmocone diameter) shows strong serration of the external, adventive and lateral lobes (Fig. 21C). This serration is much more prominent than in most other representatives of the genus and affects not only the lobe bases but migrates upwards to their flanks with the presence of very small notches. The external lobe is parallel sided and the adjacent ventrolateral saddle is narrower than the strongly serrated adventive lobe.

The small specimen MB.C.25216 (Ali Bashi N, −3.10 m) provides insight into the morphology of the intermediate growth stage (Fig. 22C). It has 40 mm conch diameter and possesses a moderately depressed whorl cross section (ww/wh = 1.54) with a broadly rounded venter. Ten coarse conical nodes are present on the midflank and migrate, on the last preserved volution, towards the ventrolateral area.

In the suture line of specimen MB.C.25216 (drawn at 40 mm phragmocone dm), the external lobe is remarkable because it possesses converging flanks and it is much deeper than the adventive lobe (Fig. 21E). Its prongs are slightly pouched and serrated with small notches at the base. The wide venter accommodates the parallel-sided, rounded ventrolateral saddle and the asymmetrical adventive lobe, which shows deeper notches on its dorsal side.

Remarks. *Paratirolites kittli* differs from the otherwise similar *P. vediensis* in the more rounded whorl cross section of the subadult stage, which in the latter is trapezoidal with a flattened venter and flattened diverging flanks.

The figure provided by Stoyanow (1910, pl. 9, figs 1, 2) shows a paratirolitid ammonoid, which has, at about 40 mm conch diameter, small and pointed ventrolateral nodes. In this large number of nodes, *P. kittli* differs from the other species of *Paratirolites*, which have a lower number of coarser, conical nodes. Stoyanow's figure shows a suture line with two notches of the prongs in the external lobe, which agrees with the material described here.

Shevyrev (1965, 1968) figured a specimen with 75 mm conch diameter. This specimen has 10 coarse ventrolateral nodes, and in this respect is dissimilar to the original description of *P. kittli*. It probably belongs to another species.

Stoyanow (1910) had only one fragment of his species *Stephanites*? *waageni*. Despite this limited original material, a rather good characterization of this species was provided. The figured specimen is a fragment of the phragmocone with a whorl height of 22 mm, meaning that the total diameter of the conch including the body chamber was at least 110 mm. It shows a ventrally depressed whorl profile with convex flanks and a broadly rounded venter. The flank shows sharp ribs, which produce sharp conical nodes in the midflank area. With this morphological inventory, it can be attributed to *P. kittli* with some certainty.

Shevyrev (1965) had 24 specimens, making it the most common species of the genus. He published three suture lines, all of which show less strongly serrated lobes when compared with the new material described here.

Stratigraphical range. *Paratirolites* Limestone; 3.35 to 1.55 m below the extinction horizon (*Paratirolites kittli* Zone to *Alibashites mojsisovicsi* Zone).

Paratirolites vediensis Shevyrev, 1965
(Figs 23, 24)

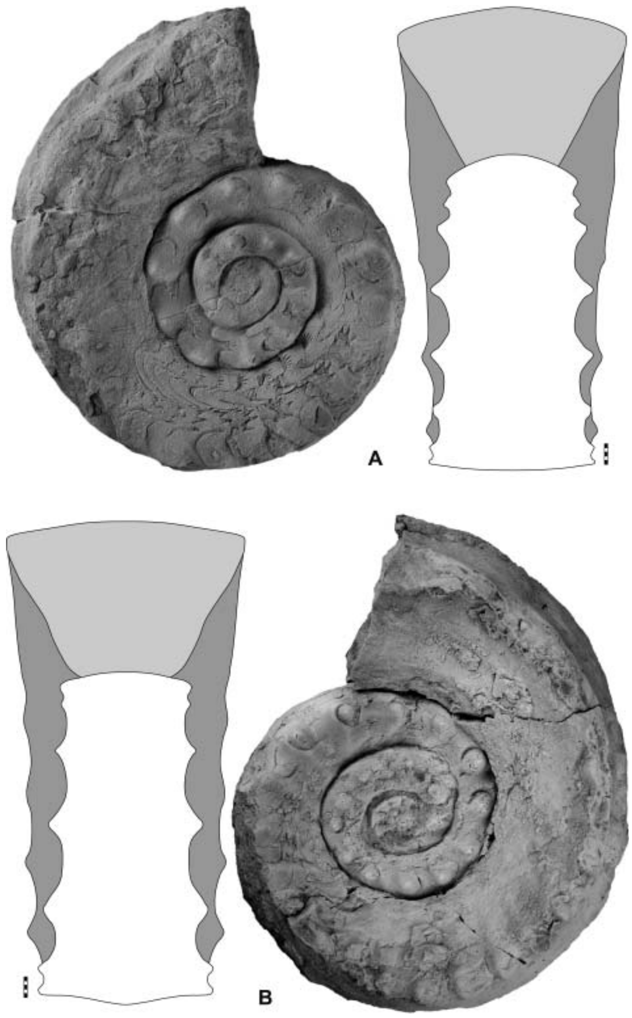

Figure 23. *Paratirolites vediensis* Shevyrev, 1965, lateral and dorsal views. **A,** MB.C.25264, Ali Bashi N, −2.65 m; **B,** MB. C.25265, Aras Valley, −3.05 m. Scale bars = 5 mm.

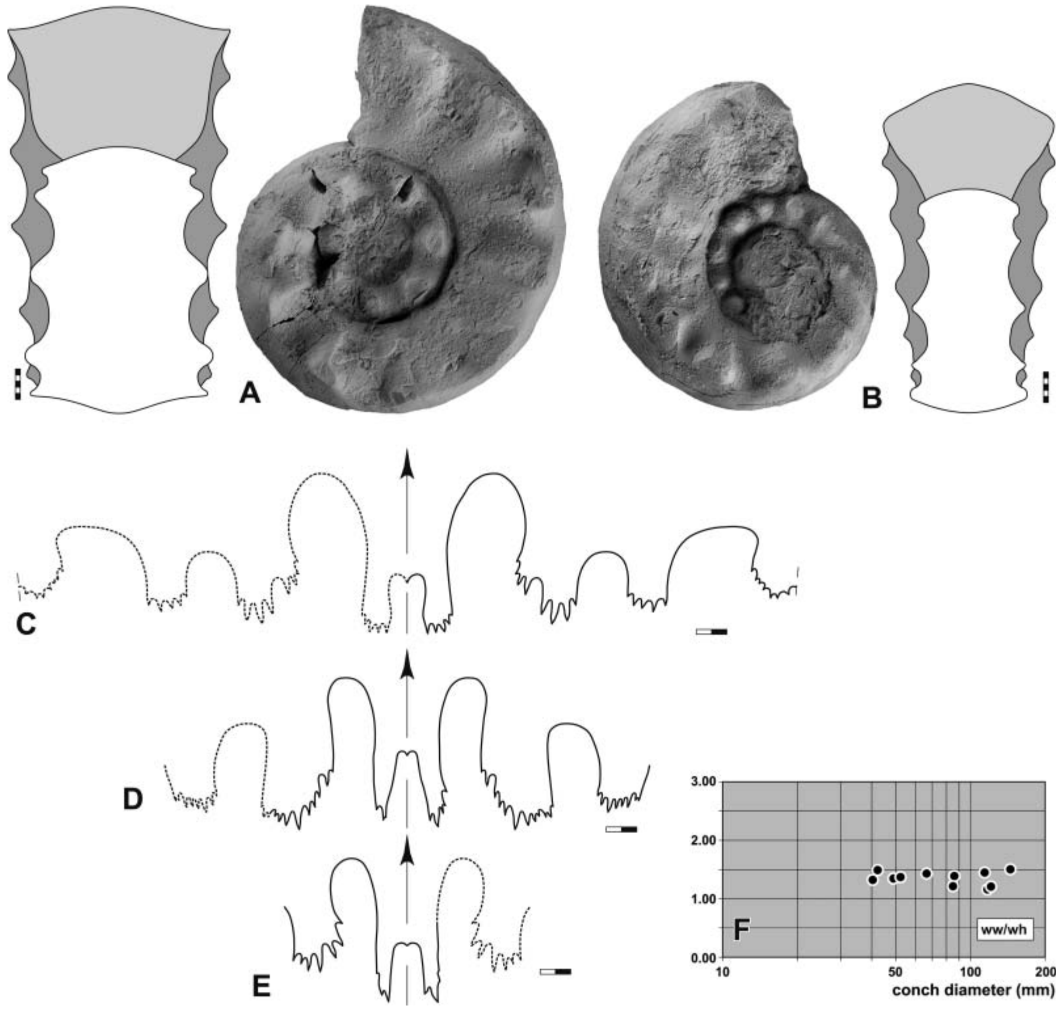

Figure 24. *Paratirolites vediensis* Shevyrev, 1965. **A, B,** lateral and dorsal views; **A,** MB.C.25266, Aras Valley, float; **B,** MB.C.25267, Ali Bashi N, −3.10 m. **C−E,** suture lines; **C,** MB.C.25268, Ali Bashi N, −2.65 m; at 20.5 mm wh; **D,** MB.C.25267, Ali Bashi N, 3.10 m; at 48.4 mm dm, 23.2 mm ww, 18.0 mm wh; **E,** MB.C.25266, Aras Valley, float; at 45.9 mm dm, 15.2 mm wh. **F,** whorl cross section proportions. Scale bars: A, B = 5 mm; C−E = 2 mm.

1965 *Paratirolites vediensis* Shevyrev: 176, pl. 23, fig. 1.
1968 *Paratirolites vediensis* Shevyrev; Shevyrev: 92, pl. 5, fig. 1.
1969 *Paratirolites vediensis* Shevyrev; Stepanov *et al*., pl. 13, fig. 5.
2014b *Paratirolites vediensis* Shevyrev; Korn in Ghaderi *et al*., text-fig. 7G.

Holotype. PIN 1478/2; illustrated by Shevyrev (1965, pl. 23, fig. 1).

Type locality and horizon. Vedi (Armenia); *Paratirolites* Limestone.

Material. Thirty-two specimens (Aras Valley, Ali Bashi N).

Diagnosis. *Paratirolites* with a conch reaching 250 mm dm. Subadult stage with trapezoidal, weakly depressed whorl cross section (ww/wh = 1.20−1.50) and flattened tectiform venter; 10−15 coarse ventrolateral nodes per volution. Adult stage with strongly trapezoidal and weakly depressed whorl cross section (ww/wh = 1.00−1.20), flattened tectiform venter and angular ventrolateral shoulder; weak ventrolateral nodes. Prongs of the external lobe usually multiply serrated; altogether 14−20 notches of the E, A and L lobes.

Description. Specimen MB.C.25264 (Ali Bashi N, −2.65 m) is an incomplete specimen with 112 mm conch diameter; preserved are one-third of the strongly weathered body chamber and two volutions of the phragmocone (Fig. 23A). The specimen is, because of strong weathering, only preserved from one side. The conch is thinly discoidal and subevolute at 86 mm dm (ww/dm = 0.42; uw/dm = 0.44) and possesses a weakly depressed trapezoidal whorl cross section (ww/wh = 1.49). The flanks are flattened and diverge strongly; they are separated from the slightly flattened venter by a subangular ventrolateral shoulder. Strong ventrolateral nodes are developed up to a

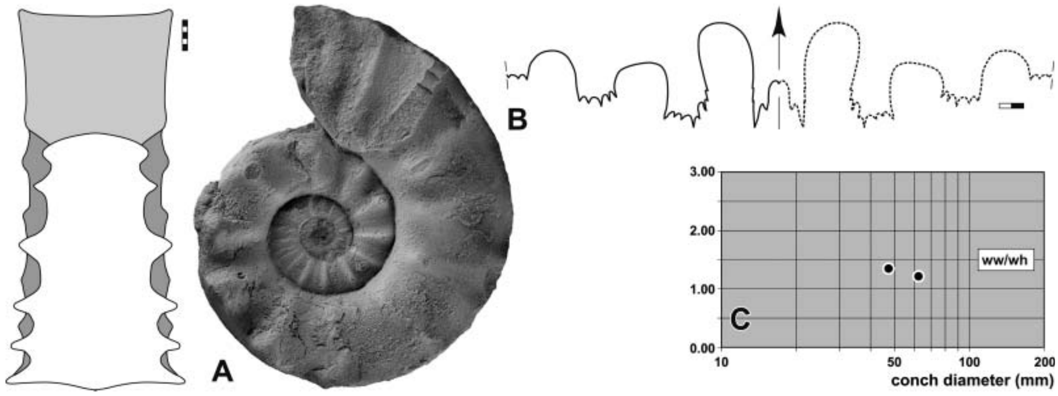

Figure 25. *Paratirolites quadratus* sp. nov., holotype, MB.C.25296, Ali Bashi N, −1.70 m. **A,** lateral and dorsal views; **B,** suture line at 30.8 mm ww, 13.9 mm wh; **C,** whorl cross section proportions. Scale bars: A = 5 mm; B = 2 mm.

conch diameter of about 85 mm; they are particularly prominent on the penultimate volution (10 per volution). On the last preserved volution these nodes become significantly weaker.

Specimen MB.C.25265 (Aras Valley, −3.05 m) has 117 mm conch diameter and closely resembles specimen MB.C.25264 in conch shape and sculpture. Its body chamber is less weathered and shows 12 weak ventrolateral nodes per half volution (Fig. 23B).

Specimen MB.C.25266 (Aras Valley, float) is a rather well preserved specimen with 66 mm conch diameter. It shows a strongly trapezoidal whorl cross section with slightly flattened, tectiform venter. The sculpture consists of coarse and pointed ventrolateral spines, which develop out of ribs on the flank (Fig. 24A). The suture line of the specimen shows a rather strongly serrated external lobe with slightly asymmetric prongs; the external lobe is deeper than the adventive lobe (Fig. 24E).

The suture line of specimen MB.C.25268 (Ali Bashi N, −2.65 m) has, at 22 mm whorl height (corresponding to 60 mm phragmocone diameter), a parallel-sided external lobe with narrow parallel-sided prongs that are strongly serrated at the base (Fig. 24C). The ventrolateral saddle appears to be slightly inflated and is broadly rounded; it is wider than the strongly serrated adventive lobe. A fine serration with a number of little notches can also be seen in the lateral and umbilical lobes, of which the latter has a position at the umbilical seam.

Remarks. *Paratirolites vediensis* differs from *P. waageni* in the strongly trapezoidal whorl cross section with flattened venter of the subadult stage, which shows a rounded venter in *P. waageni*. It differs from *P. trapezoidalis*, which possesses a very similar conch geometry, in the much coarser ribs of the adult stage (which in *P. trapezoidalis* are much more numerous and delicate), and in the stronger serrated prongs of the external lobes (usually multiply serrated in *P. vediensis*, but simple or bifid in *P. trapezoidalis*).

Shevyrev (1965) based his new species on only one specimen, but the newly collected specimens confirm his idea for a separation. In most cases, separation from the otherwise similar *P. waageni* is rather easy and justifies the introduction of this species.

Stratigraphical range. *Paratirolites* Limestone; 3.30 to 2.10 m below the extinction horizon (*Paratirolites kittli* Zone to lower part of the *Stoyanowites dieneri* Zone).

Paratirolites quadratus sp. nov.
(Fig. 25)

Derivation of name. After the nearly quadrate whorl profile of the adult stage.

Holotype. MB.C.25296 (Fig. 25A).

Type locality and horizon. Ali Bashi N section; 1.70 m below the top of the *Paratirolites* Limestone (*Stoyanowites dieneri* Zone).

Material. Two specimens (Aras Valley).

Diagnosis. *Paratirolites* with a conch reaching 90 mm dm. Subadult stage with trapezoidal, weakly depressed whorl cross section (ww/wh = 1.35) and broadly rounded venter; about 12 ribs ending in spiny ventrolateral nodes. Adult stage with weakly trapezoidal to nearly quadrate and weakly depressed whorl cross section (ww/wh = 1.20), weakly concave venter and angular ventrolateral shoulder; coarse and shallow ribs on the flanks. Prongs of the external lobe multiply serrated; altogether about 17 notches of the E, A and L lobes.

Description. Holotype MB.C.25296 is a well-preserved specimen with 62 mm conch diameter; preserved are a part of the body chamber (half of the last volution) and the last three volutions of the phragmocone (Fig. 25A). The conch is thinly discoidal and subevolute in the last volution (ww/dm = 0.40; uw/dm = 0.39). It shows a subtrapezoidal, ventrally depressed whorl cross section (ww/wh = 1.21) at the largest diameter. The specimen shows a narrow and oblique umbilical wall and slightly concave and diverging flanks, which are separated from the flattened, slightly concave venter by an angular margin. The sculpture of the juvenile stage (up to 12 mm dm) consists of rounded ribs, which become more pronounced during ontogeny. At 22 mm dm, these ribs develop spiny ventrolateral nodes, of which 10 can be counted for one volution (up to 49 mm dm). At a larger diameter (above 49 mm dm), these ventrolateral nodes are weakened but the ribs produce sharp dorsolateral nodes.

The suture line, drawn at 14 mm whorl height (representing about 40 mm phragmocone diameter) of the holotype possesses a parallel-sided external lobe with narrow prongs that display two narrow notches (Fig. 25B). The ventrolateral saddle has a slightly bulbous shape and is slightly asymmetrical and dorsally inclined. On the venter follows an asymmetrical adventive lobe with seven little notches.

Remarks. *Paratirolites quadratus* differs from the other species of *Paratirolites* in the slightly trapezoidal, nearly quadrate whorl profile in the adult conch and the very long, spiny ventrolateral nodes.

Stratigraphical range. *Paratirolites* Limestone; 1.70 m below the extinction horizon (*Stoyanowites dieneri* Zone).

Paratirolites multiconus sp. nov.
(Fig. 26)

Derivation of name. From Latin *multi* = many, and *conus* = cone, because of the large number of ventrolateral nodes.

Holotype. MB.C.25298 (Fig. 26A).

Type locality and horizon. Dorasham (Azerbaijan); *Paratirolites* Limestone.

Material. Two specimens (Aras Valley, Ali Bashi N).

Diagnosis. *Paratirolites* with a conch reaching 100 mm dm. Subadult stage with trapezoidal, weakly depressed whorl cross section (ww/wh = 1.10) and rounded venter; 20 weak ribs, which end in conical ventrolateral nodes, per volution. Adult stage with slightly trapezoidal and weakly compressed whorl cross section (ww/wh ~0.85), rounded venter and narrowly rounded ventrolateral shoulder; numerous small ventrolateral nodes. Prongs of the external lobe multiply serrated; about 18 notches of the E, A and L lobes.

Description. Specimen MB.C.25298 (Ali Bashi N, −1.10 m) is unfortunately a somewhat corroded specimen, but nevertheless shows a number of characters (Fig. 26A). It has a diameter of 82 mm, and more than half of the last volution belongs to the body chamber. The phragmocone shows a trapezoidal whorl cross section with broadly rounded venter; it is ornamented with ribs, which become stronger with distance to the umbilicus and end in conical ventrolateral nodes. About 20 such ribs

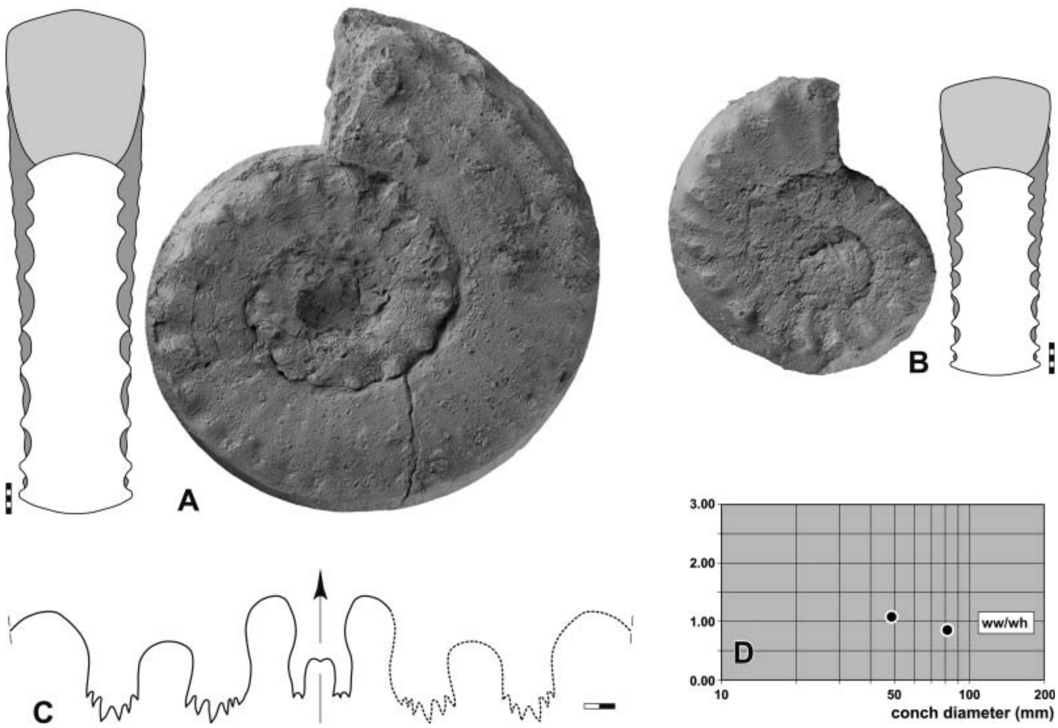

Figure 26. *Paratirolites multiconus* sp. nov. **A, B,** lateral and dorsal views; **A,** holotype, MB.C.25298, Ali Bashi N, −1.10; **B,** paratype, MB.C.25299, Aras Valley, −1.15 m; **C,** holotype, MB.C.25298, suture line at 16.5 mm wh. **D,** whorl cross section proportions. Scale bars: A, B = 5 mm; C = 2 mm.

occupy the flanks of one volution. The ribs become much finer on the adult body chamber, where they are visible as numerous (about 25 per half volution) weak riblets ending in small ventrolateral nodes.

The suture line of specimen MB.C.25298 (drawn at 16.5 mm wh, corresponding to a phragmocone diameter of 55 mm) possesses an external lobe, which is pouched in the lower half (Fig. 26C). Its prongs are slightly asymmetrical, being bifid and trifid with small secondary notches. The adventive and lateral lobes are strongly serrated with six small notches each.

The smaller specimen MB.C.25299 (Ali Bashi N, −1.15 m) is also not very well preserved. It has, at 49 mm conch diameter, a thinly discoidal and subevolute shape (ww/dm = 0.36; uw/dm = 0.43) with a trapezoidal whorl cross section (ww/wh = 1.06) and a rounded venter. It possesses 20 weak ribs on the last preserved volution; these ribs form slightly elongate ventrolateral nodes (Fig. 26B). The venter is smooth.

Remarks. *Paratirolites multiconus* differs from the other species of *Paratirolites* in the slender conch and the larger number of ventrolateral nodes.

Stratigraphical range. *Paratirolites* Limestone; 1.15 to 1.10 m below the extinction horizon (*Abichites abichi* Zone).

Paratirolites serus sp. nov.
(Fig. 27)

Derivation of name. From Latin *serus* = late, because of the high stratigraphical occurrence.

Holotype. MB.C.25300 (Fig. 27A).

Type locality and horizon. Ali Bashi N section, 0.65 m below the top of the *Paratirolites* Limestone (*Abichites stoyanowi* Zone).

Material. Five specimens (Aras Valley, Ali Bashi N, Ali Bashi 1).

Diagnosis. *Paratirolites* with a conch reaching 80 mm dm. Subadult stage with strongly trapezoidal, moderately depressed whorl cross section (ww/wh = 1.60) and rounded venter; 12 weak ribs, which end in coarse conical ventrolateral nodes, per volution. Adult stage with slightly trapezoidal and moderately depressed whorl cross section (ww/wh = 1.60), flattened venter and angular ventrolateral shoulder; numerous sharp ribs on the flank. Prongs of the external lobe simple; altogether about eight notches of the E, A and L lobes.

Description. Holotype MB.C.25300 (Ali Bashi N, −0.65 m) is an incomplete specimen with 51 mm conch diameter; most of the specimen represents the phragmocone and only about a quarter of the body chamber is preserved (Fig. 27A). The maximum diameter of the phragmocone is 40 mm; the conch is discoidal in this stage with a trapezoidal, weakly depressed whorl cross section (ww/wh = 1.30), which has a tectiform venter. The last volution of

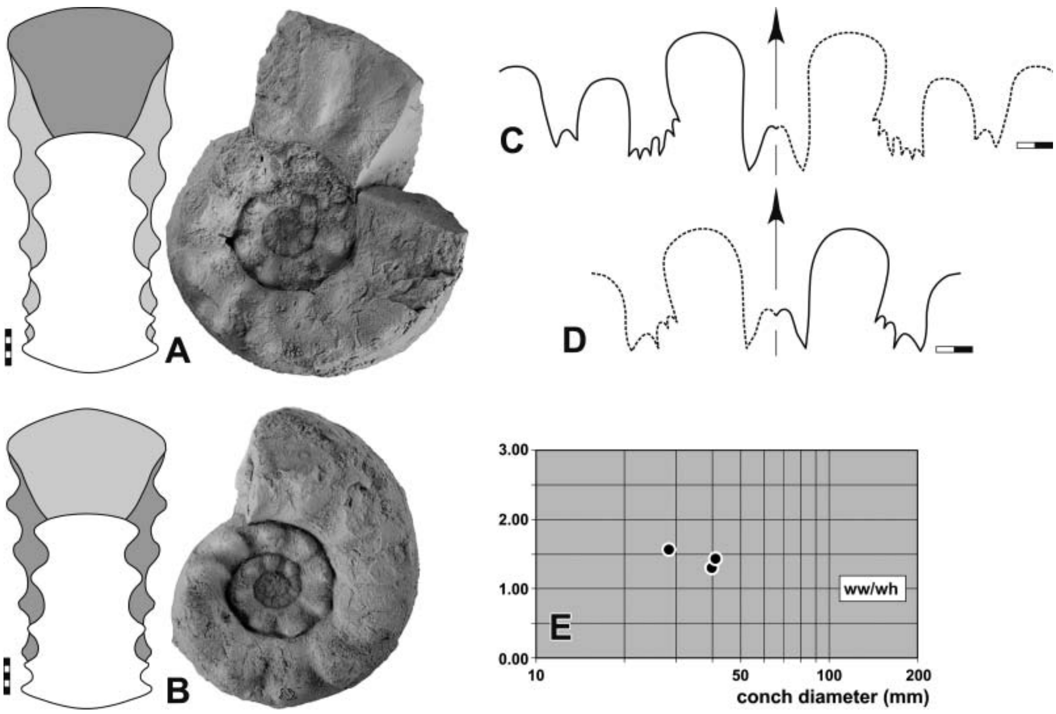

Figure 27. *Paratirolites serus* sp. nov. **A, B,** lateral and dorsal views; **A,** holotype, MB.C.25300, Ali Bashi N, −0.65 m; **B,** paratype, MB.C.25301, Ali Bashi N, −0.85 m. **C, D,** suture lines; **C,** holotype, MB.C.25300, at 10.5 mm wh; **D,** paratype, MB.C.25301, at 9.5 mm wh. **E,** whorl cross section proportions. Scale bars: A, B = 5 mm; C, D = 2 mm.

the phragmocone is ornamented with 10 rounded ribs on the flank, which end in coarse conical ventrolateral nodes. These nodes become much weaker on the body chamber and are replaced by elongate dorsolateral nodes.

The suture line of the holotype (drawn at 10.5 mm wh) shows a rather narrow, parallel-sided external lobe, which possesses narrowly V-shaped, unsubdivided prongs (Fig. 27C). The inflated ventrolateral saddle is broadly rounded, the adventive lobe possesses six notches and the lateral lobe is bifid.

The smaller paratype MB.C.25301 (Ali Bashi N, −0.85 m) is fully chambered with 41 mm conch diameter. It has a pentagonal whorl cross section with tectiform venter and diverging flanks (Fig. 27B). The ornament consists of 10 conical ventrolateral nodes on the last phragmocone volution, the penultimate volution possessing eight such nodes. The suture line has an unsubdivided external lobe.

Remarks. Subadult specimens of *Paratirolites serus* resemble some stratigraphically older species such as *P. waageni* and particularly *P. vediensis*. The new species differs from these in the smaller conch diameter (40 mm maximum phragmocone diameter in contrast to 70−80 mm in *P. waageni* and *P. vediensis*), the presence of elongate dorsolateral nodes on the body chamber, and in the much simpler suture line with an unsubdivided external lobe.

The two species *Alibashites mojsisovicsi* and *A. ferdowsii* are similar in the subadult stage, but they possess a square-shaped (*A. mojsisovicsi*) or subtrapezoidal (*A. ferdowsii*) body chamber with a flat venter.

Stratigraphical range. *Paratirolites* Limestone; 0.95 to 0.55 m below the extinction horizon (lower part of the *Abichites stoyanowi* Zone).

Genus ***Julfotirolites*** gen. nov.

Derivation of name. Named after the similarity with *Tirolites* and *Paratirolites*, and the town of Julfa.

Type species. *Julfotirolites kozuri* sp. nov., North-west Iran.

Diagnosis. Representatives of the family Dzhulfitidae with large conch; maximum adult diameters are about 105 mm. Adult stage with oval, compressed whorl cross section. Subadult stage with large conical ventrolateral nodes, adult stage with weak ribs. Suture line with deep external lobe; the depths of external lobe and adventive lobe are nearly identical.

Remarks. The monospecific new genus *Julfotirolites* differs from *Paratirolites* and *Alibashites* in the shape of the adult stage, which shows an oval cross section in *Julfotirolites* but is trapezoidal in *Paratirolites* and subtrapezoidal in *Alibashites*.

Julfotirolites kozuri sp. nov.
(Fig. 28)

Derivation of name. Named after H. W. Kozur (1942−2013) for his stratigraphical work on the Permian−Triassic boundary beds in Iran.

Holotype. MB.C.25305 (Fig. 28A).

Type locality and horizon. Aras Valley section; float of the *Paratirolites* Limestone.

Material. Three specimens (Aras Valley, Ali Bashi N).

Diagnosis. *Julfotirolites* with a conch reaching 105 mm dm. Subadult stage with oval, weakly depressed whorl cross section (ww/wh = 1.20) and rounded venter; 10 coarse conical ventrolateral nodes per volution. Adult stage with oval and weakly compressed whorl cross section (ww/wh = 0.65), rounded venter and rounded ventrolateral shoulder; weak ribs on the midflank. Prongs of the external lobe trifid; altogether 13−15 notches of the E, A and L lobes.

Description. Holotype MB.C.25305 (float) is a rather well preserved internal mould of a fully septate specimen

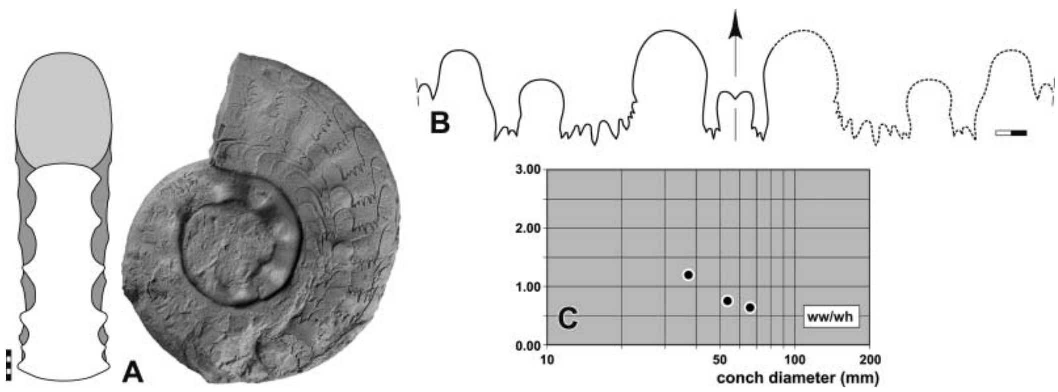

Figure 28. *Julfotirolites kozuri* sp. nov., holotype, MB.C.25305, Aras Valley, float. **A,** lateral and dorsal views; **B,** suture line at 49.8 mm dm, 19.2 mm wh; **C,** whorl cross section proportions. Scale bars: A = 5 mm; B = 2 mm.

with a conch diameter of 54 mm (Fig. 28A). The specimen shows a change of conch shape and sculpture already before the end of the phragmocone; the whorl cross section becomes slender on the last preserved volution and the ww/wh ratio is reduced from 1.20 at 37 mm dm to 0.76 at 54 mm dm. The ribs become weaker at the same time; the number of ribs changes from 10 per whorl to eight per half whorl.

The suture line of the holotype shows, at 50 mm dm, a rather narrow external lobe with narrow prongs, which possess three little notches (Fig. 28B). The ventrolateral saddle is broadly rounded and almost symmetrical. The adventive lobe is strongly serrated with nine small notches of irregular size, while the lateral lobe has only three notches.

Paratype MB.C.25306 (Ali Bashi N, −2.65 m) has, with 66 mm conch diameter, a conch and sculpture similar to the holotype. The specimen is rather poorly preserved, but shows the rapid weakening of the ornament from conical midflank nodes to fine ribs within one volution.

Remarks. *Julfotirolites kozuri* differs from *Paratirolites* species in the rounded venter and the compressed whorl cross section.

Stratigraphical range. *Paratirolites* Limestone; about 2.85 m below the extinction horizon (*Paratirolites kittli* Zone).

Genus ***Alibashites*** gen. nov.

Derivation of name. Named after the Ali Bashi Mountains east of Julfa.

Type species. *Xenodiscus* (*Paratirolites*?) Mojsisovicsi Stoyanow, 1910.

Included species. *Alibashites ferdowsii* sp. nov. (North-west Iran); *Xenodiscus* (*Paratirolites*?) Mojsisovicsi Stoyanow, 1910 (Azerbaijan) ; *Alibashites stepanovi* sp. nov. (North-west Iran) ; *Alibashites uncinatus* sp. nov. (North-west Iran).

Diagnosis. Representatives of the family Dzhulfitidae with moderately large to large conch; maximum adult diameters are between 85 and 110 mm. Adult stage with subtrapezoidal or quadrate whorl cross section. Subadult stage with large conical ventrolateral nodes, adult stage with weak ribs. Suture line with deep external lobe; the depths of external lobe and adventive lobe are nearly identical.

Remarks. *Alibashites* has an intermediate morphological position between *Paratirolites* and *Abichites*. It possesses the subadult sculpture with conical ventrolateral nodes of *Paratirolites* but lacks the trapezoidal whorl profile of that genus. *Abichites* has a similar adult conch morphology with a rectangular or subtrapezoidal whorl profile but does not possess the strong ventrolateral nodes developed in *Alibashites*.

Alibashites mojsisovicsi (Stoyanow, 1910)
(Fig. 29)

1910 *Xenodiscus* (*Paratirolites*?) Mojsisovicsi Stoyanow: 79, pl. 8, fig. 1.
1965 *Abichites mojsisovicsi* (Stoyanow); Shevyrev: 180, pl. 23, fig. 4.
1968 *Abichites mojsisovicsi* (Stoyanow); Shevyrev: 95, pl. 4, fig. 3.
1969 *Abichites mojsisovicsi* (Stoyanow); Stepanov *et al*., pl. 13, fig. 4.

Lectotype. The specimen figured by Stoyanow (1910, pl. 8, fig. 1).

Type locality and horizon. Dorasham (Azerbaijan); *Paratirolites* Limestone.

Material. Eighteen specimens (Aras Valley, Ali Bashi N, Ali Bashi 4, Ali Bashi 1).

Diagnosis. *Alibashites* with a conch reaching 90 mm dm. Subadult stage with circular, weakly depressed whorl cross section (ww/wh = 1.00−1.20) and rounded venter; 13 coarse ventrolateral nodes per volution. Adult stage with quadrate and weakly compressed whorl cross section (ww/wh = 0.95−1.00), almost flat venter and subangular ventrolateral shoulder; low ribs on the flanks, forming very weak dorsolateral and ventrolateral nodes. Prongs of the external lobe variable, simple to trifid; 8−13 notches of the E, A and L lobes.

Description. Specimen MB.C.25308 (Ali Bashi 4, −1.35 m) is a fairly well-preserved specimen with 62 mm conch diameter; preserved are the partly weathered body chamber (last half volution) and the last two volutions of the phragmocone (Fig. 29A). The conch is extremely discoidal and subevolute in the last volution (ww/dm = 0.30; uw/dm = 0.44) and possesses, at the largest diameter, a trapezoidal whorl cross section with about equal values for whorl width and whorl height (ww/wh = 0.98). At this stage, the flanks are slightly concave and diverge slowly towards the flattened venter; flanks and venter are separated by a subangular margin. One volution earlier (at about 32 mm dm), the ww/wh ratio is much higher (ww/wh = 1.45) due to coarse ventrolateral nodes. The venter is broadly rounded in this growth stage. The sculpture changes significantly in the growth stage at 37 mm dm. While the last two volutions of the phragmocone possess very strong, spiny ventrolateral nodes (8−10 per volution), they become rapidly weaker at the terminal body chamber and are replaced there by densely spaced sharp ribs, which terminate in weak nodes placed at the ventrolateral edge.

The smaller specimen MB.C.25310 (Ali Bashi 4, −1.70 m) is also rather well preserved and has a conch diameter of 44 mm. The last half volution belongs to the

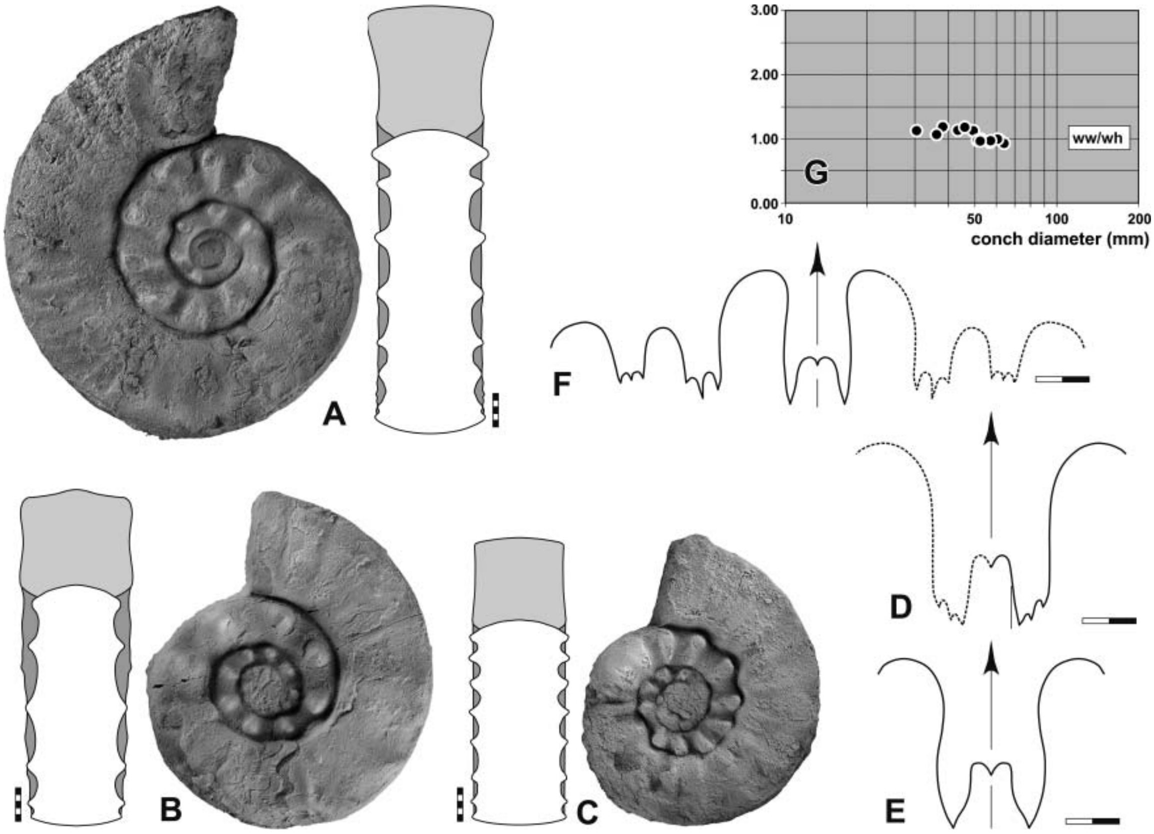

Figure 29. *Alibashites mojsisovicsi* (Stoyanow, 1910). **A–C,** lateral and dorsal views; **A,** MB.C.25308, Ali Bashi 4, −1.35 m; **B,** MB. C.25309, Ali Bashi 4, −1.55 m; **C,** MB.C.25310, Ali Bashi N, −1.70 m. **D–F,** suture lines; **D,** MB.C.25310, Aras Valley, −1.40 m; at 14.5 mm ww, 12.5 mm wh; **E,** MB.C.25309, at 11.4 mm ww, 10.0 mm wh; **F,** MB.C.25310, at 11.5 mm ww, 9.7 mm wh. **G,** whorl cross section proportions. Scale bars: A–C = 5 mm; D–F = 2 mm.

body chamber and one and a half volutions of the phragmocone are preserved (Fig. 29C). At 44 mm dm, the conch is extremely discoidal and subevolute in the last volution (ww/dm = 0.34; uw/dm = 0.44) and possesses a subquadrate whorl cross section (ww/wh = 1.13). The flanks are nearly flat in this stage and are separated from the flattened venter by a subangular margin. The last portion of the phragmocone possesses prominent ventrolateral nodes (11 per volution), which perform as obstacles for the umbilical wall of the following volution. On the body chamber, the ventrolateral nodes are weak and less pronounced than the sharp dorsolateral nodes.

The suture line of specimen MB.C.25310, drawn at 8 mm whorl height (about 25 mm phragmocone diameter) has a slightly pouched external lobe with narrow lanceolate prongs (Fig. 29F). The broadly rounded ventrolateral saddle is asymmetrical and ventrally inclined. The adventive and lateral lobes have a position on the flank. Both are serrated with converging flanks; the adventive lobe shows one small and two large notches, whereas the lateral lobe has three very small notches.

Suture lines of other specimens differ particularly in the shape of the external lobe. Specimen MB.C.25309 (Ali Bashi 4, −1.55 m; wh = 10 mm, corresponding to a phragmocone diameter of 32 mm) has pouched prongs (Fig. 29E), and specimen MB.C.25310 (Ali Bashi 1, −1.40 m; wh = 12.5 mm, corresponding to a phragmocone diameter of 40 mm) possesses asymmetrical ventral prongs with three little notches (Fig. 29D).

Remarks. *Alibashites ferdowsii* has coarse nodes in the subadult stage like *A. mojsisovicsi*, but this species shows a much wider whorl cross section (ww/wh = 1.25–1.50) than *A. mojsisovicsi* (ww/wh = 0.95–1.00) in the adult stage.

Alibashites mojsisovicsi differs from the species of *Abichites*, which may develop a similar adult stage, in the coarse subadult ventrolateral nodes.

Stratigraphical range. *Paratirolites* Limestone; 1.90 to 1.15 m below the extinction horizon (*Alibashites mojsisovicsi* Zone and lower part of the *Abichites abichi* Zone).

Alibashites ferdowsii sp. nov.
(Fig. 30)

Derivation of name. After Hakim Abu ’l-Qasim Ferdowsi Tusi (940–1020), important and influential Persian poet and author of the epic Shahnameh.

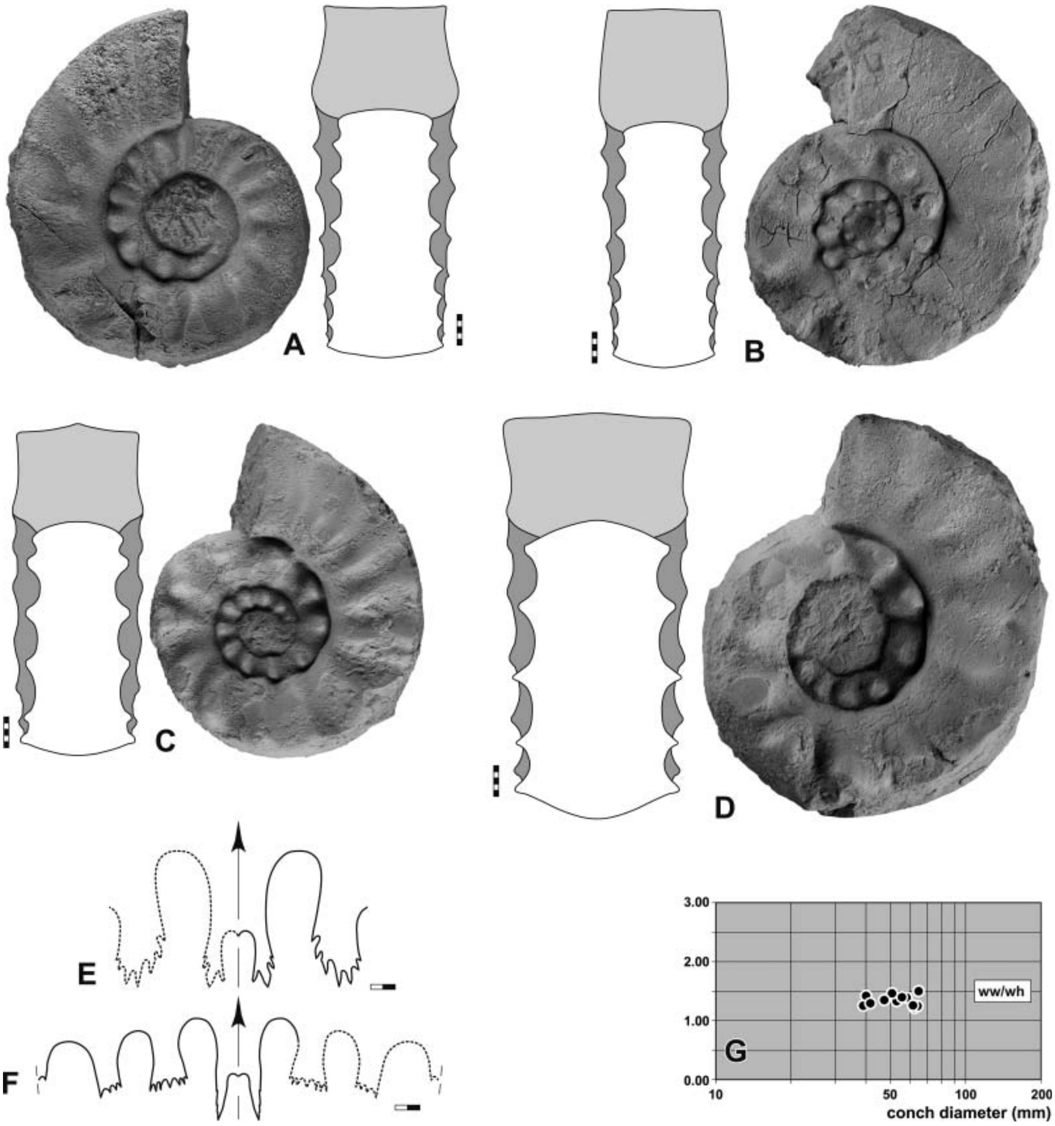

Figure 30. *Alibashites ferdowsii* sp. nov. **A−D,** lateral and dorsal views; **A,** holotype, MB.C.25327, Aras Valley, float; **B,** paratype, MB.C.25328, Aras Valley, float; **C,** paratype, MB.C.25329, Ali Bashi N, float; **D,** paratype, MB.C.25330, Aras Valley, −1.75 m. **E, F,** suture lines; **E,** paratype, MB.C.25331, Ali Bashi N, float; at 14.0 mm wh; **F,** paratype, MB.C.25328, Aras Valley, float; at 16.0 mm ww, 11.6 mm wh. **G,** whorl cross section proportions. Scale bars: A−D = 5 mm; E, F = 2 mm.

Holotype. MB.C.25327 (Figs 30A).

Type locality and horizon. Aras Valley section; float of the *Paratirolites* Limestone (probably *Stoyanowites dieneri* Zone).

Material. Eight specimens (Aras Valley, Ali Bashi N).

Diagnosis. *Alibashites* with a conch reaching 100 mm dm. Subadult stage with circular to subtrapezoidal, weakly depressed whorl cross section (ww/wh = 1.25−1.50) and broadly rounded venter; 10−12 very coarse ventrolateral nodes. Adult stage with subtrapezoidal and weakly depressed whorl cross section (ww/wh = 1.20−1.50) with converging flanks, almost flat venter and angular ventrolateral shoulder; sharp ribs on the flanks, forming short dorsolateral nodes and stronger ventrolateral nodes. Prongs of the external lobe variable in shape, bifid to multiply serrated; altogether 15−18 notches of the E, A and L lobes.

Description. Holotype MB.C.25327 (Aras Valley, float; 58 mm conch diameter) shows a part of the body chamber (less than half volution) and about one fairly well preserved volution of the phragmocone (Fig. 30A). The conch is thinly discoidal and subevolute in the last volution (ww/dm = 0.42; uw/dm = 0.42) and shows a subtrapezoidal, ventrally depressed whorl cross section (ww/wh = 1.38). The whorls are, in the adult stage, thickest at the broadly rounded umbilical margin and the flanks converge slowly toward the subangular ventrolateral shoulder. This separates the shallow tectiform venter from the flanks. The last preserved volution displays the transition from the strongly ribbed subadult stage with prominent conical ventrolateral nodes into the adult stage with sharp ribs and low elongate dorsolateral and ventrolateral nodes.

Paratype MB.C.25329 (Aras Valley, −1.75 m; 53 mm conch diameter) closely resembles the holotype in conch shape and sculpture. Differences can be seen in the shape of the venter, which in specimen MB.C.25330 shows a shallow keel on the last half volution (Fig. 30C).

Morphologically similar are also paratypes MB. C.25330 (Ali Bashi N, float; 65 mm dm; Fig. 30D) and MB.C.25328 (Aras Valley, float; 58 mm dm; Fig. 30B). MB.C.25330 shows a rather well-rounded venter until 48 mm conch diameter.

The suture line is somewhat variable in the new species. The two figured paratypes MB.C.25331 (Fig. 30E) and MB.C.25328 (Fig. 30F) differ in the pronunciation of the secondary notches of the external lobe (rather large in MB.C. 25331, but barely visible in MB.C.25328), and in the shape of the adventive lobe (deep and semicircular in MB.C.25331, but flattened in MB.C.25328).

Remarks. This species shows an intermediate morphological position between the genera *Paratirolites* and *Abichites*. Characteristic for *Paratirolites* is the intermediate growth stage with trapezoidal whorl cross section with the prominent conical ventrolateral nodes; similar to *Abichites* is the flat venter in the adult stage. The intermediate position of *Alibashites ferdowsii* is also visible in the suture line; on the one side is the more complex external lobe in *Paratirolites* (with serrated prongs of the external lobe), and on the other side is *Abichites* (with a trend towards unserrated prongs of the external lobe).

Alibashites ferdowsii differs from *A. mojsisovicsi* in the wide and weakly depressed whorl cross section (ww/wh = 1.25−1.50) and in the ribbed adult stage, which displays dorsolateral as well as ventrolateral nodes.

Stratigraphical range. *Paratirolites* Limestone; 1.85 to 1.45 m below the extinction horizon (*Alibashites mojsisovicsi* Zone and lowest part of the *Abichites abichi* Zone).

Alibashites uncinatus sp. nov.
(Fig. 31)

Derivation of name. From the Latin *uncinatus* = hook shaped, because of the form of the ribs.

Holotype. MB.C.25335 (Fig. 31A).

Type locality and horizon. Aras Valley section; 1.90 m below the top of the *Paratirolites* Limestone (*Stoyanowites dieneri* Zone).

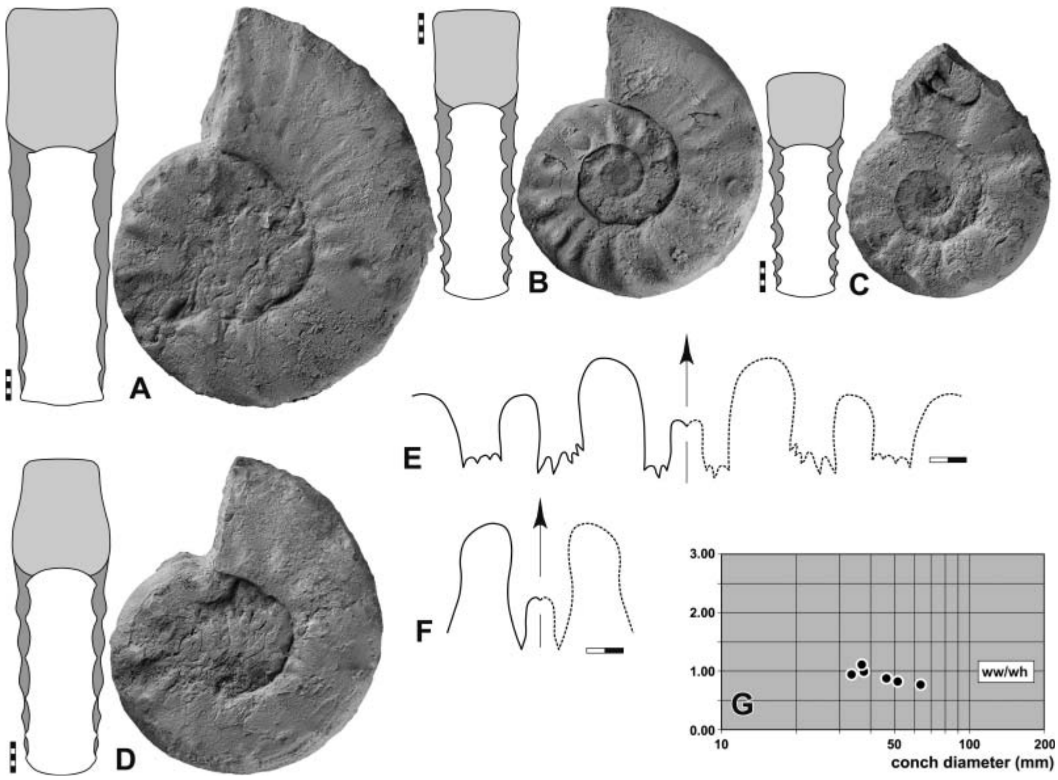

Figure 31. *Alibashites uncinatus* sp. nov. **A−D,** lateral and dorsal views; **A,** holotype, MB.C.25335, Aras Valley, −1.90 m; **B,** paratype, MB.C.25336, Aras Valley, float; **C,** paratype, MB.C.25337, Aras Valley, float; **D,** paratype, MB.C.25338, Aras Valley, −1.45 m. **E, F,** suture lines; **E,** holotype, MB.C.25335, at 13.2 mm wh; **F,** paratype, MB.C.25338, at 12.3 mm wh. **G,** whorl cross section proportions. Scale bars: A−D = 5 mm; E, F = 2 mm.

Material. Ten specimens (Aras Valley, Ali Bashi N, Ali Bashi 4).

Diagnosis. *Alibashites* with a conch reaching 85 mm dm. Subadult stage with trapezoidal whorl cross section (ww/wh = 1.00) and flattened venter; 10−12 shallow ribs forming pointed dorsolateral and ventrolateral nodes. Adult stage with subtrapezoidal and weakly compressed whorl cross section (ww/wh = 0.70−0.80), flattened or concave venter and angular ventrolateral shoulder; weak dense ribs on the flanks, forming weak nodes in the ventrolateral area. Prongs of the external lobe simple to multiply serrated; altogether 12−16 notches of the E, A and L lobes.

Description. Holotype MB.C.25335 (Aras Valley, −1.90 m) is a fairly well preserved specimen with 64 mm conch diameter (Fig. 31A). It displays the transformation from the subadult into the adult stage, characterized by the change of the whorl cross section from trapezoidal (widest in the ventrolateral area) to subtrapezoidal (widest near the umbilicus). The ornament changes parallel to the whorl cross-section shape: the subadult stage shows coarse ribs with conical ventrolateral nodes, while the adult stage possesses weaker ribs with dorsolateral nodes and weaker ventrolateral nodes.

Similar conch proportions can be seen in paratype MB. C.25338 (Aras Valley, −1.95 m) at 51 mm conch diameter. This specimen shows a subtrapezoidal whorl cross section, which is widest near the rounded umbilical margin. The slightly concave flanks converge towards the flattened, barely convex venter (Fig. 31D). One volution earlier, the whorl cross section is trapezoidal and widest in the ventrolateral area. A transformation of the ornament is also visible on the last volution; the ventrolateral conical nodes lose their strength while the dorsolateral nodes become more prominent.

The smaller paratypes MB.C.25336 and MB.C.25337 (both Aras Valley, float) display, at 46 and 37 mm conch diameter, respectively, the subtrapezoidal whorl cross section of the subadult stage. In both specimens the ventrolateral nodes show a hook-shaped ending; they are the dominant ornament feature (Fig. 31B, C).

The suture line of holotype MB.C.25335 possesses a rather wide external lobe with nearly parallel flanks (Fig. 31E). The prongs show a trifurcation at the base and the adventive and lateral lobes have five and four small notches, respectively. The suture line of specimen MB. C.25338 differs in the simple and narrow external lobe without any secondary serration (Fig. 31F).

Remarks. *Alibashites uncinatus* differs from *A. stepanovi* in the shape of the subadult whorl cross section, which is wider (ww/wh = 1.00) than in *A. uncinatus* (ww/wh = 0.70−0.80). Another distinguishing feature is the more pronounced ventrolateral nodes in the subadult stage of *S. unicatus*. *Alibashites mojsisovicsi* possesses much coarser ventrolateral nodes in the subadult stage.

Stratigraphical range. *Paratirolites* Limestone; 1.95 to 1.45 m below the extinction horizon (uppermost part of the *Stoyanowites dieneri* Zone and lowest part of the *Abichites abichi* Zone).

Alibashites stepanovi sp. nov.
(Fig. 32)

1973 *Paratirolites mojsisovicsi* (Stoyanow); Teichert & Kummel in Teichert *et al.*: pl. 6, fig. 8, 9, pl. 7, fig. 6.

Derivation of name. Named after D. L. Stepanov, one of the pioneers of Permian−Triassic stratigraphy in the Ali Bashi Mountains.

Holotype. MB.C.25345 (Fig. 32).

Type locality and horizon. Ali Bashi M section; 1.60 m below the top of the *Paratirolites* Limestone (*Stoyanowites dieneri* Zone).

Material. Twenty-six specimens (Aras Valley, Ali Bashi N, Ali Bashi M).

Diagnosis. *Alibashites* with a conch reaching 110 mm dm. Subadult stage with trapezoidal, weakly compressed whorl cross section (ww/wh = 0.70−0.80) and rounded venter; 25 biconvex ribs forming small umbilical nodes and ending in elongate ventrolateral nodes. Adult stage with subtrapezoidal, weakly compressed whorl cross section (ww/wh = 0.60−0.70) and moderately wide umbilicus (uw/dm = 0.40−0.45), flattened venter and subangular ventrolateral shoulder; very weak dense ribs on the flanks, coarsest in the dorsolateral and ventrolateral areas. Prongs of the external lobe usually bifid; 9−15 notches of the E, A and L lobes.

Description. Holotype MB.C.25345 (Ali Bashi M, −1.60 m) is at 83 mm conch diameter the largest of the specimens (Fig. 32A). It is incomplete, with the last half volution belonging to the body chamber. At this stage, the conch is extremely discoidal and subevolute (ww/dm = 0.22; uw/dm = 0.42) with a weakly compressed whorl cross section (ww/wh = 0.70). The whorls are widest near the rounded umbilical wall and converge slowly towards the subangular ventrolateral shoulder. The flanks are slightly concave and the venter is flat. The ornament consists of weak ribs on the phragmocone, forming elongate sharp nodes in the dorsolateral and ventrolateral areas. The ornament is very similar on the body chamber, but the ribs are more numerous (20 on half a volution) and weaker.

The two smaller paratypes MB.C.25346 and MB. C.25347 (Aras Valley, −1.85 m), both with 60 mm conch diameter, are very similar in their conch proportions and

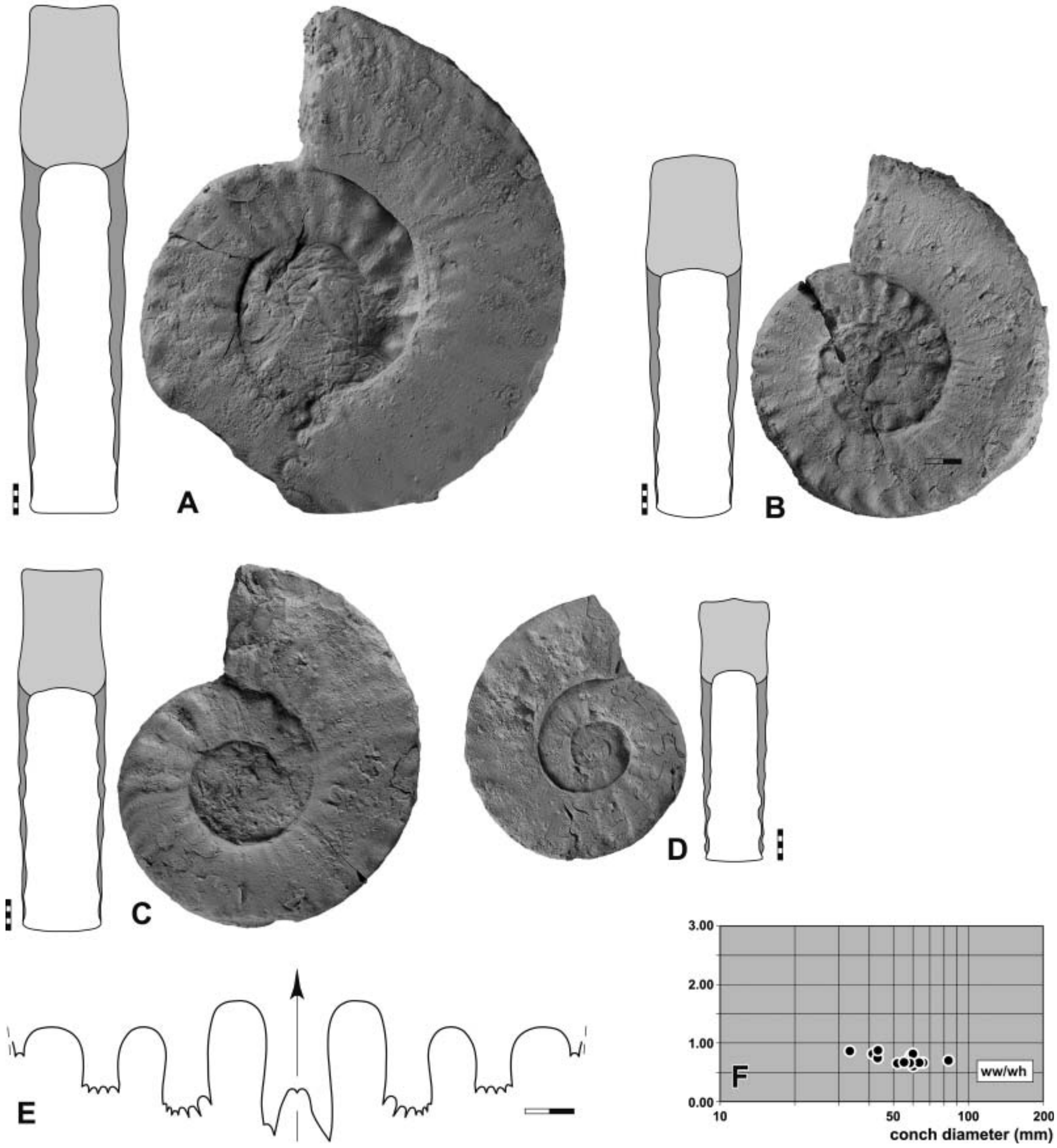

Figure 32. *Alibashites stepanovi* sp. nov. **A–D,** lateral and dorsal views; **A,** holotype, MB.C.25345, Ali Bashi M, −1.60 m; **B,** paratype, MB.C.25346, Aras Valley, −1.85 m; **C,** paratype, MB.C.25347, Aras Valley, −1.85 m; **D,** paratype, MB.C.25348, Aras Valley, −1.45 m; **E,** paratype, MB.C.25348, suture line at 9.3 mm ww, 10.0 mm wh. **F,** whorl cross section proportions. Scale bars: A–D = 5 mm; E = 2 mm.

ornament (Fig. 32B, C). They differ only in the shape of the whorl cross section, with the first specimen showing nearly parallel flanks but the second showing slightly concave flanks. Furthermore, specimen MB.C.25346 shows weaker riblets on the body chamber in comparison with specimen MB.C.25347.

Paratype MB.C.25348 (Aras Valley, −1.45 m) shows the immature morphology and ornament at 43 mm diameter (Fig. 32D). The conch proportions are similar to those seen in the larger specimens; the flanks are slightly trapezoidal and the venter is a flattened tectiform.

The suture line of paratype MB.C.25348 has, at 10 mm wh, a rather simple external lobe, which is asymmetrical with respect to secondary subdivision (one prong being subdivided into two notches). The flanks of the external lobe are parallel, the ventrolateral saddle is nearly symmetrical and the adventive and lateral lobes show parallel flanks. They are subdivided into seven and five secondary notches, respectively (Fig. 32E).

Remarks. *Alibashites stepanovi* differs from the superficially similar *Stoyanowites dieneri* in the converging flanks of the adult stage and much denser ribs, which in *A. stepanovi* are short but in *S. dieneri* are developed into longer spines. A similar species is *A. uncinatus*, but this species has a stouter subadult stage (ww/wh = 1.00, in contrast to 0.70−0.80 in *A. stepanovi*) and coarser ventrolateral nodes in the subadult stage.

Stratigraphical range. *Paratirolites* Limestone; 1.90 to 1.45 m below the extinction horizon (*Alibashites mojsisovicsi* Zone and lowermost part of the *Abichites abichi* Zone).

Genus *Abichites* Shevyrev, 1965

Type species. *Kashmirites*? *stoyanowi* Kiparisova, 1947 by original designation.

Included species. *Abichites abichi* Shevyrev, 1965 (Azerbaijan); *Abichites alibashiensis* sp. nov. (North-west Iran); *Abichites ariaeii* sp. nov. (North-west Iran); *Abichites paucinodus* sp. nov. (North-west Iran); *Abichites shahriari* sp. nov. (North-west Iran); *Kashmirites*? *stoyanowi* Kiparisova, 1947 (Azerbaijan); *Abichites subtrapezoidalis* sp. nov. (North-west Iran); *Abichites terminalis* sp. nov. (North-west Iran).

Diagnosis. Representatives of the family Dzhulfitidae with small to moderately large conch; maximum adult diameters are between 30 and 90 mm. Adult stage with quadrate, rectangular or oval whorl cross section. Subadult stage with weak to moderately strong lateral ribs; adult stage with weak ornament. Suture line with deep external lobe; the depths of the external lobe and adventive lobe are nearly identical.

Remarks. The species of *Abichites* show a quadrate, rectangular or oval adult whorl cross section with parallel flanks, subangular or angular ventrolateral shoulder and flattened venter. The ontogeny shows a rather sudden morphological change from the more or less strongly ribbed intermediate stage to the more delicately ribbed adult stage.

A comparison of the newly collected material from the North-west Iranian localities with the specimens described by Shevyrev (1965, 1968) from Dorasham indicates some differences: '*A. mojsisovicsi*' is better placed in another genus based on the shape of the whorl profile. The figured specimen of *A. stoyanowi* has a more compressed whorl cross section (ww/dm = 0.25; ww/wh = 0.70–0.90) than any of the specimens from North-west Iran. This discrepancy cannot be explained here.

Within the genus *Abichites*, two morphological trends can be observed, and in this respect the genus displays a morphological evolution like that of *Paratirolites*:

1. A significant size decrease, from a maximum conch diameter of 90 mm in the stratigraphically older species to 25–30 mm in the stratigraphically youngest species.
2. A simplification of the suture lines, visible in the decreased number of sutural notches.

Shevyrev (1965, 1968) illustrated four suture lines of the three species included by him in the genus *Abichites* (including *A. mojsisovicsi*). These suture lines were drawn from specimens between 10 and 13 mm whorl height – that is, corresponding to a phragmocone diameter of 30–40 mm. Three of the four suture lines show serrated prongs of the external lobe. This is in striking contrast to this study, in which the majority of the material shows simple lanceolate prongs of the external lobe.

Species of *Abichites* were found to occur only in the upper half of the *Paratirolites* limestone; they show a successive stratigraphical occurrence with limited overlaps. The stratigraphical succession (in metres below the top of the *Paratirolites* Limestone) of the species is *A. subtrapezoidalis* (2.10–1.45 m) – *A. abichi* (1.50–0.65 m) – *A. alibashiensis* (1.40–0.50 m) – *A. ariaeii* (1.15–0.70 m) – *A. stoyanowi* (0.95–0.35 m) – *A. paucinodus* (0.70–0.35 m) as well as *A. shahriari* and *A. terminalis* in the uppermost beds of the *Paratirolites* Limestone. Serrated prongs of the external lobe have been found particularly in the stratigraphically older species, whereas the two youngest species usually show simple prongs. According to the conch shape and sculpture, the stratigraphically successive species of *Abichites* may not represent a morphocline and probably not a phylogenetic sequence.

Suture lines of a number of specimens between 3.0 and 14.5 mm whorl height (i.e. corresponding to a phragmocone diameter between 9 and 45 mm) are presented here to demonstrate the wide variability within the material. It is evident that specimens which share the same conch morphology and sculpture may differ strikingly in the outline of the external lobe. In some cases, asymmetrical external lobes can be seen, and larger specimens tend to more often possess serrated lobes.

Abichites subtrapezoidalis sp. nov.
(Figs 33, 34)

Derivation of name. Named after the subtrapezoidal whorl cross section.

Holotype. MB.C.25371 (Fig. 33D).

Type locality and horizon. Aras Valley section (North-west Iran); *Paratirolites* Limestone.

Material. Eighteen specimens (Aras Valley, Ali Bashi N, Ali Bashi 4).

Diagnosis. *Abichites* with a conch reaching 90 mm dm. Subadult stage with circular, weakly compressed to depressed whorl cross section (ww/wh = 0.90–1.10) and rounded venter; 20 weak ribs per volution. Adult stage with a subtrapezoidal or quadrate, weakly depressed whorl cross section (ww/wh = 1.00–1.05), venter nearly flat; numerous sharp ribs forming sharp dorsolateral and

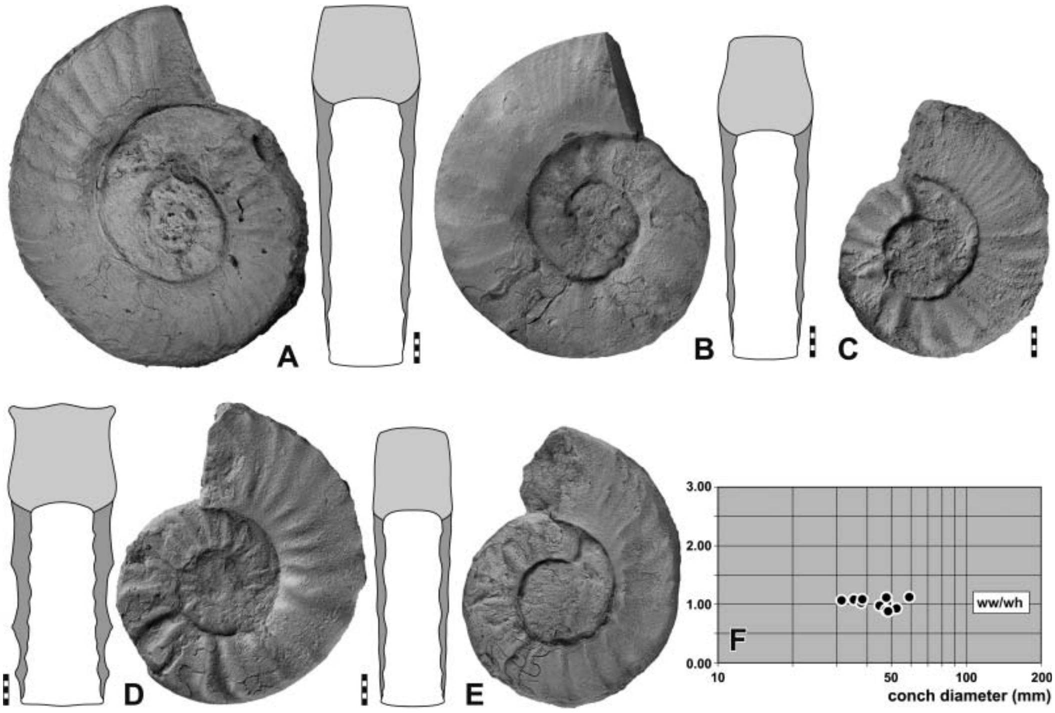

Figure 33. *Abichites subtrapezoidalis* sp. nov. **A–E,** lateral and dorsal views; **A,** paratype, MB.C.25372, Aras Valley, float; **B,** paratype, MB.C.25373, Ali Bashi 4, −2.01 m; **C,** paratype, MB.C.25374, Aras Valley, −1.45 m; **D,** holotype, MB.C.25371, Aras Valley, float; **E,** paratype, MB.C.25375, Aras Valley, float. **F,** conch proportions. Scale bars = 5 mm.

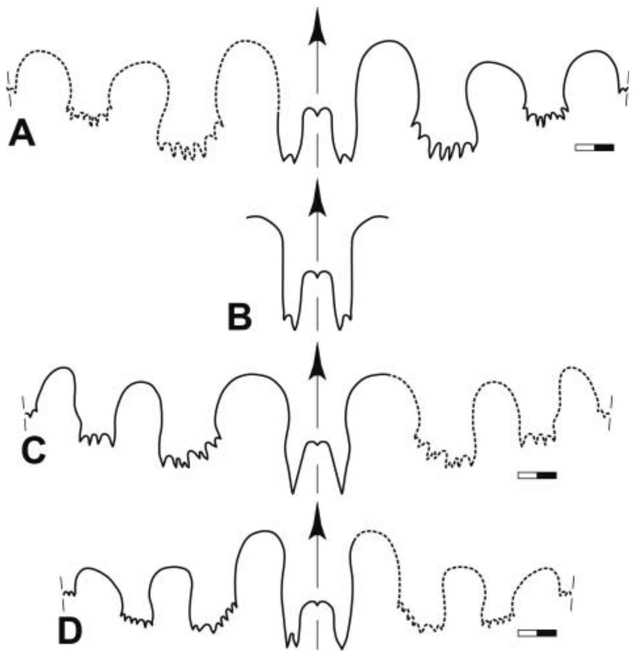

Figure 34. *Abichites subtrapezoidalis* sp. nov., suture lines. **A,** paratype, MB.C.25372, Aras Valley, float; at 11.7 mm ww, 14.6 mm wh; **B,** paratype, MB.C.25373, Ali Bashi 4, −2.01 m; at 12.0 mm ww, 12.3 mm wh; **C,** holotype, MB.C.25371, Aras Valley, float; at 33.8 mm dm, 13.4 mm ww, 11.4 mm wh; **D,** paratype, MB.C.25375, Aras Valley, float; at 9.7 mm ww, 9.5 mm wh. Scale bars = 2 mm.

ventrolateral nodes. Prongs of the external lobe simple or bifid; altogether 12−13 notches of the E, A and L lobes.

Description. Paratype MB.C.25373 (Ali Bashi 4, −2.01 m) is extremely discoidal and widely umbilicate (ww/dm = 0.29; uw/dm = 0.46). The whorl cross section is subquadrate (ww/wh = 0.92) and widest near the rounded umbilical margin, from where the flanks converge concavely towards the sharp ventrolateral shoulder that separates the flank from the flattened venter (Fig. 33B). The last third of the last volution belongs to the body chamber; on this the sculpture consists of faint ribs, which are sharpest near the umbilicus and fade out towards the venter. The phragmocone is poorly preserved but shows weak and rounded ribs.

Paratype MB.C.25372 (Aras Valley, float) with 59 mm conch diameter is very similar in conch shape and ornament but has a weakly depressed whorl cross section (ww/wh = 1.11) (Fig. 33A). This specimen shows the suture line (drawn at 14.6 mm wh, corresponding to a conch diameter of about 50 mm) with a parallel-sided external lobe and bifid prongs. The adventive lobe and also the lateral lobe are strongly serrated with seven and eight small notches, respectively (Fig. 34A).

Holotype MB.C.25371 (Aras Valley, float) has a diameter of 48 mm and shows the last part of the phragmocone with septal crowding at 35 mm diameter as well as a part of the body chamber (Fig. 33D). Its general conch

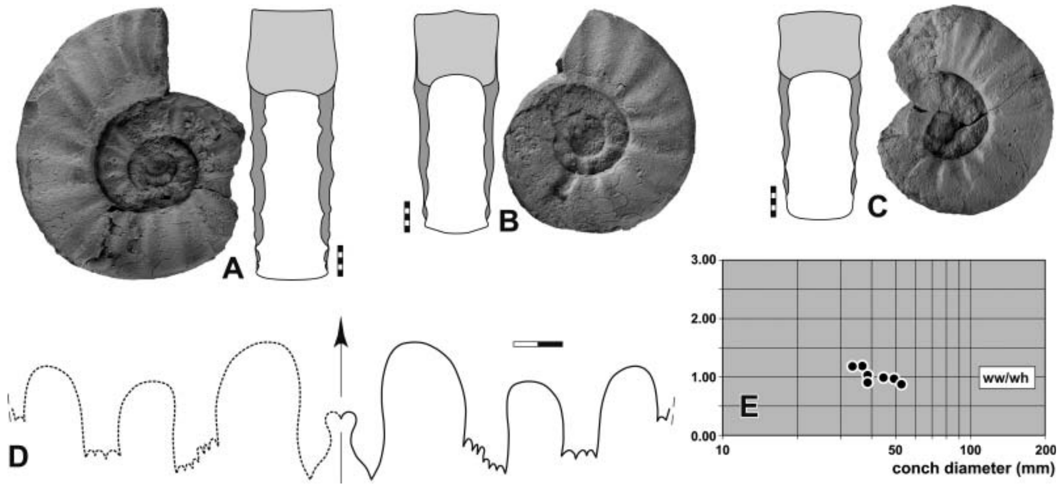

Figure 35. *Abichites abichi* Shevyrev, 1965. **A–C,** lateral and dorsal views; **A,** MB.C.25389, Ali Bashi 1, −0.65 m; **B,** MB.C.25390, Ali Bashi N, −0.85; **C,** MB.C.25391, Ali Bashi N, −0.85 m. **D,** MB.C.25389, suture line at 32.3 mm dm, 14.4 mm ww, 11.8 mm wh. **E,** whorl cross section proportions. Scale bars: A–C = 5 mm; D = 2 mm.

morphology is thinly discoidal and subevolute (ww/dm = 0.35; uw/dm = 0.43) with a moderate coiling rate (WER = 2.22). The phragmocone displays a circular whorl cross section and possesses sharp, slightly curved ribs on the flank (two per volution). Shape and sculpture change on the body chamber; the whorl cross section is quadrate (ww/wh = 1.02) with slightly concave flanks that are separated from the flattened venter by an angular ventrolateral shoulder. The ribs become weaker and form sharp and elongate dorsolateral and ventrolateral nodes on the body chamber. The suture line of holotype MB. C.25371 (drawn at 9.7 mm wh) possesses a pouched external lobe with lanceolate, unserrated prongs, a broadly rounded inflated ventrolateral saddle and a multiply serrated adventive lobe (Fig. 34C).

Paratype MB.C.25375 (Aras Valley, float; 9.5 mm wh, corresponding to a phragmocone diameter of 30 mm) displays a suture line with a slightly pouched external lobe with subparallel flanks (Fig. 34D). The lobe shows differently shaped prongs; one is lanceolate and the other is bifid. The ventrolateral saddle as well as the lateral saddle are nearly symmetrical and have parallel flanks. The adventive lobe has a position on the outer flank; it is slightly asymmetrical like the lateral lobe and strongly serrated.

Remarks. *Abichites subtrapezoidalis* differs from the other species of *Abichites* in the whorl cross section, which in this species is widest near the umbilicus and shows flanks converging toward the flattened venter. In this respect it resembles *A. ferdowsii*, which, however, possesses coarse conical ventrolateral nodes in the subadult stage. The adult ornament of *A. subtrapezoidalis* consists of fine sharp ribs, which form sharp elongate nodes around the umbilicus and on the outer flanks; this separates the species from most of the others, which possess coarse ribs or subadult ventrolateral nodes.

Stratigraphical range. *Paratirolites* Limestone; 2.10 to 1.45 m below the extinction horizon (*Stoyanowites dieneri* Zone and lowest part of the *Abichites abichi* Zone).

Abichites abichi Shevyrev, 1965 (Fig. 35)

1910 *Xenodiscus* aff. *kapila* (Diener); Stoyanow: 87, pl. 9, fig. 3.
1965 *Abichites abichi* Shevyrev: 181, pl. 24, fig. 4.
1968 *Abichites abichi* Shevyrev; Shevyrev: 96, pl. 4, fig. 4.

Holotype. PIN 1252/137; illustrated by Shevyrev (1965, pl. 24, fig. 4).

Type locality and horizon. Dorasham 2 section; *Paratirolites* Limestone.

Material. Ten specimens (Aras Valley, Ali Bashi N, Ali Bashi 4, Ali Bashi 1, Ali Bashi P).

Diagnosis. *Abichites* with a conch reaching 75 mm dm. Subadult stage with subquadrate, weakly depressed to compressed whorl cross section (ww/wh = 1.20) and slightly flattened venter; with 15 rounded straight ribs on the flanks. Adult stage with quadrate whorl cross section (ww/wh = 1.00), parallel flanks and flattened venter; with weak rounded ribs on the flanks. Prongs of the external lobe usually simple; 7–12 notches of the E, A and L lobes.

Description. Specimen MB.C.25389 (Ali Bashi 1, −0.65 m) is an incomplete specimen with 44.5 mm conch diameter. Preserved are a part of the body chamber (less then half of the last volution) and one and a half volutions of the phragmocone (Fig. 35A). The conch is extremely discoidal and subevolute in the last volution (ww/dm = 0.33; uw/dm = 0.42) and possesses, at the largest diameter, a quadrate whorl cross section (ww/wh = 1.00) with slightly concave flanks and venter. The flanks are separated from the tabulate venter by an angular edge. The last volution displays 20 sharp ribs, which form weak umbilical nodes. The penultimate volution shows rounded ribs.

The suture line of specimen MB.C.25389 (drawn at 32 mm dm) shows a parallel-sided external lobe with simple, slightly pouched prongs (Fig. 35D). The adventive lobe is asymmetrical and deeper on the umbilical side; it is serrated with seven small notches. The lateral lobe has only four notches.

The two smaller specimens MB.C.25390 (Fig. 35B) and MB.C.25391 (Fig. 35C) (both Ali Bashi N, −0.85 m) with 37 and 34 mm diameter, respectively, are similar in conch shape and ornament. They differ from specimen MB. C.25389 in the subquadrate, ventrally depressed whorl cross section (ww/wh = 1.18). The venter is a flattened tectiform in the two specimens.

Remarks. *Abichites abichi* differs from the otherwise similar species *A. subtrapezoidalis* in the quadrate adult whorl cross section (subtrapezoidal in *A. subtrapezoidalis*). The body chamber of *A. abichi* has stronger ribs than *A. subtrapezoidalis* does. *Abichites alibashiensis* has a similar body chamber, but differs from *A. abichi* in the coarse ventrolateral nodes of the subadult stage.

Stratigraphical range. *Paratirolites* Limestone; 1.50 to 0.65 m below the extinction horizon (*Abichites abichi* Zone and lower part of the *Abichites stoyanowi* Zone).

Abichites alibashiensis sp. nov.
(Fig. 36)

1910 *Balatonites* (?) cf. *euryomphalus*; Stoyanow: 91, pl. 7, fig. 6.

Derivation of name. Named after the Ali Bashi Mountains.

Holotype. BM2011-072 (Fig. 36A).

Type locality and horizon. Ali Bashi N section; 1.40 m below the top of the *Paratirolites* Limestone (*Stoyanowites dieneri* Zone).

Material. Eleven specimens (Aras Valley, Ali Bashi N, Ali Bashi 1).

Diagnosis. *Abichites* with a conch reaching 70 mm dm. Subadult stage with oval, weakly depressed whorl cross section (ww/wh = 1.25) and slightly flattened venter; 12 prominent midflank ribs. Adult stage with quadrate and weakly depressed whorl cross section (ww/wh = 1.10−1.25), flattened venter and subangular ventrolateral shoulder; sharp ribs on the flanks. Prongs of the external lobe simple or bifid; 7−10 notches of the E, A and L lobes.

Description. Holotype MB.C.25399 (Ali Bashi N, −1.40 m) is an incomplete specimen with 48 mm conch diameter; only a quarter of a volution of the phragmocone and half a volution of the body chamber are preserved (Fig. 36A). It is extremely discoidal and subevolute (ww/dm = 0.31; uw/dm = 0.44) with a quadrate, weakly depressed whorl cross section (ww/wh = 1.06). The last portion of the phragmocone shows wide-standing and coarse ribs on the outer flank; they end in prominent elongate ventrolateral nodes. The ribs are much weaker on the body chamber, where they are more densely spaced, sharper and ending in small ventrolateral nodes. The flat venter is smooth.

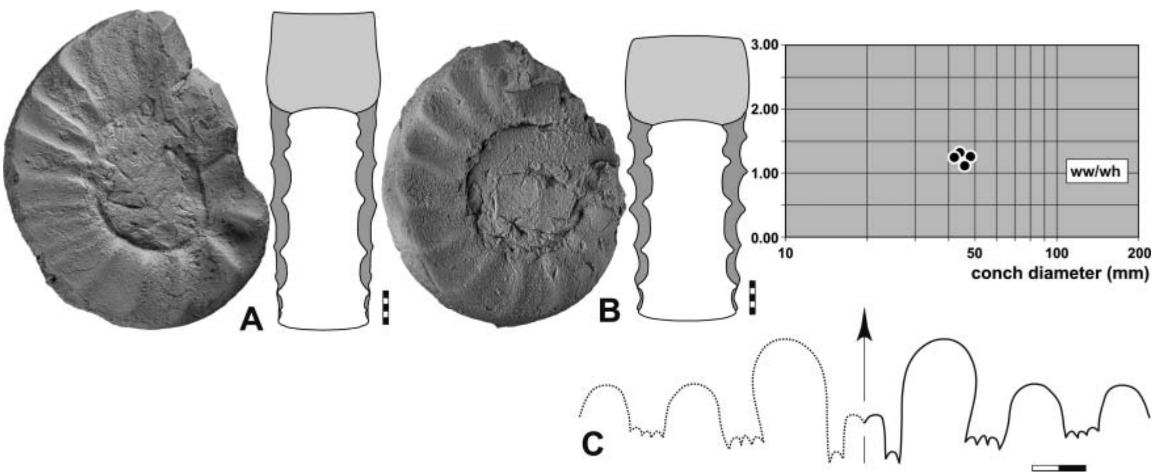

Figure 36. *Abichites alibashiensis* sp. nov. **A, B,** lateral and dorsal views; **A,** holotype, MB.C.25399, Ali Bashi N, −1.40 m; **B,** paratype MB.C.25400, Ali Bashi 1, −0.71 m; **C,** holotype, MB.C.25399, suture line at 9.7 mm wh. **D,** whorl cross section proportions. Scale bars: A, B = 5 mm; C = 2 mm.

The suture line of the holotype (drawn at 9.7 mm wh, corresponding to a phragmocone diameter of 30 mm), shows a parallel-sided external lobe with bifid prongs (Fig. 36C). The ventrolateral saddle is slightly inflated, the parallel-sided adventive lobe has four small secondary notches and the lateral lobe has a similar shape with four notches.

Remarks. *Abichites alibashiensis* differs from *A. abichi*, *A. stoyanowi* and *A. subtrapezoidalis* in the sharp ribs of the subadult stage. Species of *Alibashites* possess subadult ribs but also ventrolateral nodes; these are *A. mojsisovicsi* (with very weak adult ribs) and *A. ferdowsii* (with a much more compressed whorl cross section).

Stratigraphical range. *Paratirolites* Limestone; 1.40 to 0.50 m below the extinction horizon (*Abichites abichi* Zone and lower part of the *Abichites stoyanowi* Zone).

Abichites ariaeii sp. nov.
(Fig. 37)

Derivation of name. Named after Ali Asghar Ariaei, the father of the geology of Eastern Iran.

Holotype. MB.C.25410 (Fig. 37A).

Type locality and horizon. Ali Bashi N locality; 1.15 m below the top of the *Paratirolites* Limestone (*Stoyanowites dieneri* Zone).

Material. Nine specimens (Aras Valley, Ali Bashi N, Ali Bashi 4, Ali Bashi P).

Diagnosis. *Abichites* with a conch reaching 85 mm dm. Subadult stage with oval, weakly compressed whorl cross section (ww/wh = 0.85–1.00) and rounded venter; 20–25 low and rounded midflank ribs. Adult stage with subquadrate and weakly compressed whorl cross section (ww/wh = 0.85–1.00), rounded venter and rounded ventrolateral shoulder but transformed into a totally flat venter at the end of the body chamber; weak and low ribs on the flanks. Prongs of the external lobe simple; 7–9 notches of the E, A and L lobes.

Description. The largest of the specimens is holotype MB.C.25410 (Ali Bashi N, −1.15 m) with 60 mm conch diameter (Fig. 37A). It is incompletely preserved, but displays the adult morphology, in which the conch is extremely discoidal and subevolute (ww/dm = 0.29; uw/dm = 0.40) with a nearly quadrate whorl cross section (ww/dm = 0.96). The whorls are widest in the midflank area and converge slightly towards the angular ventrolateral shoulder. The venter is nearly flat in this growth stage, but flattening of the venter appears only during the last half volution. The sculpture is visible on the last one and a quarter whorls; it consists of rounded ribs, which appear to be strongest on the outer flank. The venter is smooth.

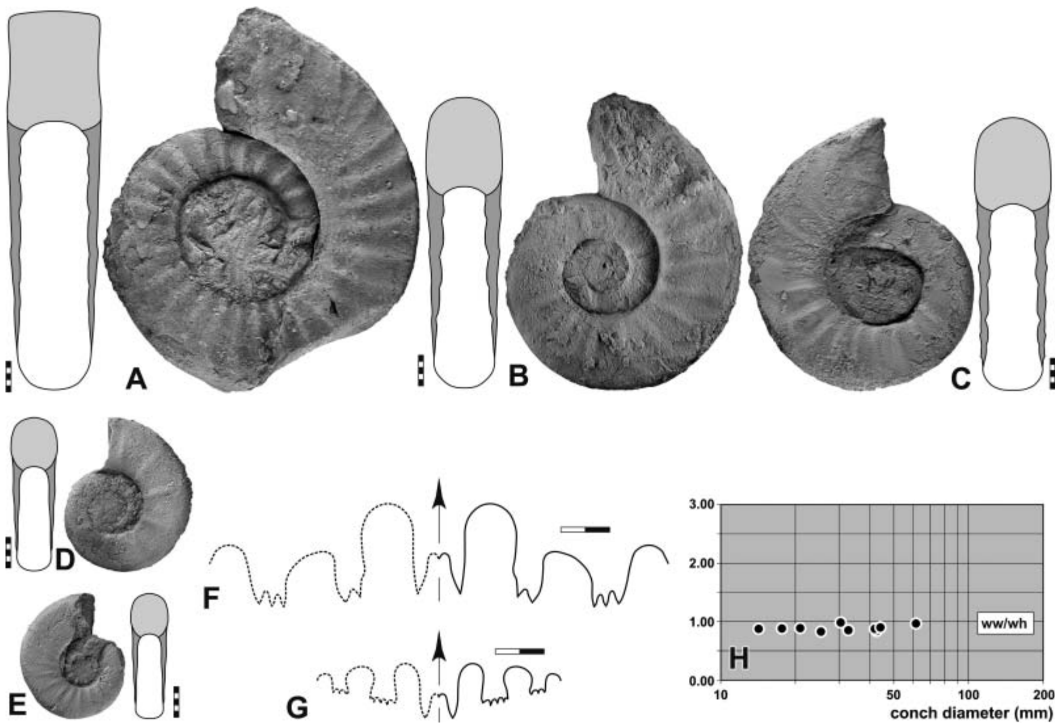

Figure 37. *Abichites ariaeii* sp. nov. **A–E,** lateral and dorsal views; **A,** holotype, MB.C.25410, Ali Bashi N, −1.15 m; **B,** paratype, MB.C.25411, Ali Bashi P, −0.70 m; **C,** paratype, MB.C.25412, Ali Bashi 4, −0.75 m; **D,** paratype, MB.C.25413, Aras Valley, −0.85 m; **E,** paratype, MB.C.25414, Aras Valley, −0.75 m. **F, G,** suture lines; **F,** paratype, MB.C.25412, at 8.1 mm ww, 7.4 mm wh; **G,** paratype, MB.C.25414, at 4.5 mm ww, 4.5 mm wh. **H,** whorl cross section proportions. Scale bars: A–E = 5 mm; F, G = 2 mm.

Paratype MB.C.25411 (Ali Bashi P, −0.70 m) is an incomplete specimen with 43 mm conch diameter; it shows a part of the body chamber (more than half of the last volution) and one volution of the phragmocone (Fig. 37B). The conch is extremely discoidal and subevolute in the last volution (ww/dm = 0.29; uw/dm = 0.43) and shows, at the largest diameter, an oval, laterally compressed whorl cross section (ww/wh = 0.84) with a rounded venter. The sculpture consists of 20 ribs on the last volution; they are shallow, rounded and strongest on the inner flank, and extend in a slightly projected direction.

Paratype MB.C.25412 (Ali Bashi N, −0.75 m; 42 mm conch diameter) is very similar to the holotype in conch shape (ww/dm = 0.30; uw/dm = 0.43) and ornament (Fig. 37C). In this specimen, the ribs are confined to the inner flank area.

The suture line of paratype MB.C.25412, drawn at 7.5 mm wh (about 24 mm phragmocone diameter) shows a parallel-sided external lobe with narrow lanceolate prongs (Fig. 37F). The ventrolateral saddle is slightly asymmetrical and broadly rounded. The adventive and lateral lobes have a position on the flank; the first possesses two notches and the latter three.

Remarks. *Abichites ariaeii* differs from the other species of the genus in the rounded venter present throughout most of its ontogeny. Unlike other species, which possess a longer adult stage with a flat venter, only the last portion of the body chamber has a flattened venter. The ornament of *A. ariaeii* shows only rather weak, rounded ribs on the flank, which is in contrast to most of the other species, which have sharp ribs or ventrolateral nodes.

Stratigraphical range. *Paratirolites* Limestone; 1.15 to 0.70 m below the extinction horizon (upper part of the *Abichites abichi* Zone and lower part of the *Abichites stoyanowi* Zone).

Abichites stoyanowi (Kiparisova, 1947)
(Fig. 38)

1910 *Xenodiscus radians* (Waagen); Stoyanow: 86, pl. 9, fig. 5.
1910 *Xenodiscus* sp. indet. Stoyanow: 87, pl. 9, fig. 6.
1947 *Kashmirites*? *stoyanowi* Kiparisova in Voinova *et al.*: 149, pl. 35, fig. 1.
1965 *Abichites stoyanowi* Kiparisova; Shevyrev: 179, pl. 24, figs 2, 3.
1968 *Abichites stoyanowi* Kiparisova; Shevyrev: 94, pl. 3, fig. 5, pl. 4, fig. 2.
2014b *Abichites stoyanowi* Kiparisova; Korn in Ghaderi *et al.*, text-fig. 7H.

Lectotype. The specimen figured by Stoyanow (1910, pl. 9, fig. 5).

Type locality and horizon. Dorasham (Azerbaijan); *Paratirolites* Limestone.

Material. Twenty specimens (Aras Valley, Ali Bashi N, Ali Bashi 1, Ali Bashi P).

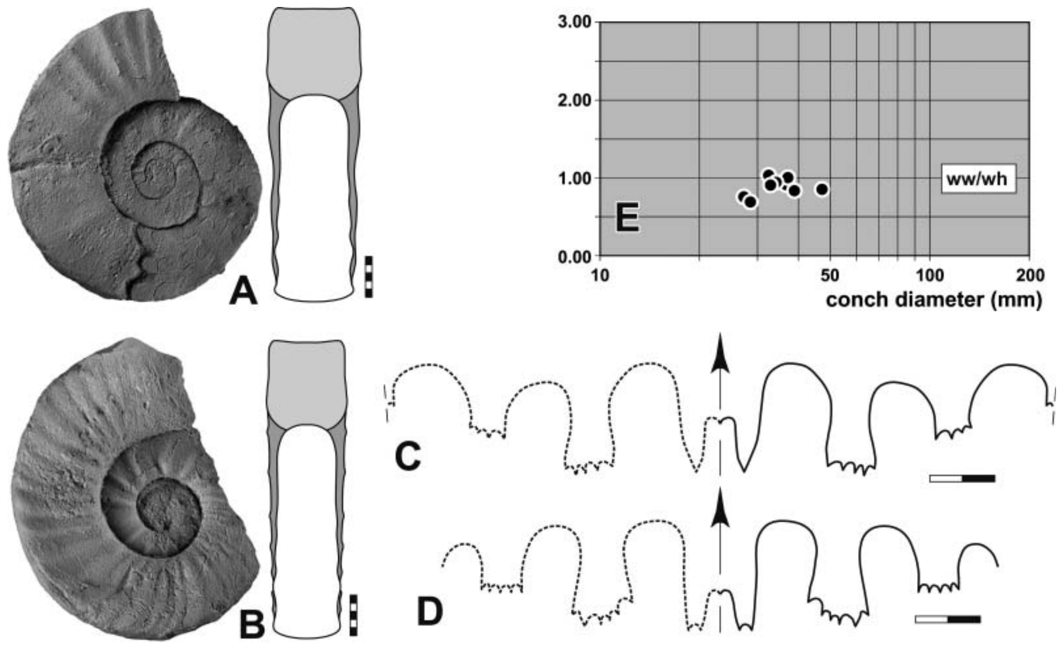

Figure 38. *Abichites stoyanowi* (Kiparisova, 1947). **A, B,** lateral and dorsal views; **A,** MB.C.25419, Ali Bashi N, −0.35 m; **B,** MB.C.25420, Ali Bashi N, float. **C, D,** suture lines; **C,** MB.C.25419, at 9.9 mm wh; **D,** MB.C.25420, at 7.5 mm ww, 9.6 mm wh. **E,** whorl cross section proportions. Scale bars: A, B = 5 mm; C, D = 2 mm.

Diagnosis. *Abichites* with a conch reaching 70 mm dm. Subadult stage with circular, weakly compressed whorl cross section (ww/wh = 0.90−1.00) and rounded venter; 16−20 moderately weak ribs per volution. Adult stage with quadrate and weakly compressed whorl cross section (ww/wh = 0.90−1.00), flat venter and subangular to angular ventrolateral shoulder; altogether 12−14 sharp concavo-convex ribs per half volution on the flanks. Prongs of the external lobe simple or bifid; 7−11 notches of the E, A and L lobes.

Description. Specimen MB.C.25420 (Ali Bashi N, −0.35 m) has 37 mm conch diameter and shows the beginning of the terminal body chamber at 28 mm dm (Fig. 38B). The body chamber has a quadrate whorl cross section (ww/wh = 1.00) with slightly concave flanks, a sharp ventrolateral margin and a slightly concave venter. The body chamber possesses rather sharp, linear ribs on the flanks and the phragmocone has rounded ribs with wide distances between them.

Specimen MB.C.25419 (Ali Bashi N, float), with 36 mm conch diameter, is rather well preserved and allows the study of the intermediate growth stage (Fig. 38A). It is extremely discoidal and subevolute (ww/dm = 0.30; uw/dm = 0.41) with a subquadrate whorl cross section (ww/wh = 0.91). The whorl is widest near the rounded umbilical margin, from where the flanks converge barely towards the sharp ventrolateral shoulder that separates the flank from the slightly concave venter. This specimen shows sharp and slightly sigmoidal ribs on the last volution, while the inner whorls possess straight and rounded ribs.

The two figured suture lines are similar in their general outline. However, they differ in the prongs of the external lobe, which are bifid in specimen MB.C.25420 (Fig. 38D) and simple in specimen MB.C.25419 (Fig. 38C).

Remarks. *Abichites stoyanowi* differs from *A. ariaeii* in the shape of the venter, which in *A. ariaeii* is rounded and flat only in the last growth stage but which becomes flat much earlier in *A. stoyanowi*. *Abichites abichi* is another similar species, but possesses much stronger ribs. *Abichites subtrapezoidalis* has a similar whorl cross section, but only very weak riblets around the umbilicus on the adult body chamber.

Stratigraphical range. *Paratirolites* Limestone; 0.95 to 0.30 m below the extinction horizon (*Abichites stoyanowi* Zone).

Abichites paucinodus sp. nov.
(Fig. 39)

Derivation of name. From the Latin *pauci* = few, and *nodus* = node, because of the few lateral nodes in the subadult stage.

Holotype. MB.C.25439 (Fig. 39A).

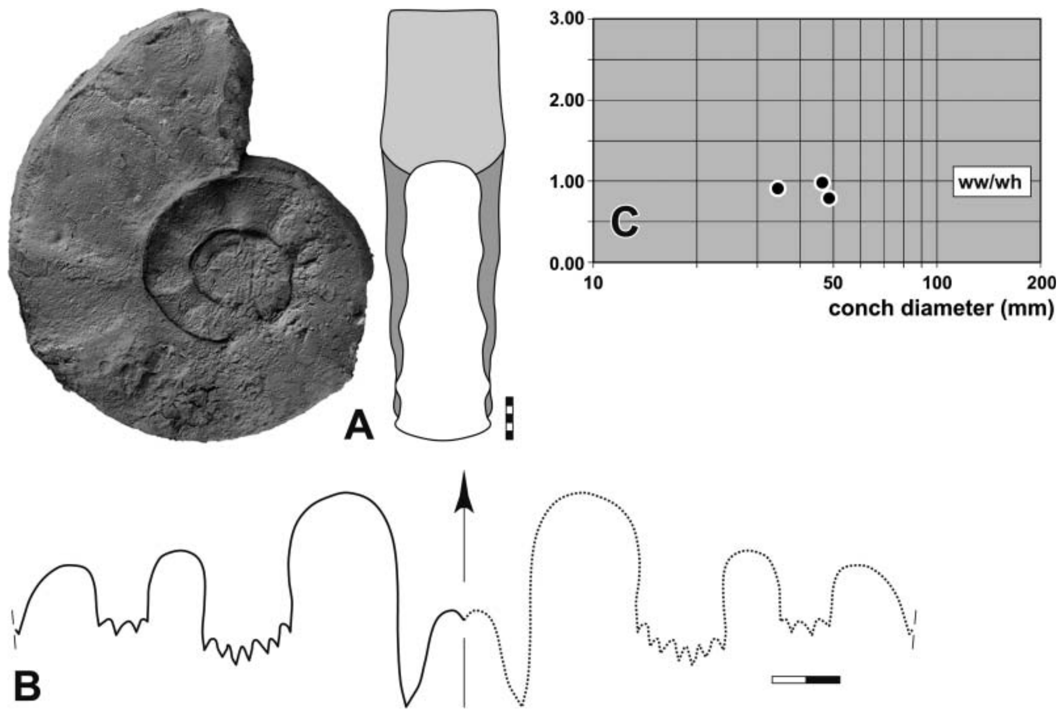

Figure 39. *Abichites paucinodus* sp. nov., holotype, MB.C.25439, Ali Bashi N, −0.35 m. **A,** lateral and dorsal views; **B,** suture line at 14.4 mm wh; **C,** whorl cross section proportions. Scale bars: A = 5 mm; B = 2 mm.

Type locality and horizon. Ali Bashi N section; 0.35 m below the top of the *Paratirolites* Limestone (*Abichites stoyanowi* Zone).

Material. Six specimens (Aras Valley, Ali Bashi N, Ali Bashi 1).

Diagnosis. *Abichites* with a conch reaching 65 mm dm. Subadult stage with oval, weakly compressed whorl cross section (ww/wh = 0.90−1.00) and rounded venter; eight low and rounded midflank ribs. Adult stage with rectangular and weakly compressed whorl cross section (ww/wh = 0.80−1.00), flattened venter and angular ventrolateral shoulder; few weak and low ribs on the flanks. Prongs of the external lobe simple; 9−12 notches of the E, A and L lobes.

Description. Holotype MB.C.25439 (Ali Bashi N, −0.35 m) is a somewhat corroded specimen with 49 mm conch diameter; a segment of 100° of the body chamber is preserved (Fig. 39A). The conch shape is extremely discoidal and subevolute (ww/dm = 0.30; uw/dm = 0.38) with a weakly compressed rectangular whorl cross section (ww/wh = 0.78) and a rather high coiling rate (WER = 2.34). The body chamber shows the transformation of the rounded venter in the subadult stage towards the flattened adult form. The sculpture of the body chamber consists of wide-standing low and rounded radial ribs, which form weak dorsolateral and ventrolateral nodes.

The suture line of holotype MB.C.25439 (drawn at 14.4 mm whorl height, corresponding to a phragmocone diameter of 44 mm) has a rectangular external lobe with parallel flanks and narrow V-shaped unserrated prongs (Fig. 39B). The adventive lobe is serrated with seven secondary notches, and the lateral lobe has four notches.

Remarks. *Abichites paucinodus* differs from the other species of *Abichites* in the narrower umbilicus (uw/dm less than 0.40 in *A. paucinodus*, but 0.43 in most of the other species).

Stratigraphical range. *Paratirolites* Limestone; 0.75 to 0.35 m below the extinction horizon (*Abichites stoyanowi* Zone).

Abichites shahriari sp. nov.
(Fig. 40)

Derivation of name. After Mohammad-Hossein Shahriar (1906−1988), the last poet of the lineage of classical legendary Iranian Azerbaijani poets.

Holotype. MB.C.25445 (Fig. 40A).

Type locality and horizon. Ali Bashi N section; *Paratirolites* Limestone (probably *Arasella minuta* Zone).

Material. Two specimens (Aras Valley, Ali Bashi N).

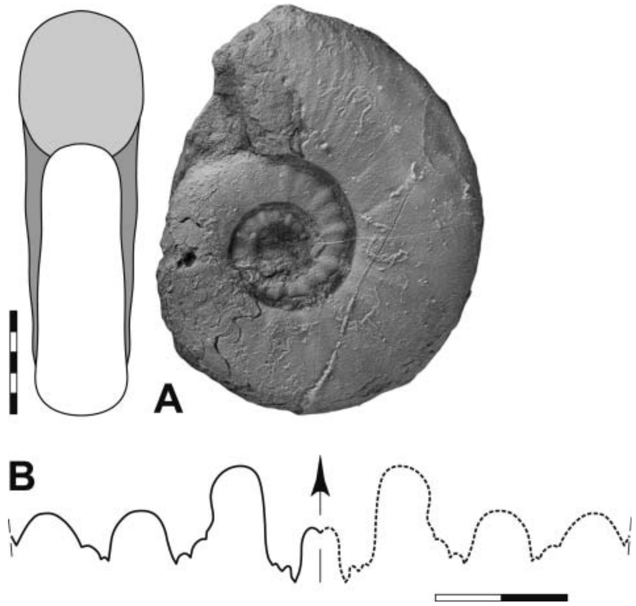

Figure 40. *Abichites shahriari* sp. nov., holotype MB.C.25445, Ali Bashi N, float. **A,** lateral and dorsal views; **B,** suture line at 12.0 mm dm, 3.6 mm wh. Scale bars: A, B = 5 mm; C = 2 mm.

Diagnosis. *Abichites* with a conch reaching 25 mm dm. Subadult and adult stage with oval, weakly compressed whorl cross section and rounded venter; 15 weak midflank ribs per volution. Adult stage with oval and weakly compressed whorl cross section (ww/wh = 0.85−0.90) and rounded venter; very faint riblets on the flanks. Prongs of the external lobe trifid; nine notches of the E, A and L lobes.

Description. Holotype MB.C.25445 (Ali Bashi N, float) is a slightly weathered specimen of 20 mm conch diameter, of which a little more than half a volution belongs to the body chamber (Fig. 40A). The conch is subevolute (uw/dm = 0.37) with an oval, weakly compressed whorl profile (ww/wh = 0.86). The ornament shows 15 rounded ribs on one volution on the phragmocone, but on the body chamber the ornament is weakened and forms weak blunt riblets, which extend in a forwards direction across the flanks and wedge out near the venter.

The suture line of holotype MB.C.25445 has, at 12 mm phragmocone diameter, a rather wide external lobe with slightly diverging flanks and with slightly serrated asymmetrical prongs (Fig. 40B). On the flanks follow the similarly asymmetrical adventive and lateral lobes, both of which possess three little notches.

Discussion. *Abichites shahriari* differs from *A. stoyanowi* in the smaller size (reaching only about half of the conch diameter) and in the profile of the adult whorl, which is oval in *A. shahriari* but rectangular in *A. stoyanowi*. *Abichites ariaeii* has a similar whorl profile but differs in the much coarser ribs at comparable conch diameters. *Abichites shahriari* differs from *A. terminalis*

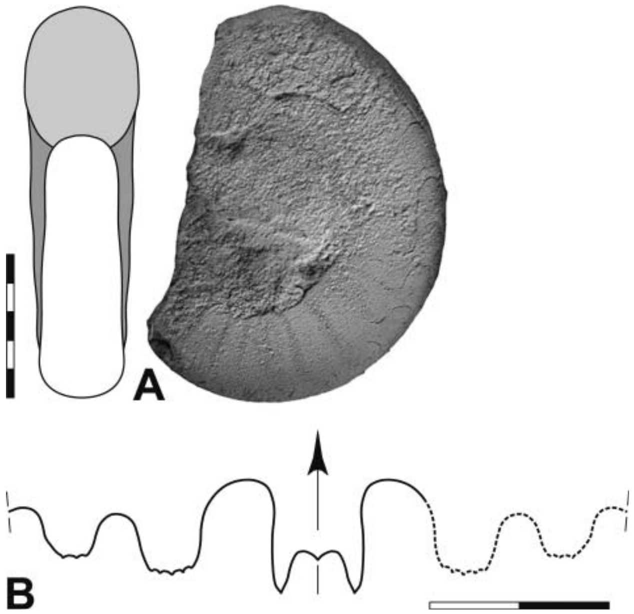

Figure 41. *Abichites terminalis* sp. nov., holotype MB.C.25447, Ali Bashi P, float. **A,** lateral and dorsal views; **B,** suture line at 2.9 mm wh. Scale bars: A = 5 mm; B = 2 mm.

in the wider whorl profile (ww/dm = 0.85 in *A. shahriari* but only 0.75 in *A. terminalis*) and the much coarser ornament.

Stratigraphical range. Top horizon of the *Paratirolites* Limestone (*Arasella minuta* Zone).

Abichites terminalis sp. nov.
(Fig. 41)

Derivation of name. From Latin *terminalis* = belonging to the boundary, because of its occurrence at the extinction horizon.

Holotype. MB.C.25447 (Fig. 41A).

Type locality and horizon. Ali Bashi P section; uppermost horizon of the *Paratirolites* Limestone (*Arasella minuta* Zone).

Material. Four specimens (Ali Bashi N, Ali Bashi P).

Diagnosis. *Abichites* with a conch reaching 20 mm dm. Subadult and adult stage with oval, weakly compressed whorl cross section and rounded venter; very weak mid-flank riblets. Adult stage with oval and weakly compressed whorl cross section (ww/wh = 0.75–0.80) and rounded venter; extremely faint riblets on the flanks. Prongs of the external lobe simple; A and L lobes rounded with very small notches.

Description. Holotype MB.C.25447 is an incomplete specimen with 11 mm diameter; it is subevolute with a weakly compressed oval whorl profile (uw/dm = 0.37; ww/wh = 0.76) and a rounded venter (Fig. 41A). The chambered portion of the specimen displays shallow straight riblets on the flank, while the body chamber appears to be nearly smooth.

The suture line of the holotype has, at 3 mm whorl height (corresponding to a phragmocone diameter of about 9 mm), a slightly pouched external lobe with nearly parallel flanks (Fig. 41B); the prongs of the external lobe are narrow and simple. Both the adventive and the lateral lobe are slightly asymmetrical; they possess a very weak serration at the bases.

Remarks. *Abichites terminalis* differs from *A. shahriari* in the narrower, more compressed whorl profile and the much weaker ornament in the subadult stage.

Stratigraphical range. Top horizon of the *Paratirolites* Limestone (*Arasella minuta* Zone).

Genus ***Stoyanowites*** Korn, 2014

Type species. *Paratirolites Dieneri* Stoyanow, 1910.

Included species. *Stoyanowites aspinosus* sp. nov. (North-west Iran); *Paratirolites dieneri* Stoyanow, 1910 (Azerbaijan).

Diagnosis. Representatives of the family Dzhulfitidae with moderately large conch; maximum adult diameters are between 80 and 95 mm. Subadult and adult stages with rectangular and compressed whorl cross section. Subadult stage with weak to moderately strong lateral ribs; adult stage with weak ornament. Suture line with an external lobe that is much shorter than the adventive lobe.

Remarks. *Stoyanowites* is separated by most of the other genera of the family Dzhulfitidae by the short external lobe, which does not reach the depth of the adventive and lateral lobes. Only *Dzhulfites* is similar in this respect, but this genus is characterized by coarse ventrolateral nodes absent in *Stoyanowites*.

Stoyanowites dieneri (Stoyanow, 1910)
(Fig. 42)

1910 *Paratirolites dieneri* Stoyanow: 83, pl. 8, fig. 2.
1934 *Paratirolites dieneri* Stoyanow; Spath: 366, text-fig. 125e.
1965 *Paratirolites dieneri* Stoyanow; Shevyrev: 178, pl. 23, figs 2, 3.
1968 *Paratirolites dieneri* Stoyanow; Shevyrev: 93, pl. 3, figs 2, 3.
1973 *Paratirolites mojsisovicsi* Stoyanow; Teichert & Kummel in Teichert *et al.*: pl. 7, fig. 1.
2014b *Stoyanowites dieneri* (Stoyanow); Korn in Ghaderi *et al.*, text-fig. 7F.

Lectotype. The specimen figured by Stoyanow (1910, pl. 8, fig. 2).

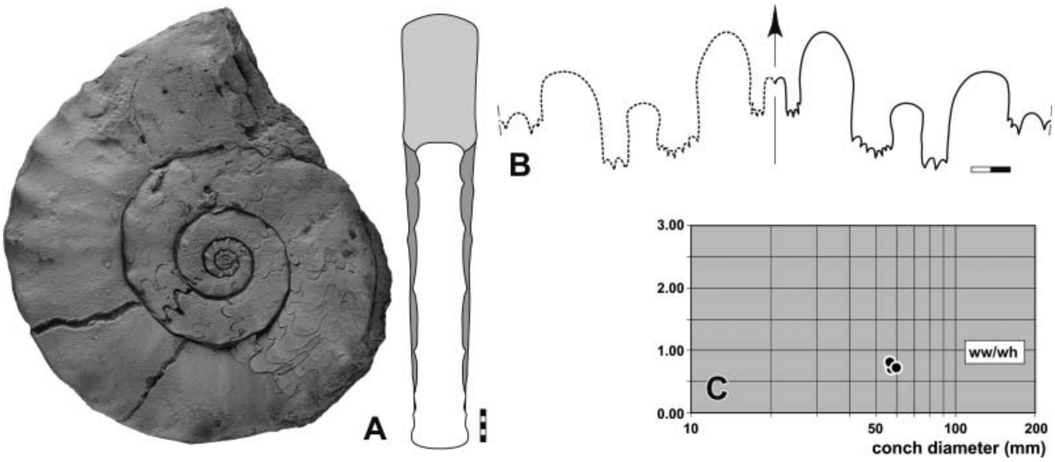

Figure 42. *Stoyanowites dieneri* (Stoyanow, 1910), MB.C.25451, Aras Valley, float. **A,** lateral and dorsal views; **B,** suture line at 12.8 mm wh; **C,** whorl cross section proportions. Scale bars: A = 5 mm; B = 2 mm.

Type locality and horizon. Dorasham section; *Paratirolites* Limestone.

Material. Seven specimens (Aras Valley, Ali Bashi N, Ali Bashi 4).

Diagnosis. *Stoyanowites* with a conch reaching 95 mm dm. Subadult stage with oval, weakly compressed whorl cross section (ww/wh = 0.80) and rounded venter; 16 fine ribs forming weak and rounded dorsolateral and ventrolateral nodes. Adult stage with parallel flanks and weakly compressed whorl cross section (ww/wh = 0.60−0.70), rounded venter and subangular ventrolateral shoulder; weak dorsolateral nodes. Prongs of the external lobe bifid; altogether 10−16 notches of the E, A and L lobes; external lobe shorter than adventive lobe.

Description. Specimen MB.C.25451 (Aras Valley, float) is a slightly deformed and weathered specimen, but still shows a number of conch, ornament and suture details (Fig. 42A). It has a conch diameter of 57 mm and half of the last whorl belongs to the body chamber. The conch is extremely discoidal (ww/dm = 0.21) with a wide umbilicus (uw/dm = 0.49) and a strongly compressed whorl cross section (ww/wh = 0.49). The flattened flanks are parallel and are separated from the flattened venter by an angular margin. Three stages of the ornament can be separated: (1) wide-standing rounded ribs in the juvenile stage; (2) predominance of weak ventrolateral nodes in the subadult stage; and (3) coupled dorsolateral and ventrolateral riblets, the latter being coarser, on the body chamber.

The suture line of specimen MB.C.25451 (13 mm wh, corresponding to a phragmocone diameter of 38 mm) shows a rather small external lobe with subparallel flanks; the prongs are parallel sided and end in a finely serrated base (Fig. 42B). The depth of the external lobe reaches only two-thirds of the adventive lobe; these lobes are separated by a narrowly rounded ventrolateral saddle. Both the adventive lobe and the lateral lobe are parallel sided; the adventive lobe is the wider of the two and possesses seven small notches; the lateral lobe has three notches.

Remarks. *Stoyanowites dieneri* differs from *S. aspinosus* in the presence of dorsolateral nodes and the lack of dense ribs on the body chamber.

Stratigraphical range. *Paratirolites* Limestone; 2.30 to 1.65 m below the extinction horizon (*Stoyanowites dieneri* Zone and *Alibashites mojsisovicsi* Zone).

Stoyanowites aspinosus sp. nov.
(Fig. 43)

Derivation of name. From Latin *spinosus* = spiny, because of the lack of dorsolateral and ventrolateral spines.

Holotype. MB.C.25458 (Fig. 43A).

Type locality and horizon. Aras Valley section; 0.95 m below the top of the *Paratirolites* Limestone (*Abichites stoyanowi* Zone).

Material. Four specimens (Aras Valley, Ali Bashi N).

Diagnosis. *Stoyanowites* with a conch reaching 80 mm dm. Subadult stage with oval, weakly compressed whorl cross section (ww/wh = 0.70) and rounded venter; 15 narrow and rounded ribs on the flanks. Adult stage with oval and weakly compressed whorl cross section (ww/wh = 0.60) and moderately wide umbilicus (uw/dm = 0.40−0.45), rounded venter and rounded ventrolateral shoulder; very weak ribs on the flanks, coarsest in the ventrolateral area. Prongs of the external lobe bifid; 8−9 notches of the E, A and L lobes.

Description. Holotype MB.C.25458 (Aras Valley, −0.95 m) is a slightly weathered specimen with 50 mm conch diameter; one-quarter of the last preserved volution belongs to the body chamber (Fig. 43A). A little more

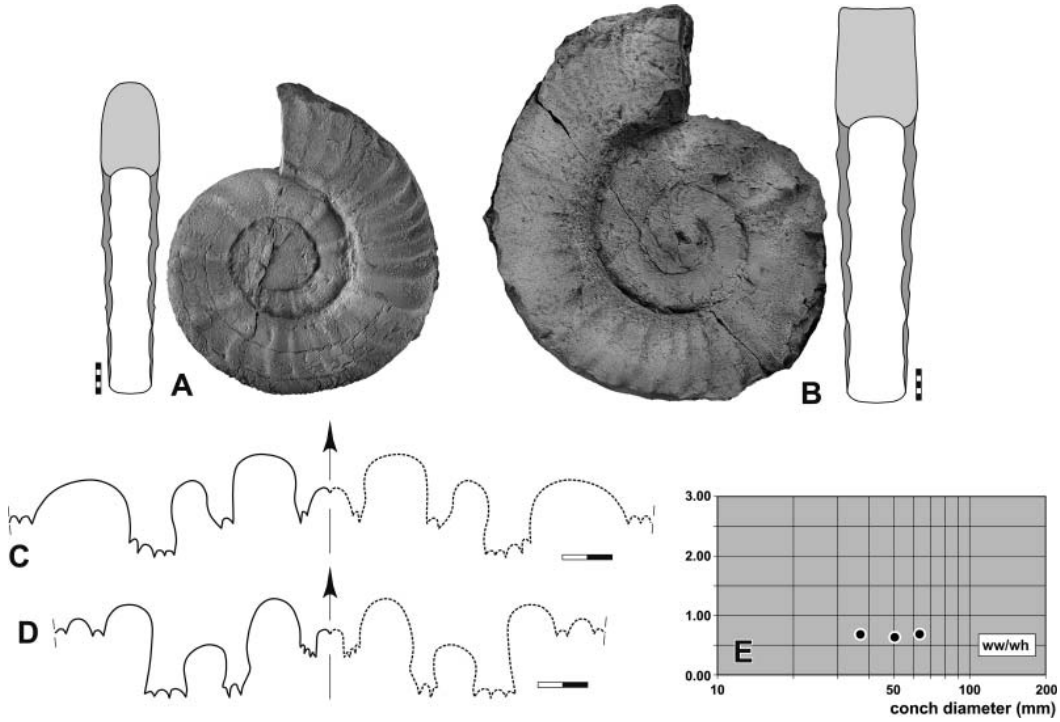

Figure 43. *Stoyanowites aspinosus* sp. nov. **A, B,** lateral and dorsal views; **A,** holotype, MB.C.25458, Aras Valley, −0.95 m; **B,** paratype, MB.C.25459, Ali Bashi N, −1.50 m. **C, D,** suture lines; **C,** holotype, MB.C.25458, at 12.5 mm wh; **D,** paratype, MB.C.25460, Ali Bashi N, float, at 9.0 mm wh. **E,** whorl cross section proportions. Scale bars: A, B = 5 mm; C, D = 2 mm.

than one volution of the phragmocone can be studied. The conch is extremely discoidal and subevolute in the last volution (ww/dm = 0.18; uw/dm = 0.44) and possesses, at the largest diameter, an oval, laterally compressed whorl cross section (ww/wh = 0.63). The coiling rate is moderate (WER = 1.86). A change in the ornament can be observed on the last volution. While the penultimate volution displays straight and rounded riblets arranged in wide distances (five riblets per half volution), the last portion of the phragmocone and the body chamber show a conspicuous tendency toward more densely spaced, sharp and concave riblets. Furthermore the riblets on the penultimate volution show low dorsolateral and ventrolateral nodes, which are not present on the last volution.

The suture line of holotype MB.C.25458 (drawn at 12.5 mm wh, corresponding to a phragmocone diameter of 37 mm) is remarkable because it differs strikingly from most of the other paratirolitid ammonoids. It possesses a parallel-sided, short external lobe with bifid prongs. The adventive lobe is very small and bifid; it reaches only half the depth of the external lobe (Fig. 43C). The lateral lobe is almost twice as wide and deep as the adventive lobe and possesses five secondary notches.

Paratype MB.C.25459 is a somewhat corroded specimen with 64 mm conch diameter (Fig. 43B). Half of the last volution belongs to the body chamber, which shows the transformation from the rounded venter to the flat and slightly concave shape of the venter, then separated by an angular margin from the flattened flanks. The body chamber shows also the changes in the ornament from rather coarse ribs ending in ventrolateral nodes to much finer, densely arranged ribs, which extend with a forward bending on the flank.

The suture line of the smaller paratype MB.C.25460 (Aras Valley, float; drawn at 9 mm wh, corresponding to a phragmocone diameter of 27 mm) has a similar outline (Fig. 43D). Its external lobe is very short and reaches only half the depth of the adventive lobe. Adventive and lateral lobes show the same depth, but the adventive lobe is narrower and is bifid, while the lateral lobe possesses four notches.

Remarks. *Stoyanowites aspinosus* differs from *S. dieneri* in the absence of dorsolateral nodes and the presence of densely spaced curved riblets on the body chamber.

Stratigraphical range. *Paratirolites* Limestone; 1.55 to 0.95 m below the extinction horizon (upper part of the *Stoyanowites dieneri* Zone and *Alibashites mojsisovicsi* Zone).

Family **Xenodiscidae** Frech, 1902

Included genera. *Arasella* Korn, 2014; *Iranites* Teichert & Kummel, 1973; *Phisonites* Shevyrev, 1965; *Shevyrevites* Teichert & Kummel, 1973; *Xenaspis* Waagen, 1879; *Xenodiscus* Waagen, 1879.

Diagnosis. Representatives of the superfamily Xenodiscoidea with small to moderate-sized conch, in which the ontogeny is usually simple with similar juvenile, subadult and adult stages. Suture line with unserrated or weakly serrated, short but rather wide external lobe; adventive, lateral and umbilical lobe often multidentate; some species with a simplified suture line without serrations.

Genus ***Arasella*** Korn, 2014

Type species. *Sinoceltites*? *minutus* Zakharov, 1983.

Remarks. The monospecific genus *Arasella* is a somewhat problematical because of its very simple suture line; an unambiguous attribution to a distinct family is therefore difficult. The shape of the external lobe speaks for placing it in the family Xenodiscidae rather than the Dzhulfitidae. The shape of the conch and the sculpture are similar to *Shevyrevites* from the lower part of the Changhsingian, but this genus has multidentate adventive and lateral lobes.

Arasella minuta (Zakharov, 1983)
(Fig. 44)

1983 *Sinoceltites*? *minutus* Zakharov: 153, pl. 15, fig. 1, 2.
2014 *Arasella minuta* (Zakharov); Korn in Ghaderi *et al*.: text-fig. 7I.

Holotype. BPI 4/813; illustrated by Zakharov (1983, pl. 15, fig. 1).

Type locality and horizon. Akhura (Azerbaijan); probably top of the *Paratirolites* Limestone.

Material. Four specimens (Aras Valley, Ali Bashi N, Ali Bashi 4).

Diagnosis. *Arasella* with a conch reaching 35 mm dm. Subadult and adult stage with circular whorl cross section (ww/wh = 0.85−1.05) and rounded venter; 20−22 sharp ribs on the flanks. External lobe with V-shaped prongs; adventive and lateral lobes broadly rounded.

Description. Specimen MB.C.25462 (Ali Bashi N, −0.10 m) is the best-preserved specimen available for study (Fig. 44A). It has 30 mm conch diameter and gives insight about two whorls, in which the conch shape and ornament does not change. The specimen is extremely discoidal with a wide umbilicus (ww/dm = 0.25; uw/dm = 0.46) and possesses an oval, weakly compressed whorl profile (ww/wh = 0.78) with broadly rounded venter. There are about 24 sharp ribs per volution; they are straight on the flanks and turn forward in the ventrolateral area and then suddenly weaken. The venter is free of ribs.

Specimen MB.C.25463 (Ali Bashi N, −0.30 m) has a conch diameter of 22 mm, but only one volution, half of which belongs to the body chamber, can be studied (Fig. 44B). The conch is extremely discoidal and evolute (ww/dm = 0.29; uw/dm = 0.45) with a circular whorl cross section (ww/wh = 1.02). The ornament consists of about 20 sharp ribs on the flank; some of these ribs end in short ventrolateral spines. The venter is smooth.

The suture line of specimen MB.C.25463 (drawn at 5.6 mm wh) shows a small and short external lobe, which reaches only half the depth of the adventive lobe (Fig. 44C). The prongs of the external lobe are V-shaped. The adventive lobe is the dominant sutural element; it is

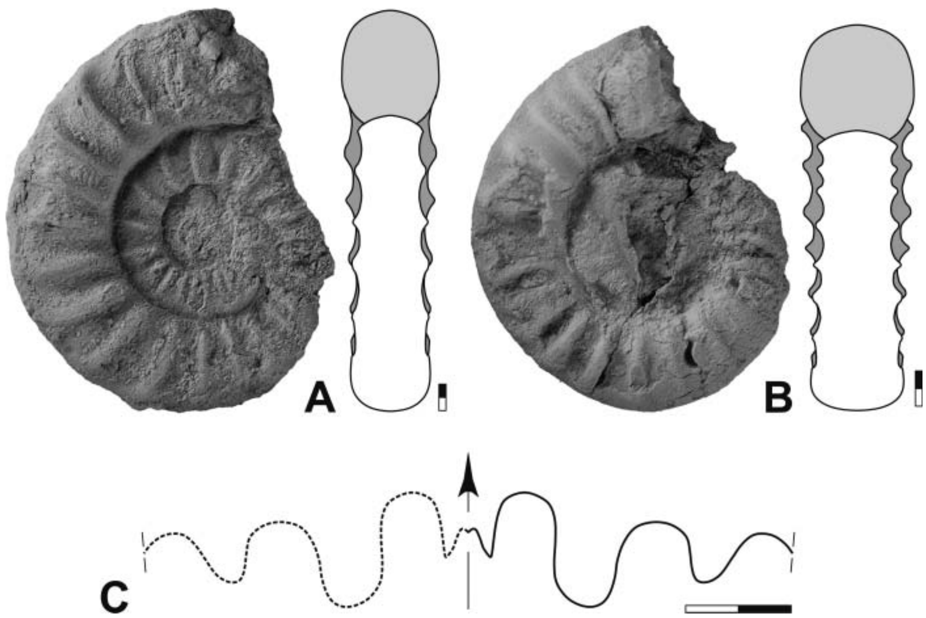

Figure 44. *Arasella minuta* (Zakharov, 1983). **A, B,** lateral and dorsal views; **A,** MB.C.25462, Aras Valley, −0.10 m; **B,** MB.C.25463, Ali Bashi N, −0.30 m. **C,** suture line at 5.6 mm wh, MB.C.25463. Scale bars = 2 mm.

nearly symmetrical and broadly rounded, while the smaller lateral lobe is more asymmetrical and narrowly rounded.

Remarks. *Arasella minuta* can easily be separated from all other ammonoids from the *Paratirolites* Limestone because of its very simple suture line with rounded adventive and lateral lobes and the short external lobe.

Stratigraphical range. *Paratirolites* Limestone; from 0.30 m below up to the extinction horizon (*Arasella minuta* Zone).

Conclusions

The region of Julfa (East Azerbaijan, Iran) and Dzhulfa (Nakhichevan, Azerbaijan) is one of only a few regions worldwide in which fossiliferous Late Permian sedimentary successions with diverse ammonoid assemblages are exposed. In this region, the latest Permian is represented by the 4 to 5 m thick *Paratirolites* Limestone, a deep shelf sediment that spans an interval of about 1.5 million years before the end-Permian mass extinction (Schobben *et al.* 2015).

From the outcrops in the Aras Valley and the Ali Bashi Mountains, we collected about 230 specimens with detailed in situ documentation; they belong to the genera *Neoaganides*, *Pseudogastrioceras*, *Dzhulfites*, *Paratirolites*, *Julfotirolites* gen. nov., *Alibashites* gen. nov., *Abichites*, *Stoyanowites* and *Arasella*. The succession of ammonoid species within the *Paratirolites* Limestone allows for a subdivision of the rock unit into eight biozones (defined by the first occurrence of the zonal index species), in ascending order: *Dzhulfites zalensis* Zone, *Paratirolites trapezoidalis* Zone, *Paratirolites kittli* Zone, *Stoyanowites dieneri* Zone, *Alibashites mojsisovicsi* Zone, *Abichites abichi* Zone, *Abichites stoyanowi* Zone and *Arasella minuta* Zone. With this fine resolution, the ammonoid stratigraphy matches the precision of the conodont stratigraphy (Kozur 2005, 2007; Shen & Mei 2010; Ghaderi *et al*. 2014b).

The material described here is, after the time-equivalent Chinese occurrences, the most diverse assemblage known from the critical interval before the end-Permian mass extinction. It is striking that the two regions (South China and Transcaucasus/North-west Iran) differ significantly in the composition of their ammonoid assemblages. While the family Dzhulfitidae (with the genera *Dzhulfites*, *Paratirolites*, *Julfotirolites*, *Alibashites*, *Abichites*, *Stoyanowites*) is absent in China, the North-west Iranian occurrences did not yield other ceratitid ammonoid families (e.g. Pseudotirolitidae, Pleuronodoceratidae) characteristic in China.

The ammonoid species richness varies within the investigated *Paratirolites* Limestone; the richest interval is in the upper part of the rock unit, followed by a decrease in diversity towards the horizon marking the end-Permian mass extinction.

Acknowledgements

We want to express our thanks to Adel Najafzadeh, Mehdi Abassi and Hossein Hobbi (Aras Free Zone Office, Julfa) for their support with the field sessions. Dieter Weyer (Berlin) is acknowledged for providing ammonoid material from Zal. We further acknowledge the intensive preparation efforts performed by Evelin Stenzel and Markus Brinkmann (Berlin), and the photography of the specimens by Jonas Jahn, Sebastian Sladeczek, Jana Suchocka and Sabine Zachert (Berlin). Many thanks also to Sonny A. Walton (Berlin) for checking the English. DK, LL and MS acknowledge financial support which was provided by the Deutsche Forschungsgemeinschaft (DFG; projects Ko1829/12-1 and Ko2011/8-1). We gratefully acknowledge the constructive peer reviews by Arnaud Brayard (Dijon) and Masayuki Ehiro (Sendai).

Supplemental material

Supplemental material for this article can be accessed here at http://dx.doi.org/10.1080/14772019.2015.1119211

References

Arakelyan, R. A., **Grunt, T. A.** & **Shevyrev, A. A.** 1965. Kratkiy stratigraficheskiy ocherk. *Trudy Paleontologicheskogo Instituta Akademiya Nauk SSSR*, **108**, 20–25.

Bando, Y. 1973. On the Otoceratidae and Ophiceratidae. *Science Report of the Tohoku University, 2nd Series (Geology), Special Volume*, **6**, 337–351.

Bando, Y. 1979. Upper Permian and Lower Triassic ammonoids from Abadeh, Central Iran. *Memoirs of the Faculty of Education, Kagawa University*, **29**, 103–138.

Brayard, A., **Escarguel, G.**, **Bucher, H.**, **Monnet, C.**, **Brühwiler, T.**, **Goudemand, N.**, **Galfetti, T.** & **Guex, J.** 2009. Good genes and good luck: ammonoid diversity and the end-Permian mass extinction. *Science*, **325**, 1118–1121.

Chao, K.-K. 1940. Upper Paleozoic cephalopods from central Hunan, China. *Journal of Paleontology*, **14**, 68–73.

Chao, K.-K. 1965. The Permian ammonoid-bearing formations of South China. *Scientia Sinica*, **14**, 1813–1826.

Diener, K. 1914. Ammoniten aus der Untertrias von Madagaskar. *Sitzungsberichte der Kaiserlichen Akademie der Wissenschaften Klasse*, **123**, 911–922.

Ehiro, M. 1996. Latest Permian ammonoid *Paratirolites* from the Ofunato district, Southern Kitakami Massif, Northeast Japan. *Transactions and Proceedings of the Palaeontological Society of Japan, New Series*, **184**, 592–596.

Frech, F. 1897–1902. *Lethaea geognostica oder Beschreibung und Abbildung der für die Gebirgs-Formationen bezeichnendsten Versteinerungen. I. Theil. Lethaea palaeozoica. 2. Band 4*. Schweizerbart, Stuttgart, pp. 257–452.

Frest, T. J., **Glenister, B. F.** & **Furnish, W. M.** 1981. Pennsylvanian–Permian cheiloceratacean ammonoid families Maximitidae and Pseudohaloritidae. *Journal of Paleontology, Supplement*, **553**, 1–46.

Furnish, W. M. 1966. Ammonoids of the Upper Permian *Cyclolobus*-Zone. *Neues Jahrbuch für Geologie und Paläontologie, Abhandlungen*, **125**, 265–296.

Ghaderi, A., **Ashouri, A. R.**, **Kozur, H. W.** & **Korn, D.** 2013. Age assignment of section 4 of Teichert et al. (1973) at Ali Bashi Mountains (Julfa, NW Iran). *Permophiles*, **58**, 36–40.

Ghaderi, A., **Garbelli, C.**, **Angiolini, L.**, **Ashouri, A. R.**, **Korn, D.**, **Rettori, R.** & **Gharaie, M. H. M.** 2014a. Faunal change near the end-Permian extinction: the brachiopods of the Ali Bashi Mountains, NW Iran. *Rivista Italiana di Paleontologia e Stratigrafia*, **120**, 27–59.

Ghaderi, A., **Leda, L.**, **Schobben, M.**, **Korn, D.** & **Ashouri, A. R.** 2014b. High-resolution stratigraphy of the Changhsingian (Late Permian) successions of NW Iran and the Transcaucasus based on lithological features, conodonts, and ammonoids. *Fossil Record*, **15**, 41–57.

Glenister, B. F. & **Furnish, W. M.** 1981. Permian ammonoids. Pp. 49–64 in M. R. House & J. R. Senior (eds) *The Ammonoidea*. Systematics Association Special Volume, London.

House, M. R. 1988. Major features of cephalopod evolution. Pp. 1–16 in J. Wiedmann & J. Kullmann (eds) *Cephalopods – present and past*. Schweizerbart, Stuttgart.

Hyatt, A. 1883–4. Genera of fossil cephalopods. *Proceedings of the Boston Society of Natural History*, **22**, 253–338.

Joachimski, M. M., **Lai, X. L.**, **Shen, S. Z.**, **Jiang, H. S.**, **Luo, G. M.**, **Chen, B.**, **Chen, J.** & **Sun, Y. D.** 2012. Climate warming in the latest Permian and the Permian–Triassic mass extinction. *Geology*, **40**, 195–198.

Korn, D. 2010. A key for the description of Palaeozoic ammonoids. *Fossil Record*, **13**, 5–12.

Korn, D., **Ebbighausen, V.**, **Bockwinkel, J.** & **Klug, C.** 2003. The A-mode sutural ontogeny in prolecanitid ammonoids. *Palaeontology*, **46**, 1123–1132.

Kozur, H. W. 2005. Pelagic uppermost Permian and the Permian–Triassic boundary conodonts of Iran. Part II: investigated sections and evaluation of the conodont faunas. *Hallesches Jahrbuch für Geowissenschaften, Reihe B, Beiheft*, **19**, 49–86.

Kozur, H. W. 2007. Biostratigraphy and event stratigraphy in Iran around the Permian–Triassic Boundary (PTB): implications for the causes of the PTB biotic crisis. *Global and Planetary Change*, **55**, 155–176.

Kummel, B. 1957. Suborder Ceratitina Hyatt, 1884. Pp. L130–L185 in R. C. Moore (ed.) *Treatise on Invertebrate Paleontology. Part L, Mollusca, Ammonoidea*, *4*. Geological Society of America and University of Kansas Press, Lawrence.

Leda, L., **Korn, D.**, **Ghaderi, A.**, **Hairapetian, V.**, **Struck, U.** & **Reimold, W. U.** 2014. Lithostratigraphy and carbonate microfacies across the Permian–Triassic boundary near Julfa (NW Iran) and in the Baghuk Mountains (Central Iran). *Facies*, **60**, 295–325.

Leonova, T. B. 2002. Permian ammonoids: classification and phylogeny. *Paleontological Journal, Supplement*, **36**, 1–114.

Leonova, T. B. 2011. Permian ammonoids: biostratigraphic, biogeographical, and ecological analysis. *Paleontological Journal*, **45**, 1206–1312.

Liang, X. 1983. New material of Permian ammonoids with discussion on the origin, migration of Araxoceratidae and the horizon of the *Paratirolites*. *Acta Palaeontologica Sinica*, **22**, 606–615.

Liu, Y. Y., **Zhu, Y. M.** & **Tian, W. H.** 1999. New magnetostratigraphic results from Meishan section, Changxing county, Zhejiang province. *Earth Science Journal of China University of Geosciences*, **24**, 151–154.

Mikesh, D., **Glenister, B. F.** & **Furnish, W. M.** 1988. *Stenolobulites* n. gen., Early Permian ancestor of predominantly Late Permian paragastrioceratid subfamily Pseudogastrioceratidae. *The University of Kansas Paleontological Contributions*, **123**, 1–19.

Muttoni, G., **Gaetani, M.**, **Kent, D. V.**, **Sciunnach, D.**, **Angiolini, L.**, **Berra, F.**, **Garzanti, E.**, **Mattei, M.** & **Zanchi, A.** 2009a. Opening of the Neo-Tethys Ocean and the Pangea B to Pangea A transformation during the Permian. *GeoArabia*, **14**(4), 17–48.

Muttoni, G., **Mattei, M.**, **Balini, M.**, **Zanchi, A.**, **Gaetani, M.** & **Berra, F.** 2009b. The drift history of Iran from the Ordovician to the Triassic. *Geological Society of London, Special Publication*, **312**, 7–29.

Plummer, F. B. & **Scott, G.** 1937. Upper Paleozoic ammonites in Texas. *University of Texas Bulletin*, **3701**, 1–516.

Popov, Y. N. 1963. Novyi rod *Daubichites* semeystva Paragastrioceratidae. *Paleontologicheskiy Zhurnal*, **1963**(2), 148–150.

Rostovtsev, K. O. & **Azaryan, N. R.** 1973. The Permian–Triassic boundary in Transcaucasia. *Canadian Society of Petroleum Geologists Memoir*, **2**, 89–99.

Ruzhencev, V. E. 1940. Opyt estestvennoi sistematiki nekotorykh verkhnepaleozoiskikh ammonitov. *Trudy Paleontologicheskogo Instituta Akademiya Nauk SSSR*, **11**, 1–134.

Ruzhencev, V. E. 1950. Verkhnekamennougolnye ammonity Urala. *Trudy Paleontologicheskogo Instituta Akademiya Nauk SSSR*, **29**, 1–220.

Ruzhencev, V. E. 1951. Nizhnepermskie ammonity yuzhnogo Urala. 1. Ammonity Sakmarskogo Yarusa. *Trudy Paleontologicheskogo Instituta Akademiya Nauk SSSR*, **33**, 1–186.

Ruzhencev, V. E. 1952. Biostratigrafiya Sakmarskogo Yarusa v Aktyubinskoy Oblasti Kazakhskoy SSR. *Trudy Paleontologicheskogo Instituta Akademiya Nauk SSSR*, **52**, 1–87.

Ruzhencev, V. E. 1957. Filogeneticheskaya sistema paleozoiskikh ammonoidei. *Byulleten' Moskovskogo obshchestva ispytatelei prirody, otdelenie geologii*, **32**(2), 49–64.

Ruzhencev, V. E. 1959. Klassifikatsia nadsemeystva Otocerataceae. *Paleontologicheskiy Zhurnal*, **1959**(2), 56–67.

Ruzhencev, V. E. 1962. Klassifikatsia semeystve Araxoceratidae. *Paleontologicheskiy Zhurnal*, **1962**(4), 88–103.

Ruzhencev, V. E. 1963. Novye dannye o semeystve Araxoceratidae. *Paleontologicheskiy Zhurnal*, **1963**(3), 56–64.

Ruzhencev, V. E. 1965. Izmenenie organicheskovo mira na rubezhe Paleozoya i Mezozoyia. *Trudy Paleontologicheskogo Instituta Akademiya Nauk SSSR*, **108**, 117–134.

Ruzhencev, V. E. 1974. O semeystvakh Paragastrioceratidae i Spirolegoceratidae. *Paleontologicheskiy Zhurnal*, **1974**(1), 19–29.

Ruzhencev, V. E., **Sarytcheva, T. G.** & **Shevyrev, A. A.** 1965. Biostratigraficheskie vyvody. *Trudy Paleontologicheskogo Instituta Akademiya Nauk SSSR*, **108**, 93–116.

Ruzhencev, V. E. & **Shevyrev, A. A.** 1965. Ammonoidei. *Trudy Paleontologicheskogo Instituta Akademiya Nauk SSSR*, **108**, 47–57.

Schindewolf, O. H. 1929. Vergleichende Studien zur Phylogenie, Morphologie und Terminologie der Ammoneen-Lobenlinie. *Abhandlungen der Preußischen Geologischen Landesanstalt, Neue Folge*, **115**, 1–102.

Schobben, M., **Joachimski, M. M.**, **Korn, D.**, **Leda, L.** & **Korte, C.** 2014. Palaeotethys seawater temperature rise and an intensified hydrological cycle following the end-Permian mass extinction. *Gondwana Research*, **26**, 675–683.

Schobben, M., **Stebbins, A.**, **Ghaderi, A.**, **Strauss, H.**, **Korn, D.** & **Korte, C.** 2015. Flourishing ocean drives the end-Permian marine mass extinction. *Proceedings of the National Academy of Sciences of the United States of America*, **112**(33), 10298–10303.

Shen, S.-Z. & **Mei, S.-L.** 2010. Lopingian (Late Permian) high-resolution conodont biostratigraphy in Iran with comparison to South China zonation. *Geological Journal*, **45**, 135–161.

Shevyrev, A. A. 1965. Nadortyad Ammonoidea. *Trudy Paleontologicheskogo Instituta Akademiya Nauk SSSR*, **108**, 166–182.

Shevyrev, A. A. 1968. Triasovye ammonoidei Yuga SSSR. *Trudy Paleontologicheskogo Instituta Akademiya Nauk SSSR*, **119**, 1–272.

Spath, L. F. 1930. The Eotriassic invertebrate fauna of East Greenland. *Meddelelser om Gronland*, **83**(1), 1–90.

Spath, L. F. 1934. *Catalogue of the fossil Cephalopoda in the British Museum (Natural History). Part IV. The Ammonoidea of the Trias*. British Museum (Natural History), London, 521 pp.

Spinosa, C., **Furnish, W. M.** & **Glenister, B. F.** 1975. The Xenodiscidae, Permian ceratoid ammonoids. *Journal of Paleontology*, **49**, 239–283.

Stampfli, G. M. & **Borel, G. D.** 2002. A plate tectonic model for the Paleozoic and Mesozoic constrained by dynamic plate boundaries and restored synthetic oceanic isochrons. *Earth and Planetary Science Letters*, **196**, 17–33.

Stepanov, D. L., **Golshani, F.** & **Stöcklin, J.** 1969. Upper Permian and Permian–Triassic boundary in North Iran. *Geological Survey of Iran, Report*, **12**, 1–72.

Stoyanow, A. A. 1910. On the character of the boundary of Palaeozoic and Mesozoic near Djulfa. *Zapiski Imperatorskago St.-Peterburgskago Mineralogiceskago Obscestva = Verhandlungen der Russisch-Kaiserlichen Mineralogischen Gesellschaft zu St. Petersburg, Serie 2*, **47**, 61–135.

Taraz, H., **Golshani, F.**, **Nakazawa, K.**, **Sgimuzu, D.**, **Bando, Y.**, **Ishi, K.-i.**, **Murata, M.**, **Okimura, Y.**, **Sakagami, S.**, **Nakamura, K.** & **Tokuoka, T.** 1981. The Permian and the Lower Triassic Systems in Abadeh Region, Central Iran. *Memoirs of the Faculty of Science, Kyoto University, Series of Geology and Mineralogy*, **47**(2), 61–133.

Teichert, C., **Kummel, B.** & **Sweet, W. C.** 1973. Permian–-Triassic strata, Kuh-e-Ali Bashi, Northwestern Iran. *Bulletin of the Museum of Comparative Zoology,* Harvard University, **145**(8), 359–472.

Tozer, E. T. 1969. Xenodiscacean Ammonoids and their bearing on the discrimination of the Permo–Triassic boundary. *Geological Magazine*, **106**, 348–361.

Tozer, E. T. 1979. The significance of the ammonoids *Paratirolites* and *Otoceras* in correlating the Permian–Triassic boundary beds of Iran and the People's Republic of China. *Canadian Journal of Earth Sciences*, **16**, 1524–1532.

Villier, L. & **Korn, D.** 2004. Morphological disparity of ammonoids and the mark of Permian mass extinctions. *Science*, **306**, 264–266.

Voinova, E. V., **Kiparisova, L. D.** & **Robinson, V. H.** 1947. Klass Cephalopoda. Golovonogie. *Atlas rukovodyashtchikh form iskopaemykh faun SSSR. VIII. Triasovaya sistema*. Pp. 124–176. Moskva-Leningrad.

von Möller, V. 1879. Üeber die bathrologische Stellung des jüngeren paläozoischen Schichtensystems von Djoulfa in Armenien. *Neues Jahrbuch für Mineralogie, Geologie und Palaeontologie*, **1879**, 225–243.

Waagen, W. H. 1879. *Productus*-limestone fossils. I. Pisces – Cephalopoda. *Memoirs of the Geological Survey of India*, **13** (1), 1–72.

Wedekind, R. 1914. Beiträge zur Kenntnis der Oberkarbonischen Goniatiten. *Mitteilungen aus dem Museum der Stadt Essen für Natur- und Völkerkunde*, **1**, 1–22.

Xu, G. & **Wie, R.** 1977. *Fossil Atlas of South-Central China. Part 2, Cephalopoda*. Geological Publishing House, Beijing, 537–582.

Yang, D.-z. & **Yang, F.** 1992. New materials of Late Permian ammonoids from Southeastern Hubei. *Acta Palaeontologica Sinica*, **31**, 595–604.

Yang, F. 1987. Late Late Permian strata and their ammonoid zones in Southwest China. *Earth Science – Journal of Wuhan College of Geology*, **1985**(10), 129–144.

Zakharov, Y. D. 1983. *Ammonoidea*. Pp. 150–157 in M. N. Gramm & K. O. Rostovtsev (eds) *Pozdnepermiskii etap evoliutsii organicheskogo mira*. NAUKA, Leningrad.

Zakharov, Y. D. 1992. The Permo–Triassic boundary in the southern and eastern USSR and its intercontinental correlation. Pp. 46–55 in W. C. Sweet, Y. Zunyi, J. M. Dickins & Y. Hongfu (eds) *Permo–Triassic events in the Eastern Tethys*. Cambridge University Press, Cambridge.

Zakharov, Y. D. & **Rybalka, S.** 1987. Etalony permi i triasa Teticheskoy oblasti. *Problemy biostratigrafii permi i triasa Vostoka SSSR, DVNTs AN SSSR*, **1987**, 6–48.

Zhao, J., **Liang, X.** & **Zheng, Z.** 1978. Late Permian cephalopods from South China. *Palaeontologia Sinica, Series B*, **12**, 1–194.

Zhao, J. & **Zheng, Z.** 1977. The Permian ammonoids from Zhejiang and Jiangxi. *Acta Palaeontologica Sinica*, **16**, 217–254.

Zheng, Z. 1981. Uppermost Permian (Changhsingian) ammonoids from Western Guizhou. *Acta Palaeontologica Sinica*, **20**(2), 107–114.

Zhou, Z. 1985. Several problems in the Early Permian ammonoids from South China. *Palaeontologia Cathayana*, **2**, 179–210.

Zhou, Z. 1987. First discovery of Asselian ammonoid fauna in China. *Acta Palaeontologica Sinica*, **26**(2), 130–148.